

TU DELFT  
Faculty of Mechanical, Materials and Maritime Engineering

# Controlled Delivery of (-)-Epigallocatechin 3-Gallate as a Therapeutic Strategy for the Degenerative Disc Disease

## Master Thesis

By

**Aikaterini-Alexandra Zafeiropoulou (4422740)**

in partial fulfilment of the requirements for the degree of

### Master of Science

in Biomedical Engineering, Tissue Biomechanics and Implants

at Delft University of Technology

Supervisors: Assoc. Prof. Amir Zadpoor  
Prof. Stephen Ferguson (ETH Zurich)  
Assis. Prof. Karin Wuertz-Kozak (ETH Zurich)

Advisors: Dr. Lidy Fratila-Apachitei  
Dr. Olga Krupkova (ETH Zurich)

June 2017

**EMBARGO END DATE: JUNE 2022**

# Acknowledgements

The master thesis “Controlled Delivery of (-)-Epigallocatechin 3-Gallate as a Therapeutic Strategy for the Degenerative Disc Disease” was obtained in the Laboratory for Orthopaedic Technology and the laboratory of Immunoengineering and Regenerative Medicine at ETH Zurich. At this point, I have to express my gratitude and thanks to people that significantly contributed to the project’s completion.

Firstly, I would like to thank prof. Stephen Ferguson and prof. Karin Wuertz-Kozak, for accepting me in their lab, their trust to give me that project and letting me work under their supervision. Also, I would like to thank Ass. prof. Amir Zadpoor and Dr. Lidy Fratila-Apachitei (TU Delft) for their encouragement and their support to venture to do my mater thesis in a foreign university and acquire the best possible benefits from this attempt.

Of course, nothing would become reality without my advisor, Dr. Olga Krupkova. Therefore, I feel the need to express my gratitude to her, for advising me throughout these months. Her valuable indications and advice were valuable for the accomplishment of this thesis. I have to acknowledge that she taught me a lot of new techniques and how to handle different aspects and requirements of the projects.

Additionally, I couldn’t forget to mention and give my credits to all the members of the lab and especially, Dmitriy Alexeev and Oddny Björgvinsdottir for their valuable advice regarding the electrospaying part of my project and their willingness to help me with any obstacle I was facing with the electrospaying apparatus.

Last but not least, I would like to express my faith, gratitude and love to my family, Athanasios, Foteini and Ioanna Zafeiropoulos, Georgios-Marios Papadopoulos, as well as those that “feel like family”, Marianna Dimantopoulou, Eleftheria Michalaki and Anastasios Nodaras, for their significant support (each one with different means), patience and encouragement to reach till the end of this attempt.

# Abstract

Degenerative disc disease (DDD) is the accelerated process of intervertebral disc decay (decrease of disc thickness, enhanced cell death, ECM damage and collagen loss etc.), accompanied with pain, as well as structural and functional failure. So far, there are no therapies that can inhibit or even reverse the degenerative progress of this disease. Regimens and treatments that eliminate the pathological symptoms of DDD are mainly used in patients suffering from DDD. Among the promising treatments of DDD in preclinical development is the use of natural bioactive compounds, such as (-) -Epigallocatechin 3-Gallate (EGCG). EGCG is a compound of green tea leaves, indicating beneficial effects against several diseases, however it is rather degradable in its free form. Hence, on-target EGCG facilitation in human body, in a manner providing protection to EGCG against degradation and dose control over time, is necessary. It was hypothesized that encapsulation could protect EGCG and attenuate DDD features, once replaced locally and released long-term. Therefore, the aim of this master thesis was the design and synthesis of a drug delivery system (DDS) for EGCG encapsulation, stabilization and protection against unrestrained release, for potential local delivery as a DDD therapy.

EGCG was encapsulated in gelatin particles via electrospraying. These particles were then embedded into HA-pNIPAM, a thermo-responsive hydrogel for further stabilization and release control. The hydrogel-particles mixture, consisting the DDS, would then be injected into degenerative disc tissue. The DDS was evaluated regarding its biocompatibility, EGCG protection and prolonged release rates. Firstly, an electrospraying protocol was established for EGCG encapsulation in gelatin microparticles. These particles were tested for their morphology and cytotoxicity. EGCG-loaded microparticles were combined with HA-pNIPAM hydrogel and tested *in vitro* (t=7days) for their ability to release EGCG and determine the activity of encapsulated EGCG via colorimetric assays and absorbance measurements.

The electrospraying conditions of 2 $\mu$ L/min (flow rate), 20kV (voltage), 4% Gelatin solution and cross-linking with 37.5 $\mu$ g/mL glutaraldehyde (GA) gave spherical, dispersed particles with average size of 669.72 nm, facilitating injectability. Their effect on cells indicated 83-88% metabolic activity, compared to control cells (100% viability), regarding cytotoxicity. Encapsulated EGCG was released up to 50% slower than free EGCG, but kept the same activity (80%). Overall, it was demonstrated that the designed DDS is a promising approach, that can limit EGCG release and possibly protect its activity.

# Table of Contents

Acknowledgements	2
Abstract	3
Table of Contents	4
Table of Figures	6
A. Introduction	8
1. Intervertebral Disc Degeneration	8
2. (-)-Epigallocatechin 3-Gallate	9
3. Micro-Particle Production & Encapsulation for Drug Delivery Systems	10
4. Motivation, Goal, Hypotheses and Aims of the Project	11
B. Materials & Methods	13
1. Materials	13
2. Sample Preparation	16
3. Electrospraying - Drug Encapsulation	17
4. Characterization of Microparticles	18
5. Solubility & Degradation of Gelatin Microparticles	19
6. Biocompatibility of Microparticles	20
7. Experimental design of the release tests	21
8. EGCG Release (Ferrous Tartrate Method)	22
9. EGCG Activity (DPPH Assay)	22
10. Encapsulation Efficiency	23
11. Statistical Analysis of the Results	24
C. Results	25
1. Synthesis of Gelatin Particles: Optimization and Characterization	25
1.1. Optimization: Electrospraying of pain gelatin	25
1.2. Optimization: Gelatin Cross-Linking	26
1.3. Optimized Electrospraying Parameters	26
2. EGCG Encapsulation in Gelatin Microparticles	29
2.1. Synthesis of Gelatin Particles Containing EGCG	29
2.2. Encapsulation Efficiency	30
3. Solubility & Degradation of Gelatin Particles	30
4. Biocompatibility of Gelatin Particles (MTT Assay)	30

5. EGCG Release Rates	32
6. Activity of Released EGCG	35
D. Discussion	37
1. Synthesis of EGCG Drug Delivery System	37
2. Evaluation of the EGCG Drug Delivery System	41
E. Conclusions	44
F. Suggestions for Future Work	44
G. References	49
H. Appendix	53
1. SEM	53
2. Encapsulation Efficiency	58
3. Biocompatibility Test - MTT Assays	59
4. EGCG Release (Ferrous Tartrate Method and UV Spectrum)	60
5. EGCG Activity During Release Experiments (DPPH Assay)	84
6. Protocols	89

# Table of Figures

Figure 1. Anatomy of the spinal column <sup>[1]</sup>	8
Figure 2. Anatomy of Intervertebral Disc and Vertebra	8
Figure 3. Healthy and Degenerated Intervertebral Disc	9
Figure 4. Chemical Structure of (-)-Epigallocatechin Gallate	10
Figure 5. Schematic Representation of the EGCG DDS against DDD	13
Figure 6. Chemical Structures of a) Gelatin and b) EGCG <sup>[19]</sup>	14
Figure 7. Cross-Linking reaction Between Gelatin and Glutaraldehyde <sup>[28]</sup>	15
Figure 8. Thermo-reversible Hydrogel HA-pNIPAM; in room temperature (25 °C) liquid is its normal state and upon heating above 32 °C, it solidifies	16
Figure 9. 4%w/v Gelatin Solution in Acetic Acid	16
Figure 10. Representation of Electrospraying Setup	17
Figure 11. Electrospraying Setup used for Gelatin Microparticles Formation	18
Figure 12. Scanning Electron Microscopy Equipment (Quanta 200F FEI) used for Particle Characterization	19
Figure 13. a) ThinCert™ Tissue Culture Inserts b) 12-well plates for cell cultures	20
Figure 14. Solution of Formazan Crystals at MTT Assay	20
Figure 15. Sterilization under UV- Radiation for the Gelatin Microparticles	21
Figure 16. a) Scheme of the release test experimental design. At the bottom of the tube, the solid mixture of HA-pNIPAM and EGCG is placed, while the rest of the tube is filled with 0.9% NaCl solution. EGCG is released from the bottom bulk in the medium and its concentration and activity are measured. b) Eppendorf Thermo-mixer. The in vitro release experiments were held there for 1 week in 37 °C with continuous stirring	22
Figure 17 . EGCG Samples reacting with Ferrous Tartrate to Violet-Purple Color. The intensity of the color is proportional to EGCG concentration in each sample	23
Figure 18. EGCG Samples Reacting with DPPH Assay. The more active the substance is, the less color intensity the sample has.	23
Table 1. Summary of different experimental settings for plain gelatin electrospaying	26
Table 2. SEM images of electrospayed particles (flow rate:4µL/min, voltage: 21kV and solution concentration: 4%) with different concentration of GA cross-linker	27
Table 3. SEM images of electrospayed particles (flow rate:2µL/min, voltage: 21-22kV and solution concentration: 4%) with different concentrations of GA cross-linker	28
Table 4. Summary of the optimal achieved gelatin particle production for plain and cross-linked gelatin and the respective experimental conditions	28
Figure 20. Solubility of Gelatin Particles, Cross-Linked (left) and Uncross-Linked (right), 2 hours after Mixture	31
Figure 21. Solubility of Gelatin Particles, Cross-Linked (left) and Uncross-Linked (right), 24 hours after Mixture	31
Figure 22. Biocompatibility Test of the Cross-Linked Gelatin Particles (62.5µg/ml GA) in Comparison with Plain Gelatin and Untreated Cells. All the data were checked for normality and groups with asterisk indicated statistical significance at p<0.05 through Kruskal-Wallis Test	32
Figure 23. Concentration of Released EGCG in the medium of NaCl 0.9%, Along Time. The respective images of the remaining gels after 1 week of experiment duration. Statistical analysis with Kruskal-Wallis test (p=0.1, n=3) (Overall Results)	33
Figure 24. % Cumulative EGCG Release Rates in 0.9% NaCl medium Along Time. The % rates have been estimated in respect of the 0.45mM amount of concentration which is the maximum amount of EGCG that can be released in each sample, as the concentration of EGCG before the addition of 10mL release medium was 5mM. (Overall Results, n=3)	34

Figure 25. EGCG Concentration Entrapped in Hydrogel by the End of the Experiment. (Overall Results) Statistical analysis with Kruskal-Wallis test ( $p=0.1$ , $n=3$ )	34
Figure 26. % Activity of Released EGCG as a Function of Time. The respective values of HA-pNIPAM control have been subtracted, to have the original activity of EGCG for Each sample. The calibration curve of L-Ascorbic Acid (Positive Control) has been added as legend on the graph (Consolidating Figure). Statistical analysis with Kruskal-Wallis test ( $p=0.05$ , $n=12$ )	35
Figure 27. % Activity of Released EGCG as a Function of Time. The normalization has been obtained in respect of concentration. By this, activity profiles of each sample have a different shape (Consolidating Figure).	36
Figure 28. Oxidization of Aldehyde to Carboxylic Acid	39
Figure 29. Individual Reactions of an Aldehyde Under Acidic or Alkaline Conditions	39
Figure 30. Possible mechanism of the cross-linking reaction between gelatin and glutaraldehyde at acidic pH values. <sup>[68]</sup>	40
Figure 31. Photographs of HA-pNIPAM samples during DDS evaluation, depicting the hydrogel collapsing during the experiments. The left column represents the gel, either containing EGCG or not, before the release and activity experiments. The right column has the images of the same samples at the end of these experiments. Gel collapsing is obvious in most of them.	43
Figure 32. Different regions of the same electrospray sample. In the first picture (a) the particles are organized in clumps, just as they were attached in the collector plate once they were electrosprayed. The second one (b) the particles are not aggregated, as they were “interrupted” by metal spatula.	46

# A. Introduction

## 1. Intervertebral Disc Degeneration

Intervertebral disc (IVD) is the structure lying between the vertebrae (Figures 1, 2) in the vertebral column (spine). [1] IVDs absorb applied pressure and shocks, distribute any stress and keep the vertebrae from wearing down against each other. The IVDs are designed to serve in favor of bearing and spreading any loads uniformly and equally on the vertebral bodies; as well as providing flexibility of the spine in all directions.

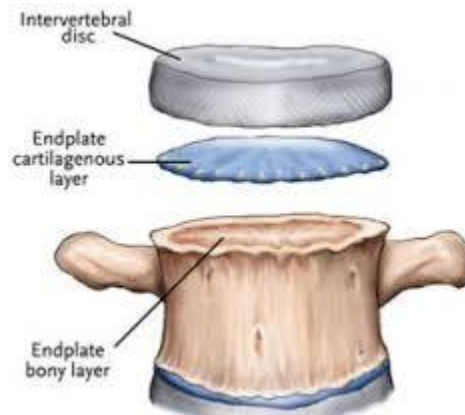


Figure 1. Anatomy of the spinal column [1]

Intervertebral discs consist of the nucleus pulposus (NP) and the annulus fibrosus (AF). NP is mainly composed by proteoglycans, hyaluronan acid and type II collagen and contains a lot of water. AF consists of radially aligned fibers of collagen type I. [2] NP tends to swell, but is resisted radially by the collagen fibers of AF and axially by the vertebral endplates. This structure enables the intervertebral discs to protect from wearing, be flexible and absorb and distribute loads.

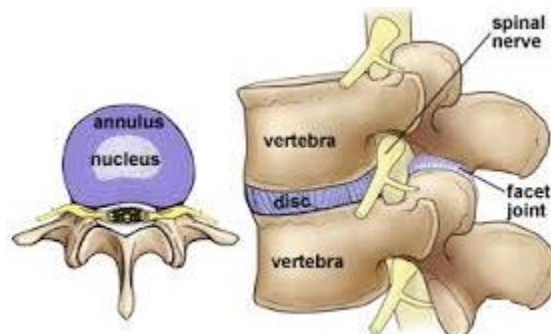


Figure 2. Anatomy of Intervertebral Disc and Vertebra

IVD degeneration starts during middle-age (30-40 years) [3] and often includes specific structural, histological, biochemical and functional changes on the intervertebral discs. [4] Degenerative disc disease is a description for the symptoms of pain, possible radiating weakness or numbness derived from a degenerated intervertebral disc. [1] It is one of the most common causes of low back pain and neck pain, accompanied by intensive inflammatory and patho-immunological processes. It is strongly age- and genetics-dependent and can be accelerated by trauma, nutritional, mechanical



and toxic factors [6]. It is initiated by an imbalance, which takes place between the anabolic and catabolic processes. This leads to collagen and proteoglycan loss, as well as to a consequent reduction of water content. All these degenerative processes result to mechanical malfunction and different stress distribution on the tissue, which can lead to increased risk for structural failure of the AF. [4] A failure to AF can cause leakage of the NP matter and accordingly, spinal nerve irritation (Figure 3). All these processes usually lead to disc degeneration. Also, nerve infiltration into the affected disc is another effect of disc degeneration. Finally, intense development of blood vessels into the tissue of compromised discs is observed, as well as nociceptive nerve fibers.

These processes are consistent with pain generation and degenerative disc disease is considered as the most common cause of neck and low back pain in adults and elderly. [4] Neck and low-back pain, as well as inflammation have laid the disc degeneration as one of the costliest diseases, requiring several and repetitive health services and treatments and resulting to reduced people productivity.



Figure 3. Healthy and Degenerated Intervertebral Disc

So far, the existing health services and treatments mainly target the pathological symptoms' elimination, which are mainly pain, via pharmacological treatment, such as analgesics, anti-inflammatories etc. Physical therapy is also applied and once in severe cases, as well as surgical interventions (discectomy, spinal fusion or disc replacement). However, these treatments do not provide cure of the disease, but aim for symptoms' elimination.

Therapies or medication that may aim to inhibit degeneration and induce disc repair are not completely developed or utilized yet, as human IVDs have only very limited self-repair capabilities. However, several new strategies and techniques are under reinforcement [4-10], most of them in preclinical stage. These therapies intend to restore normal disc height and load distribution, while reducing degenerative changes on the discs.

## 2. (-) -Epigallocatechin 3-Gallate

(-) -Epigallocatechin 3-gallate (EGCG) (Figure 4) is a biologically active compound, abundantly found in green tea leaves. [4, 11] It belongs to catechins' category, a group of natural polyphenols, and has indicated many advantageous and favorable effects on human tissue. [12] More specifically, EGCG has indicated beneficial effects, in concentration range of 0-100 $\mu$ M, for a treatment of number of clinical conditions, including cancer, obesity, atherosclerosis, diabetes, liver and neurodegenerative diseases. [5, 11-18, 20]

EGCG is responsible for the anti-oxidant, anti-aging and anti-inflammatory properties provided by green tea. These EGCG effects are exhibited via either direct or indirect interaction with cell molecules [12, 15], intervention on cell signaling [4, 22] and chemo-preventive effects in both *in vitro* and

*in vivo* systems <sup>[15]</sup>. Research studies have shown that EGCG has beneficial effects on cartilage tissue and intervertebral disc. It has been reported that EGCG causes a significant decrease of the inflammatory mediators' expression, as well as matrix metalloproteinases' production in IVD cells cultured *in vitro* and inhibits pain behavior *in vivo* <sup>[4]</sup>.

However, the use of EGCG is still limited. EGCG is in most cases unstable and degrades rapidly once released in its free form. Its degradability reduces its bioavailability, while the formed degradation products might cause side-effects. The time that EGCG degrades in each case, depends highly on the ambient conditions, like pH, temperature and partial oxygen pressure, the initial concentration of EGCG, as well as the presence of oxygen or other anti-oxidants. <sup>[12, 23]</sup> More specifically, free EGCG is quite unstable in human body, considering the ambient conditions that obtain there. In case of oral administration, it degrades even faster as it is sensitive to rapid pH changes (from extreme acidic environment in stomach to alkaline environment in intestinal system). <sup>[12]</sup> Also, EGCG indicates poor absorption through gastro-intestinal tract, because only 1 $\mu$ M of it reach in blood plasma. <sup>[12]</sup> In biological fluids, such as PBS and cell culture medium, the half-life time of EGCG is 90min and 30-60min, respectively. <sup>[12]</sup> EGCG indicates optimal stability and activity in acetic environment, pH=2-5.5, while the pH in human blood fluid is equal to 7.4 <sup>[11]</sup>, and in temperatures lower than 4 °C. Also, EGCG stability is favored while released in initial concentrations of mM range and the environmental oxygen concentration is lower than 110mm Hg.

In order to overcome these limitations, it has been aimed to protect free EGCG and control its release (10-100 $\mu$ M) once introduced into human body, by encapsulating the active compound into a polymer carrier. In this way, encapsulated EGCG is released in a sustainable way, retains its biological effectiveness and enhances its bioavailability <sup>[11, 15]</sup>. Also, it can limit possible unwanted side-effects, while the required effective dose is decreased with encapsulation <sup>[16]</sup>. The most common polymers used as carriers for EGCG encapsulation are PLA-PEG, gelatin, chitosan etc. <sup>[9, 11, 13, 15-17]</sup> More specifically, it has been proved that chitosan encapsulated EGCG enhances the intestinal absorption of EGCG <sup>[9, 11, 13, 18]</sup>.

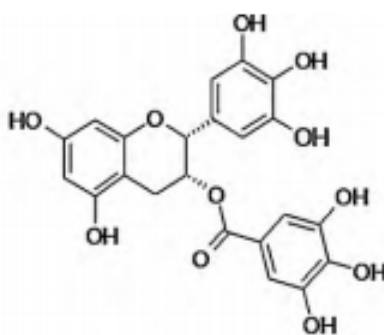


Figure 4. Chemical Structure of (-)-Epigallocatechin Gallate

### 3. Micro-Particle Production & Encapsulation for Drug Delivery Systems

Many drugs, such as natural bioactive compounds<sup>1</sup> (EGCG), peptides, proteins and DNA-based therapeutics are unstable in their free form, non-soluble or susceptible to enzymatic degradation. Therefore, drug encapsulation in sub-micron sized particles or other structures (fibers <sup>[5, 26, 28, 33, 34]</sup>,

<sup>1</sup> Bioactive compounds are essential and non-essential compounds (e.g., peptides, lipids, vitamins etc.) that occur in nature, are part of the food chain, and are shown to have a biological activity or effect on living organism, tissue, cell or in human health. <sup>[37, 38]</sup>

rods <sup>[35]</sup>, pellets <sup>[35]</sup>) is preferred. These drug delivery systems are designed to protect unstable therapeutic compounds, ensure their sustained release at exact time and concentration and target their delivery at specific location in the body <sup>[11]</sup>. This leads to an increased compliance and minimized side effects <sup>[13]</sup>. Additionally, they are designed to be biocompatible<sup>2</sup>, and increase drug bioavailability<sup>3</sup>. However, several challenges still have to be overcome, including difficulties in large-scale manufacturing, possible inactivation of the drug during fabrication, and limited control of the drug release rates.

There are several different methods of microparticle production, including drop-wise addition with lyophilizing (freeze-drying) or centrifugation, standard solvent evaporation method, emulsification cross-linking, coacervation/precipitation, as well as spray-drying, emulsion-droplet coalescence and ionic gelation. <sup>[9, 18, 66, 72]</sup> Also, particles are produced via emulsion-droplet coalescence and emulsion-droplet coalescence. <sup>[18]</sup> Synthesis methods can be classified in two main categories, top-down and bottom up processes. Among the methods belonging to the top-down category is electrospraying.

#### 4. Motivation, Goal, Hypotheses and Aims of the Project

##### ❖ Motivation

Degenerative disc disease is very common, a lot of people suffer from it, costs a lot of money to national health systems <sup>[56]</sup> and people's job performance is significantly decreased, due to the disease's symptoms (inflammation, pain). Recently, it has been shown that EGCG can reduce the degenerative decay, pain and inflammation in degenerative discs. <sup>[4]</sup> However, EGCG is mostly unstable in its free form. EGCG is sensitive to extreme ambient conditions and degrades rapidly. Therefore, a DDS of EGCG will be synthesized, in order to protect the compound and facilitate it at the suffering tissue, as well as protect the compound from rapid degradation and provide prolonged release of it in the disc. Degradation prevention will assure the compound's biological activity retention, while prolonged release will provide sustained therapeutic effect. <sup>[11, 15]</sup>

Preliminary tests revealed that gelatin can be used as EGCG carrier, as well as electrospraying can be applied as a method for particle formation and is suitable for EGCG encapsulation. <sup>[74]</sup> The results indicated formation of well-defined EGCG-gelatin particles. <sup>[74]</sup> However, microparticle formation needs optimization and gelatin requires implementation, in order to retard its rapid dissolution in aqueous environment and control better EGCG release. Therefore, implementation with electrospraying procedure and chemical cross-linking of gelatin with glutaraldehyde were considered applicable for these aims. Cross-linked EGCG-gelatin particles will be combined with thermo-reversible hydrogel HA-pNIPAM and constitute the designed DDS for this project. HA-pNIPAM can operate as carrier for intradiscal injections and further protection from degradation and unrestrained release.

##### ❖ Goal

The goal of this project is the design and synthesis of a drug delivery system (DDS) for EGCG encapsulation, stabilization and protection against unrestrained release, for potential local

---

<sup>2</sup> Biocompatibility: Biocompatibility is a general term describing the property of a material being compatible with living tissue. Biocompatible materials do not produce a toxic or immunological response when exposed to the body or bodily fluids.

<sup>3</sup> Bioavailability: The ability of a drug or other substance to be absorbed and used by the body.

delivery as a DDD therapy via injection. More specifically, the optimization of EGCG encapsulation technique, in order to stabilize EGCG, retain its activity and control its release (1-100µM), is intended for this project. The particles will be produced via electrospraying and have to be spherical structures encompassing and protecting EGCG molecules. The designed DDS will be completed with a hydrogel association in order to render the particles injectable in the target tissue and provide further protection to the bioactive compound.

#### ❖ Hypotheses

According to the state-of-the-art literature [5, 9, 10, 12, 14, 18, 19, 21, 28, 34, 39, 40], the following hypotheses were formulated; (1) microparticles can be effectively created via the method of electrospraying [5, 18, 33, 34, 51], (2) these microparticles enhance EGCG stability and provide prolonged release, (3) these particles can then be embedded into thermo-responsive HA-pNIPAM carrier, to form an injectable mixture and (4) this mixture constitutes an injectable DDS of EGCG for local application and delivery against DDD. [9]

#### ❖ Aims

In order to confirm or refute the hypothesis above, the following aims were set;

- I. Synthesis of the EGCG DDS; trials to optimize the preparation of gelatin particles, including cross-linking (Glutaraldehyde) of gelatin, electrospraying and Scanning Electron Microscopy. Upon successful gelatin particles formation, EGCG incorporation and hydrogel addition follows.
- II. Evaluation of the created DDS: biocompatibility testing (MTT assay) of gelatin particles, *in vitro* tests of encapsulated EGCG release rates (Ferrous-Tartrate Method, UV Spectrum) and its activity (DPPH assay).

# B. Materials & Methods

## 1. Materials

Gelatin polymer was chosen for EGCG encapsulation in this project (Figure 6). Acetic acid was selected as solvent for gelatin dilution. <sup>[19, 25, 26]</sup> Glutaraldehyde was combined with gelatin for cross-linking, in order to make gelatin particles less soluble upon facilitation in discs. <sup>[28, 57-59, 62]</sup> Once the microparticles were produced, HA-pNIPAM hydrogel (Figure 8) was used as injection and control carrier for the particles. <sup>[9, 39,40]</sup> These combined materials give the complete DDS of our project (Figure 5).

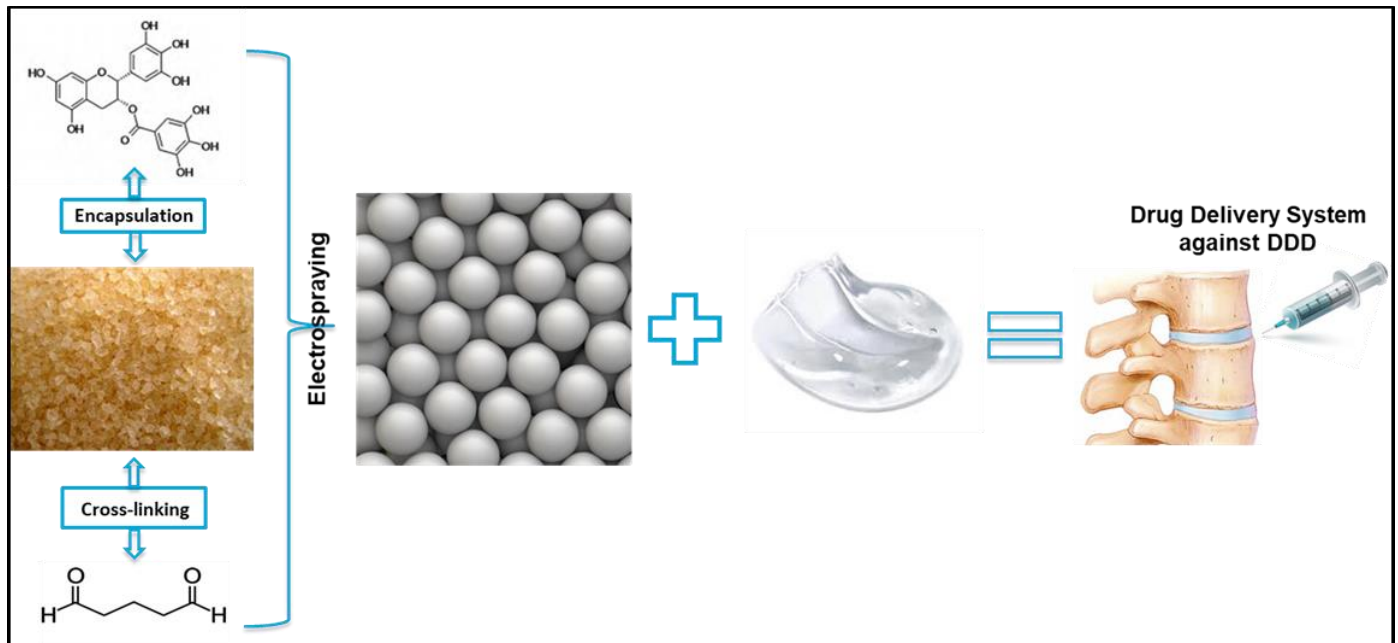


Figure 5. Schematic Representation of the EGCG DDS against DDD

Gelatin is a natural polymer, ideal for biology applications, as it is biocompatible and biodegradable. In general, natural polymers exhibit better biocompatibility and clinical functionality than synthetic polymers and some exhibit intrinsic antibacterial properties. <sup>[34]</sup> Gelatin has been used widely at bulk state in food technology for thickening and stabilizing purposes mostly. <sup>[26]</sup> It can be easily obtained from partial hydrolysis of collagen <sup>[19]</sup> with low cost. It is a structural element of skin, bones and tendons. Its mechanical and electrical properties make gelatin suitable for a wide range of applications. It has been extensively used in pharmaceutical industry for the manufacture of hard and soft capsules and especially in the field of drug controlled release, to protect drugs from external agents, such as atmospheric oxygen or light. <sup>[25]</sup> Additionally, gelatin has been widely used for enhancing elasticity, stability and consistency of food products <sup>[26]</sup> and bioactive compounds <sup>[5, 17, 26, 28]</sup>. Also, one of the most interesting properties of gelatin is its ability to form thermo-reversible hydrogels in water due to formation of collagen-like triple helices. <sup>[19]</sup>

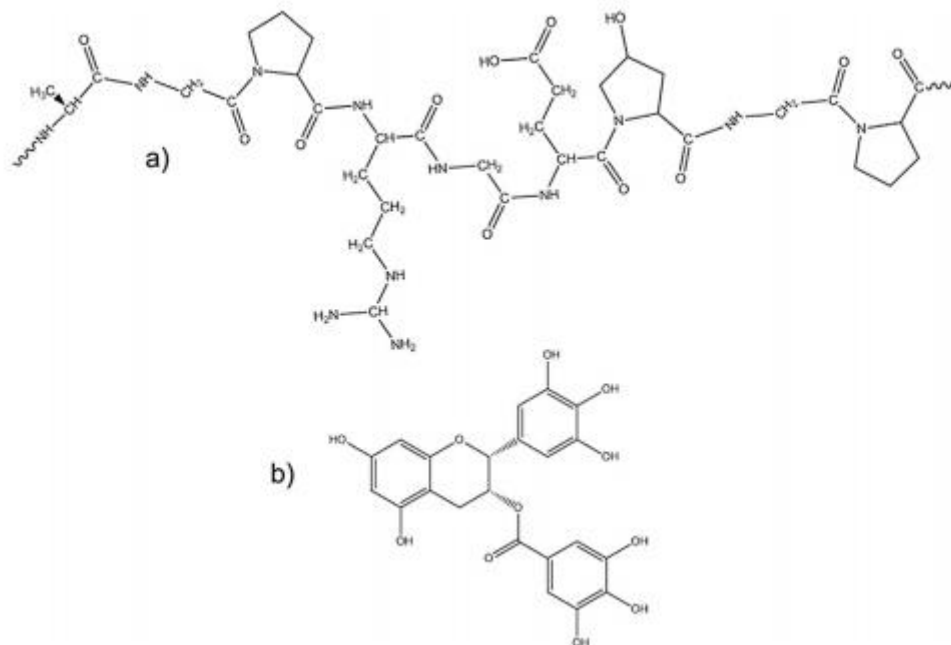


Figure 6. Chemical Structures of a) Gelatin and b) EGCG [19]

Acetic Acid is a colorless liquid organic compound with the chemical formula  $\text{CH}_3\text{COOH}$ . It is a carboxylic acid with antibacterial and antifungal properties [60], volatile and non-toxic. Volatility is desirable in processes like electrospraying, because particles can dry even faster, while low toxicity favors IVD cell viability. Acetic acid as a solvent, favors the formation of fine polymer fibers or particles through electrospinning or electrospraying. It doesn't cause any cytotoxicity for solution concentrations lower than 25%. [61] In aqueous solution containing acid (e.g. citric acid, tartaric acid, acetic acid), gelatin swells and dissolves more rapidly than in pure water, thus used extensively as solvent in gelatin solutions prepared for electrospraying/electrospinning. [19, 26, 61]

Glutaraldehyde (GA) is an organic compound with chemical formula  $\text{CH}_2(\text{CH}_2\text{CHO})_2$ , a pungent colorless oily liquid, used for sterilization, decontamination, preservative and cross-linking agent. [27] It is toxic above particular concentrations [48-50] (e.g.  $63.76\mu\text{g/mL}$  ( $3.4\mu\text{L/mL}$ ) for fibroblasts or  $73.8\text{ mg/L}$  for *Thamnocephalus platyurus*), but quite potent and commercially available and thus, widely used [57-59, 62]. Small amounts of GA ( $6.52\mu\text{g/mL}$ ) were proved to be nontoxic and at the same time active enough to increase the mechanical strength of gelatin via cross-linking mechanism. More specifically the mechanical strength of GA-modified gelatin was increased by two-fold, compared to the uncross-linked gelatin. [28] The cross-linking effects, that glutaraldehyde has on gelatin, is based on a condensation reaction. During this reaction, the amino-groups that interact with the carbonyl oxygen and water molecules, are formatted and eliminated (Figure 7).

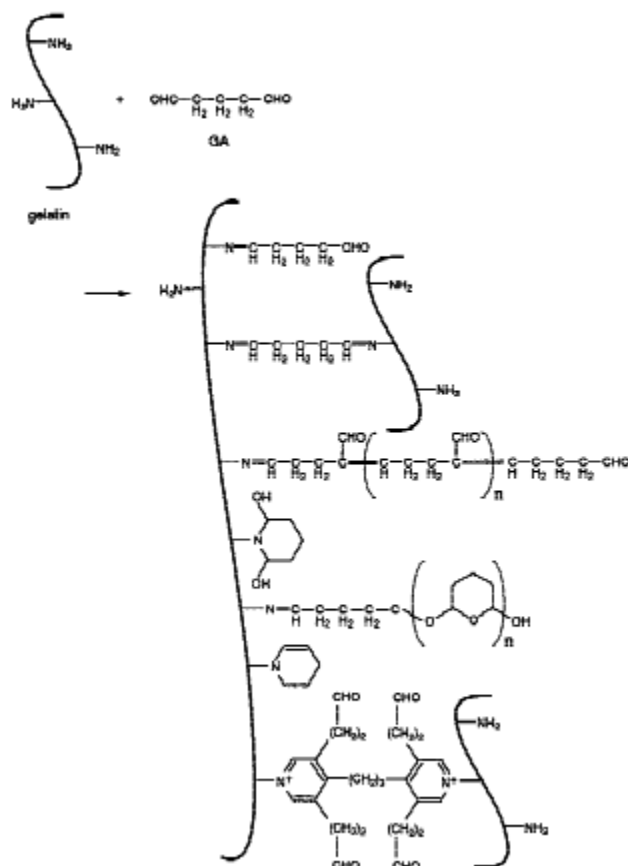


Figure 7. Cross-Linking reaction Between Gelatin and Glutaraldehyde [28]

HA-pNIPAM is a copolymer of thermoresponsive poly(N-isopropylacrylamide) (pNIPAM) and hyaluronic acid (HA) (Figure 8). HA-pNIPAM belongs to the injectable hydrogels, capable of delivering cells and drugs and gelling *in situ* without producing any toxic byproducts. [9, 39, 40] HA is a major component of the extracellular matrix in connective, epithelial, and neural tissue and is a favorable polymer for cell and drug delivery applications. Thermoresponsive PNIPAM has a gelling temperature below body temperature ( $\sim 32$  °C). [40] It is liquid at room temperature (25 °C) (Figure 8) with a sufficiently low viscosity to facilitate cell encapsulation under low shear conditions and/or mixing of additional drugs and bioactive agents. Therefore, it appears to be injectable through a needle at room temperature. It is solid at 37 °C (body temperature) with suitable mechanical properties and features rapid thermo-responsive gelling kinetics. Most important, pNIPAM (and HA-pNIPAM), as well as their degradation products, are cytocompatible. [40] A thermo-responsive hydrogel that behaves as an injectable solution at room temperature and will form a solid gel upon temperature elevation by implantation into the IVD is particularly attractive for cell, particle or drug encapsulation. [9, 39]

In our project, thermo-reversible hydrogel HA-pNIPAM was provided by the AO Research Institute in Davos in a membrane-like form and processed to powder before use. Gelatin-EGCG microparticles were dispersed in liquid HA-pNIPAM at room temperature, to give a liquid mixture. This mixture enables the particles to be injected and situated in discs. Upon laying in disc tissue and heated at 37 °C, HA-pNIPAM solidifies and a bulk of HA-pNIPAM including scattered

microparticles comes up. Bulk HA-pNIPAM allows water flow through it, promoting a slow but stable and consistent release of encapsulated EGCG. Thus, the overall designed DDS is considered to release EGCG, upon water flow and gelatin dissolution, acting against local inflammation and degenerative processes. Without HA-pNIPAM presence and supportive role, EGCG-gelatin particles would be floated away, gelatin would dissolve faster and EGCG would release unsustainably.

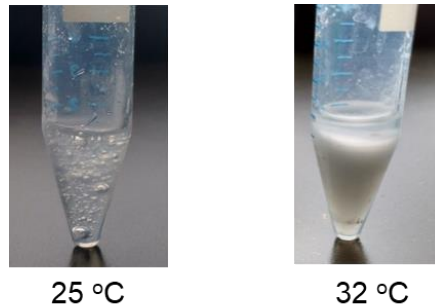


Figure 8. Thermo-reversible Hydrogel HA-pNIPAM; in room temperature (25 °C) liquid is its normal state and upon heating above 32 °C, it solidifies

## 2. Sample Preparation<sup>4</sup>

Before electro spraying process, gelatin solution was prepared. 6 or 4% w/v solution of gelatin (porcine skin gelatin type A, G1890 Sigma) was mixed with 20% v/v acetic acid in H<sub>2</sub>O (33209, Sigma) in advance, stirred on 40 °C for 4-6 hours (until gelatin was totally dissolved in the mixture) and kept at room temperature overnight before spraying (Figure 9) [19, 28].

In aqueous environment and temperatures above 30 °C, gelatin tends to swell and dissolve rapidly [44-47] and thus, GA (25%w/v in H<sub>2</sub>O, G6257 Sigma) was used as cross-linking agent, to extend the lifetime of gelatin particles. Three different amounts of GA were tested for their effectiveness to gelatin crosslinking process and particle formation; 37.5 µg/mL, 62.5 µg/mL and 87.5 µg/mL of 5% w/v GA solution in PBS were added in gelatin solution [28, 26], instantly mixed and electro sprayed to form solid particles.

For EGCG encapsulation, free EGCG in powder form (E4143, Sigma) was mixed with gelatin-GA solution and electro sprayed.



Figure 9. 4%w/v Gelatin Solution in Acetic Acid

<sup>4</sup> For more details, the respective protocol is quoted in the appendix



### 3. Electrospaying - Drug Encapsulation<sup>4</sup>

Electrospaying is one of the methods for synthesis of polymer particles or fibers with applications in various fields. Electrospaying has proved to be suitable in drug delivery domain, as there have been synthesized efficient drug carriers suitable for oral, local, injectable, inhalable administration [5, 14, 26, 35, 53, 55], including polymer micro-particles used in immunotherapy. Drug-loaded electrospayed particles facilitate augmented dissolution rates, because of their sub-micron size. This consequently increases the drug's bioavailability, because of particles' increased surface area. Gelatin, chitosan, PLGA, collagen and hyaluronic acid are some of the most commonly used polymers for drug encapsulation and successfully implemented by electrospaying (or electrospinning). [5, 11, 13, 14, 26, 31, 74, 90]

A common electrospay setup (Figure 10) consists of the poled emitter (nozzle) and a collector plate connected with a grounded electrode. During electrospaying, large particles are divided in tinier microparticles, through the application of an electric field via a voltage supply [5]. Electrospaying constitutes a one step process, which means that the particle formation and the solvent removal take place simultaneously. [21] Except of the applied voltage, no harsh conditions such as high temperatures or toxic solvents are used during the electrospaying process. [19] In more details, the operating principle of electrospay is based on the effect of an electric field for the generation of a very fine liquid aerosol. During this process, a nozzle, which is usually a syringe needle, is connected with the poled cable of an electric circuit. Through this nozzle, a liquid comes through. Once the electric field is applied on the nozzle, the liquid gets charged and a jet of tiny, fine droplets is generated [13]. While travelling in the air, the solvent of the liquid evaporates and the droplets shrink, get dried and become particles, whose diameter ranges between some nanometers and a few microns. These particles get finally attached at a metallic surface (collector), which is connected with the grounded electrode of the circuit in a distance (d) from the nozzle [13].

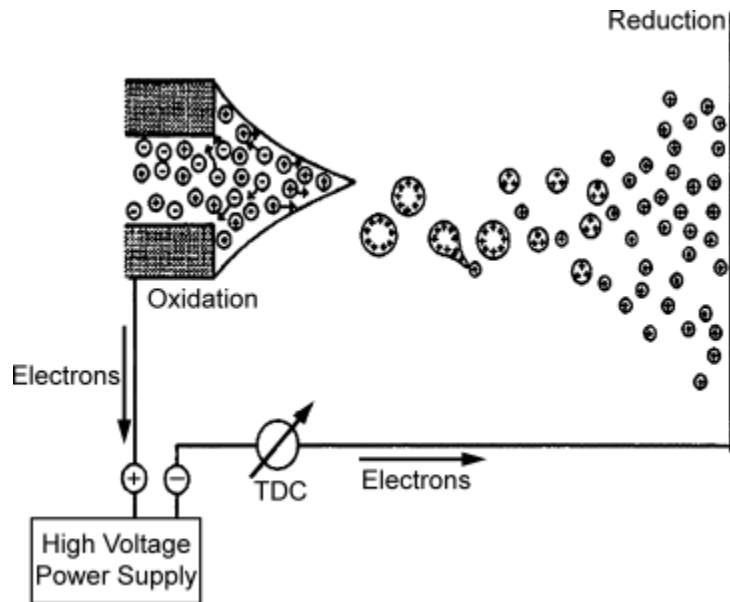


Figure 10. Representation of Electrospaying Setup

Similarly, high voltage utilization on a polymer solution, based on the same set up, can result in fine fibers, instead of tiny particles, called electrospinning. The morphology of the structures (either fibers or particles) obtained through this method can be varied depending on the operation parameters adjustment (voltage magnitude, flow rate, needle cross-section etc.) and, for a certain material (gelatin, PLGA, PLA etc.), the size and diameter depend on the polymer concentration in the solution, the distance between the collector and the needle. [26]

The main advantages of electro spraying against other particle production methods, are the low cost and the high versatility to produce particles and/or fibers (via electrospinning) of micron and nano-magnitude diameters. This capability facilitates high surface to volume ratio. Electro spraying technology corresponds to particle synthesis needs, such as high encapsulation efficiency, scalability and reproducibility [5, 26]. Electro spraying technique facilitates the synthesis of protein-based encapsulation structures, without any organic solvents and other harsh conditions (e.g. high temperatures) that could compromise the bioactive compound [19, 26]. On the other hand, a drawback of electro spraying technique is the possibility to induce some macromolecule degradation [5]. This may happen because stress is applied on the sprayed material during the whole procedure, like thermal stress during drying or shear stress into the nozzle.

In this particular project, the electro spraying apparatus consists of a variable high voltage (0-30 kV) power supply and a stainless-steel needle (cross section 1mm, 20gauge) connected through a plastic tube to a 5-mL plastic syringe of inner diameter  $\approx 12$ mm (Figure 11). The anode of the circuit is attached on the needle. The syringe, containing gelatin solution is placed horizontally on a digitally controlled syringe pump. On the opposite side of the needle there is a stainless-steel plate, which is connected with the ground electrode. On this plate, the produced electro sprayed particles are attached and collected. The user can inspect the droplet and the spraying progress from computer screen, using a micro-camera set above the needle. The distance between the needle and the collector was set at 10 cm. The experimental setup is housed in a chamber for environmental control (temp. 24 °C and humid. 40%). The produced particles were obtained using a voltage ranging from 17-25 kV and a flow rate of 2-8  $\mu$ L/min. [7, 18, 19, 26, 28]

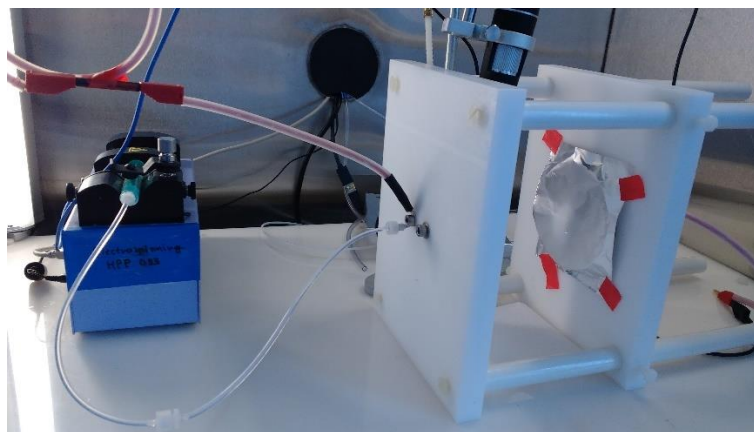


Figure 11. Electro spraying Setup used for Gelatin Microparticles Formation

#### 4. Characterization of Microparticles

For characterization of the electro sprayed gelatin particles scanning electron microscopy (SEM) was used. Generally, SEM is used for size measurements and morphology observation of dry particles. An electron beam scans the particles, electrons interact with the sample surface and

secondary electrons are reflected. These electrons are collected and implemented leading to an image acquisition. [30, 41, 42] The acquired image displays the morphology and characteristics of the specimen.

Electron transmission and thus, SEM image acquisition is exclusively possible for electrically conductive specimens. Samples also must be electrically grounded to prevent electrostatic charge accumulation at the surface. [42, 43] In case of nonconductive specimens, these are sputtered and coated with a thin film of an electrically conductive material (i.e. gold), under low vacuum conditions. In other cases, the coating takes place through high-vacuum evaporation. [30, 42] Among the advantages of SEM are the measurement of particles smaller than 1  $\mu\text{m}$ , as well as the illustration of the particles' shape and morphological characteristics.

At this project, SEM was conducted on an electron microscope (SEM Quanta 200F FEI, Figure 12) at an accelerating voltage of 10 kV and a working distance of 10 mm. Gelatin particles were sputtered with gold coating under vacuum for 90 seconds [43], before their morphology was checked via SEM. Size and diameter of the electrospayed particles were measured by SEM micrographs. [14]



Figure 12. Scanning Electron Microscopy Equipment (Quanta 200F FEI) used for Particle Characterization

## 5. Solubility & Degradation of Gelatin Microparticles

The effect of the cross-linking procedure on particles' solubility was roughly investigated. The progress of their dissolution in aquatic environment was observed optically, compared with plain gelatin particles. For this test, specific amounts (15, 30, 60mg) of electrospayed, cross-linked or plain, gelatin particles were collected and added in ThinCert™ Tissue Culture Inserts (transwell cups) (figure 13.a), on cell 12-well plates ((figure 13.b) filled with 2mL of cell culture medium (aquatic environment). Transwell cups, featuring pores of 1  $\mu\text{m}$  diameter on their walls, were placed above each well, so that cell culture medium could insert in the cup through the pores. In this way, the gelatin particles are gradually immersed in the cell medium and get dissolved through time. Photos of the different samples were taken on specific time points (1 hour, 1, 2, 3, 4, 5 days), once gelatin was mixed with cell culture medium, in order to record their solubility progress along time.

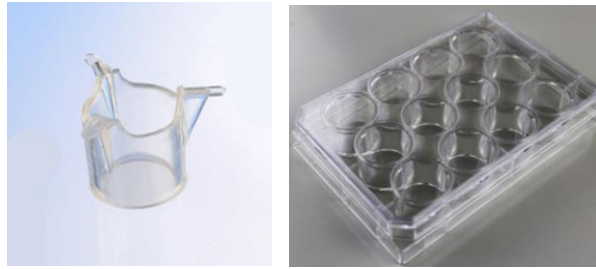


Figure 13. a) ThinCert™ Tissue Culture Inserts b) 12-well plates for cell cultures

## 6. Biocompatibility of Microparticles

The cytotoxic effects of GA, which was included to the gelatin particles, and consequently the particles' biocompatibility was tested on human IVD cells with MTT assay. These cells came from NP tissue of donors that have undergone spinal surgeries for degenerative disc degeneration. MTT is an in vitro colorimetric assay using tetrazolium salt thiazolyl blue. MTT assay has initially a yellowish shade, which turns into insoluble violet-blue formazan crystals, upon its reduction by enzymes and other agents produced by cellular metabolic activity. [61, 70] In general, a specific amount of the tetrazolium MTT compound (3- [4, 5-dimethylthiazol-2-yl]-2, 5-diphenyltetrazolium bromide) is added to the cell well-plates and the cultures are kept in 37 °C for 2-3 hours. Afterwards, DMSO is added to the wells, dissolving the purple formazan crystals in the medium. The upcoming purple solution's absorbance is determined via a spectrophotometer at 570 nm.

After electrospraying, the produced gelatin particles were collected from the aluminum foils, weighted, divided in specific doses (15, 30, 60mg) and kept in glass vials. Respectively, the amounts of GA included in these gelatin doses were 23.44, 46.88, 93.76 µg. Cultures of human intervertebral disc cells were treated with these specific doses of the electrosprayed gelatin microparticles, 15, 30 and 60mg, either plain or crosslinked. The cells were cultured in tissue culture plates. Before treatment, the gelatin particles were sterilized under UV-c irradiation for 3 hours (Figure 15), in order to eliminate any source of infection for the cells. 5 days after treatment, MTT assay was added to determine the cellular metabolic activity. The acquired absorbance values are plotted, in respect to untreated control cells (100%), allowing quantification of changes in cell proliferation and viability. The rate of tetrazolium reduction is proportional to the rate of cell metabolic activity. [61, 70, 71]

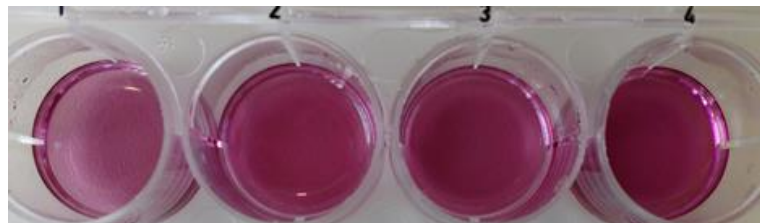


Figure 14. Solution of Formazan Crystals at MTT Assay



Figure 15. Sterilization under UV- Radiation for the Gelatin Microparticles

## 7. Experimental design of the release tests<sup>5</sup>

A set of particular experiments was designed in order to study *in vitro* the ability of the encapsulated EGCG to be released out of the gelatin particles, as well as the activity of the released EGCG. The concept of these experiments was to simulate in a preliminary way the human body environment, where the EGCG – Gelatin microparticles are intended to be placed in IVDs and act against DDD. Therefore, EGCG-gelatin microparticles were mixed with HA-pNIPAM hydrogel and put in tubes at 37 °C, which is the normal body temperature. Upon solidification of HA-pNIPAM at 37 °C, water is supposed to flow through the bulk of HA-pNIPAM, dissolving and releasing the encapsulated EGCG in a controlled manner, compared with free EGCG. 0.9% Sodium Chloride (NaCl) solution (7647-14-5 Fisher chemical) in H<sub>2</sub>O was added as release medium (Figure 16.a). The tubes containing particles and hydrogel were kept for one week at 37 °C, in Eppendorf thermo-mixer (Figure 16.b) with continuous stirring, while the 0.9% NaCl medium was collected and replaced in specific time points (1h, 1, 3, 5, 7d) along that week. Free EGCG mixed with HA-pNIPAM (control 1), free EGCG in water (control 2) and bare HA-pNIPAM (control 3) were used as controls for these experimental sets. Each experiment was performed in duplicates. The collected release

<sup>5</sup> For more details about this experiment and the measurements, see the respective protocols in the Appendix

medium was subjected to absorbance measurements, in order to specify the containing EGCG concentration and its anti-oxidant activity.

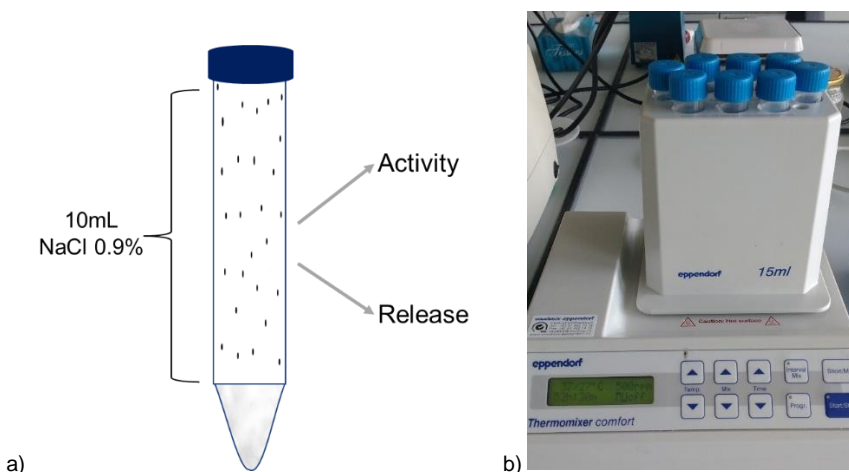


Figure 16. a) Scheme of the release test experimental design. At the bottom of the tube, the solid mixture of HA-pNIPAM and EGCG is placed, while the rest of the tube is filled with 0.9% NaCl solution. EGCG is released from the bottom bulk in the medium and its concentration and activity are measured. b) Eppendorf Thermo-mixer. The *in vitro* release experiments were held there for 1 week in 37 °C with continuous stirring

## 8. EGCG Release (Ferrous Tartrate Method)<sup>6</sup>

The concentration of released EGCG was determined via Ferrous Tartrate assay. This method is colorimetric and is based on reaction between a dyeing solution and the tanning substances that tea catechins, like EGCG, contain [73]. This reaction gives a violet color to the colorless solution. The color intensity is proportional to EGCG concentration [73] (Picture 17).

Ferrous Tartrate solution consists of dyeing solution (ferrous sulfate, potassium sodium tartrate tetrahydrate in distilled water) mixed with potassium phosphate buffer (pH 7.5), 4 ml distilled water and 15 ml buffer (0.067 M potassium phosphate, pH 7.5). Absorbance measurements were made using a spectrophotometer at 540 nm. As an alternative method, and in order to confirm the results, absorbance measurements in UV spectrum (274 nm) were obtained for bare EGCG samples.

## 9. EGCG Activity (DPPH Assay)<sup>6</sup>

Apart from release rates of encapsulated EGCG, the activity of released EGCG was determined, too. For these measurements, DPPH (2,2-diphenyl-1-picrylhydrazyl) radical scavenging method was applied. DPPH assay is the most common method used to detect the antioxidant activity of tea catechins, such as EGCG [73] (Figure 18). Mixture of this assay and the collected EGCG samples was incubated at 25 °C in dark for 60 min. Absorbance at 517 nm was measured using a spectrophotometer, methanol (O2860, Sigma) as negative control and ascorbic acid (A5960, Sigma) as positive control. Antioxidant activity was expressed as percentage inhibition of the DPPH radical and was determined by the following equation [22]:

$$(\%)DPPH = \frac{[Negative\ Control\ Optical\ Density\ (OD) - Sample\ OD]}{Negative\ Control\ Optical\ Density\ (OD)} * 100$$

<sup>6</sup> For more details about this experiment and the measurements, see the respective protocols in the Appendix

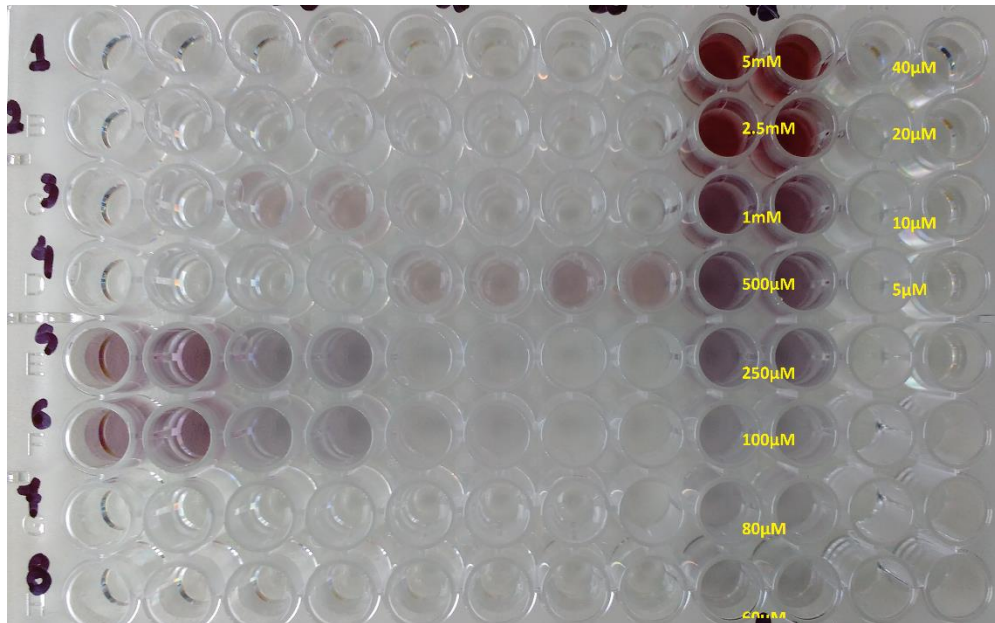


Figure 17 . EGCG Samples reacting with Ferrous Tartrate to Violet-Purple Color. The intensity of the color is proportional to EGCG concentration in each sample

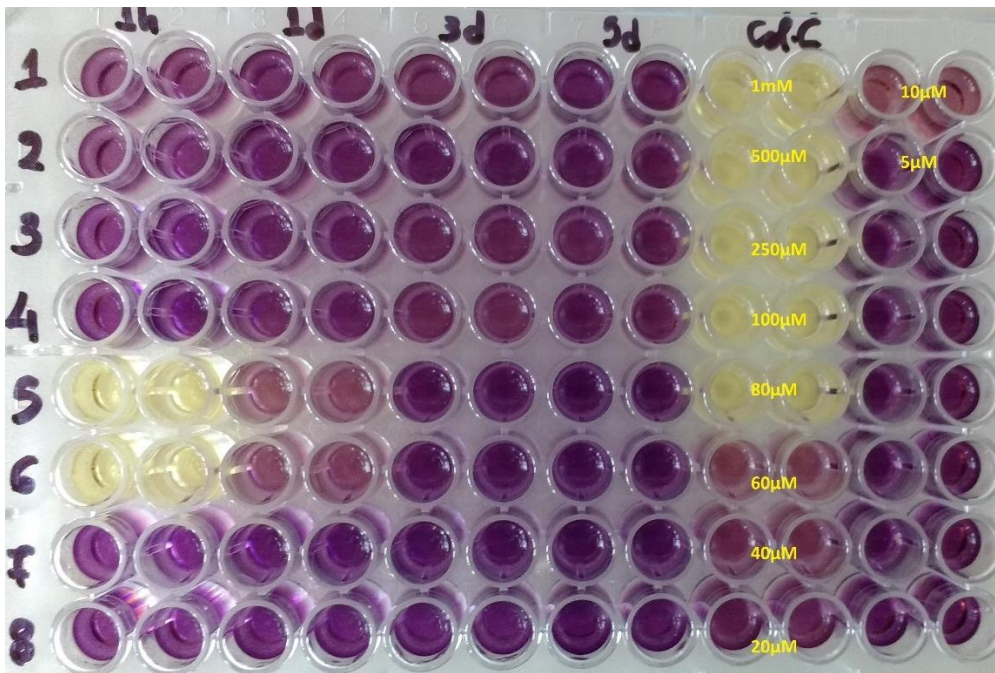


Figure 18. EGCG Samples Reacting with DPPH Assay. The more active the substance is, the less color intensity the sample has.

## 10. Encapsulation Efficiency

The calculation of encapsulation efficiency is an important part of the drug encapsulation procedure and the overall efficiency of the DDS itself. Encapsulation efficiency affects the release rates of the encapsulated compound and thus, the required dose to be administered in the patient. Encapsulation efficiency largely depends upon parameters, such as the method used for particle

formation, the solution pH, as well as the physicochemical properties of the drug. <sup>[18, 37]</sup> Regarding the used method, electrospraying has been indicated as the most effective method regarding encapsulation efficiency, because it provides values ranging between 90-100%. <sup>[5, 11, 19, 26, 33]</sup> Encapsulation efficiency can be tested in several ways according to literature and other research projects. In this project, it was aimed to measure encapsulation efficiency via Ferrous Tartrate assay. An amount of electrosprayed EGCG-Gelatin particles are collected in glass vial, weighted ( $m=0.81\text{mg}$ ) and diluted in acetic acid ( $V=1\text{mL}$ ). Considering that for 1mL of solution and 5mM EGCG concentration, an amount of 42.3mg EGCG-gelatin particles is required. In our case there is a  $95.75\mu\text{M}$  ( $\sim 100\mu\text{M}$ ) EGCG solution. This solution is measured with Ferrous tartrate regarding its EGCG content. As control, EGCG-Gelatin solution of 5mM (solution to be sprayed) is also measured, as well as standard EGCG solutions (calibration curve of 5mM-5 $\mu\text{M}$ ). Then, considering the results and the formula <sup>[19]</sup> below, the encapsulation efficiency will be calculated:

$$EE(\%) = \frac{\text{Actual EGCG Content in the Capsules}}{\text{Theoretical EGCG content in the capsules}} \cdot 100\%$$

## 11. Statistical Analysis of the Results

Statistical analysis was obtained over the results, in order to confirm their validity. Firstly, data's normal distribution was tested by Schapiro-Wilk test. Statistical significance among the groups was evaluated by either by ANOVA test for normal distributed data or by Kruskal-Wallis Test for non-normal distributed data. All results (particle size, MTT test, Ferrous Tartrate, UV, DPPH assay etc.) displayed in graphs, feature average values and standard deviations, while asterisks indicate a significance level of  $p < 0.05$ .



# C. Results

The goal of this project was the synthesis and evaluation of a DDS, that would encapsulate and protect bioactive EGCG via electro spraying method, and delivered through single-injection administration, as a potential treatment of degenerative disc disease. In order to investigate this concept, the individual parts of this DDS were synthesized, combined and evaluated. Electro sprayed EGCG-gelatin microparticles were produced, characterized, combined with HA-pNIPAM and evaluated.

## 1. Synthesis of Gelatin Particles: Optimization and Characterization

The first step for synthesis of the EGCG DDS was the preparation of gelatin particles. The criteria for particle synthesis optimization were the particle shape, their size distribution and the presence of fibers or other structures among the particles. The goal was the production of spherical, uniform and dispersed particles, without fibers among them. A protocol describing the preparation, experimental procedure and production of electro sprayed gelatin particles was established (Appendix, Protocols). The preparation of gelatin solutions and the determination of the operational electro spraying parameters were conducted according to literature [5, 7, 14, 19, 23, 26, 28, 67]. Different gelatin solutions in acetic acid, with or without cross-linking agent, were prepared and sprayed. [19, 28] The cross-linking agent, Glutaraldehyde (GA), was used in concentrations of 37.5 µg/mL, 62.5 µg/mL and 87.5 µg/mL.

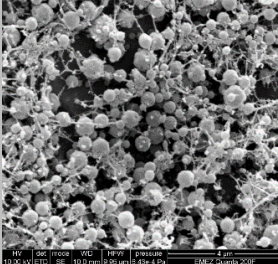
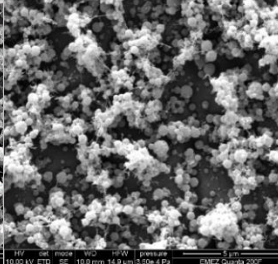
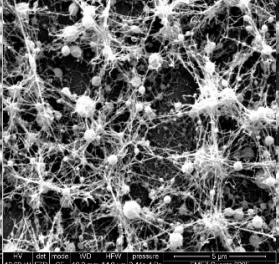
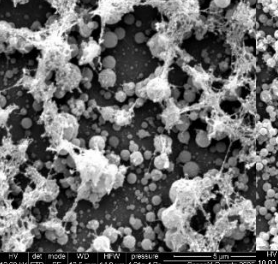
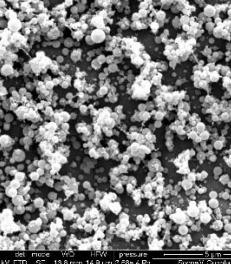
### 1.1. Optimization: Electro spraying of plain gelatin

Plain gelatin was sprayed with flow rates ranging between 2-4 µL/min and a voltage supply 17-22kV. The gelatin solution concentration was 6 or 4%. The aim was to detect the set of experimental parameters that gives the best formed particles. A summary of different experimental settings for these trials is shown in Table 1 and Appendix (Figures 28-32). Each set of conditions gave different morphology of particles. The parameters of 4 µL/min flow rate, 22kV of voltage and 6% gelatin solution, gave a combination of mainly fibers and some beads, while the rest of the parameter combinations gave rather particles, with few sparse fibers among them. The particle size acquired in each case ranged between 470-650nm.

The tests revealed that the best conditions for electro spraying plain gelatin particles were 4µL/min, 21kV, and 4% gelatin concentration (Table 1 and Appendix Figure 34). As shown by SEM, the particles were well-shaped, their size distribution was uniform ( $476.23 \pm 125.05$  nm), with less aggregations and less fibers among the particles, compared to the particles produced under different conditions. The size difference is not statistically significant<sup>7</sup> from the case giving  $474.62 \pm 267.96$ nm of particle size (2µL/min, 17kV, and 6% gelatin concentration), but statistically significant<sup>7</sup> from the case giving  $647.65 \pm 155.36$ nm of particle size (2µL/min, 22kV, and 4% gelatin concentration). More specifically for this case, the gelatin solution concentration was lower than the respective values applied on other trials, while the flow rate and voltage were higher. According to other research studies, it has been indicated [33, 51, 52] that high solution concentrations favor fibrous formations. Indeed, 4% gelatin concentration, instead of 6%, showed an effective decrease of fibrous structures among the beads.

<sup>7</sup> Statistical analysis obtained through Kruskal-Wallis test ( $\alpha=0.05$ ).

Table 1. Summary of different experimental settings for plain gelatin electrospaying

<b>Sol. Concentration (%)</b>	6	4	6	4	6
<b>Flow rate (<math>\mu\text{L}/\text{min}</math>)</b>	2	4	4	2	2
<b>Voltage (kV)</b>	17	21	22	22	20
<b>Distance (cm)</b>	10	10	10	10	10
<b>Particles' shape (SEM)</b>					
<b>Particle Size (nm)</b>	474.62 $\pm$ 267.96	476.23 $\pm$ 125.05	--	647.65 $\pm$ 155.36	--

## 1.2. Optimization: Gelatin Cross-Linking

In order to prevent rapid dissolution of gelatin particles in aqueous environment, glutaraldehyde was used for polymer cross-linking. Our goal regarding cross-linking was to retard gelatin dissolution, without interrupting the particle formation and shape criteria. Cross-linked gelatin solution was sprayed via electrospaying using experimental conditions selected for plain gelatin (flow rate:  $4\mu\text{L}/\text{min}$ , voltage:  $21\text{kV}$  and solution concentration:  $4\%$ ). The respective SEM images of particles cross-linked with either  $37.5$ ,  $62.5$  or  $87.5\ \mu\text{g}/\text{mL}$  of glutaraldehyde, are shown in Table 2. In all cases, the results of the particles have remarkable differences comparing with those of plain gelatin (Table 1), produced with the same experimental conditions. The main difference is the presence of many fibrous structures among beads. For the case of  $37.5\ \mu\text{g}/\text{mL}$  GA cross-link (Table 2), the formed particles appear to be not properly dried before reaching the collector surface. The particles don't have a proper spherical shape, but rather a flattened morphology [67], which refers to droplet appearance, introducing clusters. Consequently, experimental conditions for electrospaying of the cross-linked gelatin required further optimization.

At first, the flow rate of the solution was decreased during electrospaying, in order to investigate its effect on particle formation. The flow rate was set to  $2\mu\text{L}/\text{min}$ , instead of  $4\mu\text{L}/\text{min}$  that was used for plain gelatin. Respective results of the produced particles are shown in Table 3. According to those, an improvement on electrospayed particles morphology was detected, especially for cross-linked gelatin with  $37,5\mu\text{g}/\text{mL}$  of glutaraldehyde, as well as for the cross-linked gelatin with  $62,5\mu\text{g}/\text{mL}$ .

## 1.3. Optimized Electrospaying Parameters

In summary, the most optimal results achieved for both plain and crosslinked gelatin microparticles are represented in Table 4. The best applying experimental setup for electrospaying particles seemed to be that of  $2\ \mu\text{L}/\text{min}$  flow rate,  $20\text{kV}$  voltage,  $4\%$  w/v gelatin concentration and  $37.5\ \mu\text{g}/\text{mL}$  of GA for cross-linking (Table 4). The average particle diameter

for this case was  $669.72 \pm 172.03\text{nm}$ . In order to confirm this indication, more electrospayed samples were prepared ( $n=7$ ) under the aforementioned experimental conditions and observed via SEM. Indeed, under these experimental conditions the produced particles are normally distributed on the substrate (no clumps or aggregations), without fibers and with uniform spherical shape. The size differences among different experimental cases are not statistically significant<sup>7</sup>, therefore it is not certain that different experimental conditions (electrospaying parameters and cross-linking) give particles of different size. Consequently, gelatin particles sprayed under  $2\mu\text{L}/\text{min}$  flow rate,  $20\text{kV}$  voltage and  $4\%$  solution concentration and cross-linked with  $37.5\mu\text{g}/\text{mL}$  GA were used for EGCG encapsulation.

Table 2. SEM images of electrospayed particles (flow rate: $4\mu\text{L}/\text{min}$ , voltage:  $21\text{kV}$  and solution concentration:  $4\%$ ) with different concentrations of GA cross-linker

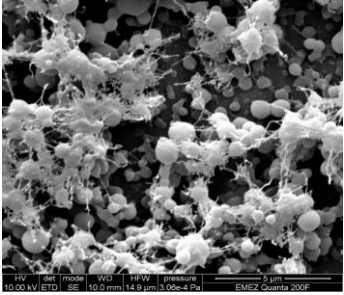
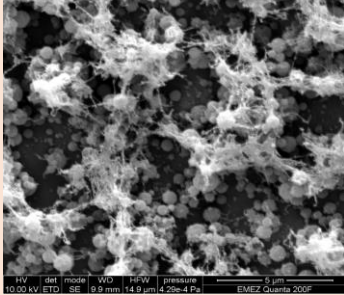
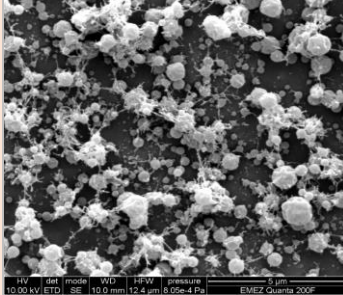
<b>Sol. Concentration (%)</b>	4	4	4
<b>Flow rate (<math>\mu\text{L}/\text{min}</math>)</b>	4	4	4
<b>Voltage (kV)</b>	21	21	21
<b>Distance (cm)</b>	10	10	10
<b>GA concentration (<math>\mu\text{g}/\text{mL}</math>)</b>	37.5	62.5	87.5
<b>Particles' shape (SEM)</b>			

Table 3. SEM images of electrospayed particles (flow rate: 2 μL/min, voltage: 21-22 kV and solution concentration: 4%) with different concentrations of GA cross-linker

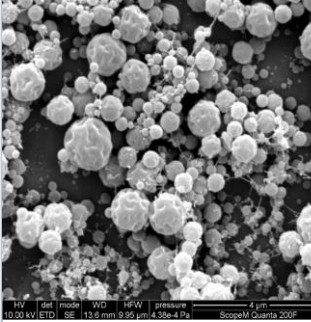
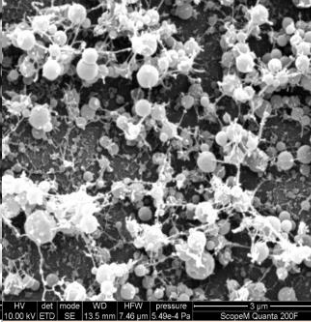
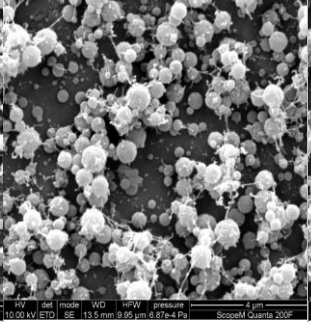
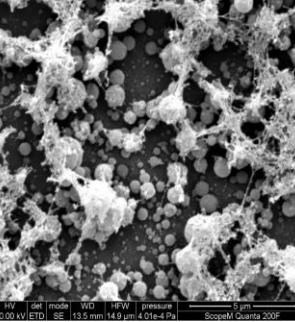
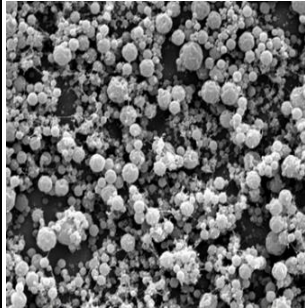
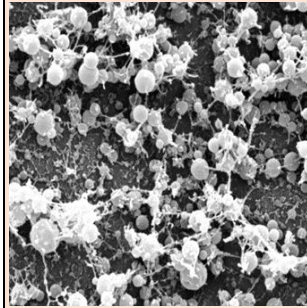
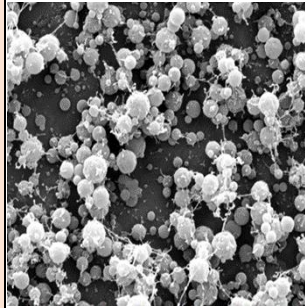
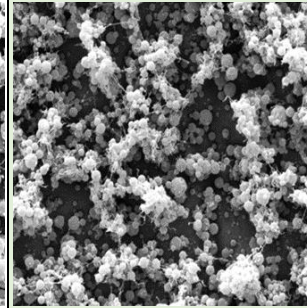
<b>Sol. Concentration (%)</b>	4	4	4	4
<b>Flow rate (μL/min)</b>	2	2	2	2
<b>Voltage (kV)</b>	22	21	21	22
<b>Distance (cm)</b>	10	10	10	10
<b>GA concentration (μg/mL)</b>	37.5	62.5	87.5	0.0
<b>Particles' shape (SEM)</b>				

Table 4. Summary of the optimal achieved gelatin particle production for plain and cross-linked gelatin and the respective experimental conditions

<b>Solution Type</b>	<b>37.5 μg/mL GA</b>	<b>62.5 μg/mL GA</b>	<b>87.5 μg/mL GA</b>	<b>Plain Gelatin</b>
<b>Sol. Concentration (%)</b>	4	4	4	4
<b>Flow rate (μL/min)</b>	2	2	2	4
<b>Voltage (kV)</b>	20	21	21	21
<b>Particles' shape (SEM)</b>				
<b>Particle size (nm)</b>	669.72 ± 172.03	492.38 ± 134.69	606.05 ± 127.58	476.23 ± 125.05

## 2. EGCG Encapsulation in Gelatin Microparticles

### 2.1. Synthesis of Gelatin Particles Containing EGCG

The experimental conditions used for EGCG encapsulation, were finally 2  $\mu\text{L}/\text{min}$  flow rate, 20kV voltage, 37.5  $\mu\text{g}/\text{mL}$  GA and 4% gelatin solution. The presence of EGCG in the polymer solution during electrospaying does not seem to have any effect on particle formation (Figure 19). This result was validated from 17 different electrospayed samples ( $n=17$ ) checked under SEM. The average particle size was  $661.08 \pm 120.98$  nm (Figure 19), which was not significantly<sup>8</sup> different from particles produced without EGCG under the same conditions. Particle-size values are normally distributed ( $n=17$ , Schapiro-Wilk & Kruskal-Wallis Test,  $p<0.05$ ).

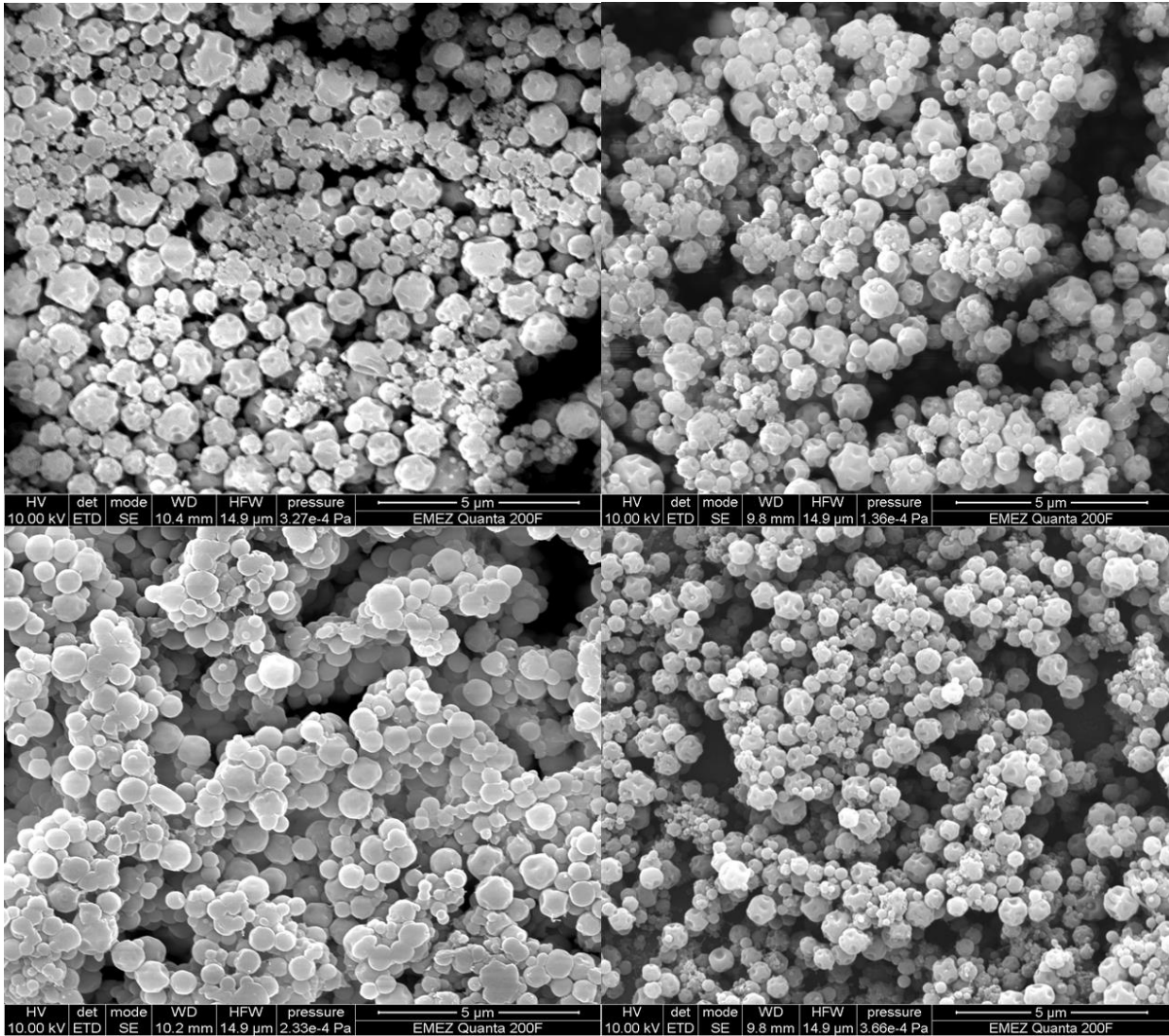


Figure 19. Gelatin Particles containing EGCG (5mM). Electrospayed with flow rate: 2 $\mu\text{L}/\text{min}$ , voltage: 20kV and solution concentration: 4% (SEM) and cross-linked with 37.5 $\mu\text{g}/\text{mL}$  GA. Average Size:  $661.08 \pm 120.98$ nm (Schapiro-Wilk & Kruskal-Wallis Test, statistical significance  $\alpha=0.05$ )

<sup>8</sup> Statistical analysis obtained through unpaired t-test ( $\alpha=0.05$ ).

## 2.2. Encapsulation Efficiency

According to absorbance measurements for encapsulation efficiency of EGCG-Gelatin particles, it seems there are significant deviations between the original concentrations of the solution and the measured ones. The respective values indicated by Ferrous Tartrate assay are represented in detail at the Appendix (Table 5). The respective measurements indicated that there was no EGCG encapsulated in the tested sample (EE=0%), instead of 100µM that was estimated. Also, control EGCG-Gel solution (5mM) measured with Ferrous Tartrate too, indicated concentration 1mM.

Obviously, a fault has occurred with the implementation procedure. Firstly, a possible cause could be that Ferrous Tartrate could have been inactivated, because it had been prepared several weeks before. In case Ferrous Tartrate assay is considered active and works properly, there must be a fault regarding the measured solutions. EGCG-Gelatin particles had been sprayed one month before the experiment and kept in fridge (4 °C). Therefore, there is a case of EGCG degradation, although it is encapsulated. If EGCG was degraded, it wouldn't react with the Ferrous Tartrate assay. Another explanation could be that EGCG-gelatin particles hadn't got dissolved in the medium once the assay was applied. Therefore, encapsulated EGCG was not released before measuring it with Ferrous Tartrate. The same case of degradation due to storage conditions, stands for the control EGCG-Gelatin solution (5mM of EGCG in 4% Gelatin solution), too. The solution was stored in fridge for more than two weeks and thus, EGCG could be degraded.

Encapsulation efficiency largely depends upon the method used for drug encapsulation, on the solution pH, as well as physicochemical properties of the drug. [18, 23] Regarding the applied encapsulation method, electrospraying seems to be the most effective method considering the encapsulation rates, because it provides values ranging between 90-100%. [14, 19, 21] Other encapsulation methods, provide encapsulation efficiency rates lower than 80%. [9] Therefore, EE must be tested again in further research on the project.

## 3. Solubility & Degradation of Gelatin Particles

Plain observations of gelatin dissolution suggest a different solubility progress between cross-linked and uncross-linked gelatin samples during the first 24 hours. The viscosity and gelation of three different samples (n=3) of both cross-linked and plain gelatin particles were roughly tested by incubation and stirring. The samples of cross-linked gelatin particles immersed in cell culture medium were jelly and viscous even 24 hours after dispersion, in comparison with the samples of plain gelatin, which seemed to be completely dissolved after 2 hours (Figures 20 and 21).

## 4. Biocompatibility of Gelatin Particles (MTT Assay)

As EGCG encapsulation in electrosprayed gelatin particles was successful, evaluation of the designed DDS had then to take place. Firstly, biocompatibility of gelatin particles was tested in IVD cell cultures (n=5). As gelatin was cross-linked with GA, which is cytotoxic, it was necessary to determine its effect on cells. More specifically, toxicity of GA in concentration of 62.5 µg/mL included in gelatin particles was tested. The revealed cell viability is represented in Figure 22, in terms of % metabolic activity of cells. The cells metabolic activity is reflected through absorbance by produced formazan crystals (MTT assay).

MTT results showed that cell viability may decrease with increasing gelatin dosage and concentration of glutaraldehyde. Nevertheless, the main decrease in cell viability was very modest and results were not significant (Figure 22). For plain gelatin, cells treated with a 15mg dosage of particles, indicated viability of  $105.53 \pm 5.8\%$ , meaning slightly higher viability than untreated cells (control 100%), while cells treated with 30mg of plain gelatin indicated  $98.3 \pm 38.6\%$ . Cells treated with cross-linked gelatin particles displayed lower viability rates. For dosage of 15mg ( $23.44\mu\text{g}$  GA), viability rate was  $87.8 \pm 23.76\%$  compared to viability of untreated cells (100%), while the respective rate for cells treated with 30mg of cross-linked gelatin ( $46.88\mu\text{g}$  GA) was  $83.32 \pm 15.07\%$ . Finally, cells treated with 60mg of cross-linked gelatin particles ( $93.76\mu\text{g}$  GA) indicated an  $82.44 \pm 35.69\%$  viability rate. For this test, data normality was tested via Schapiro-Wilk test ( $p < 0.05$ ), while statistical significance among groups was evaluated with Kruskal-Wallis test, with  $\alpha = 0.05$ .

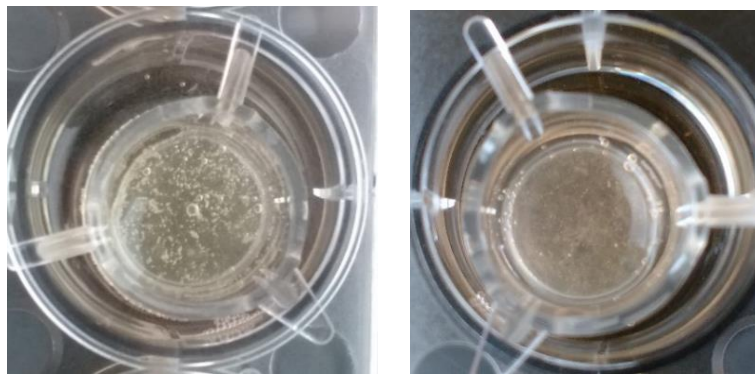


Figure 20. Solubility of Gelatin Particles, Cross-Linked (left) and Uncross-Linked (right), 2 hours after Mixture

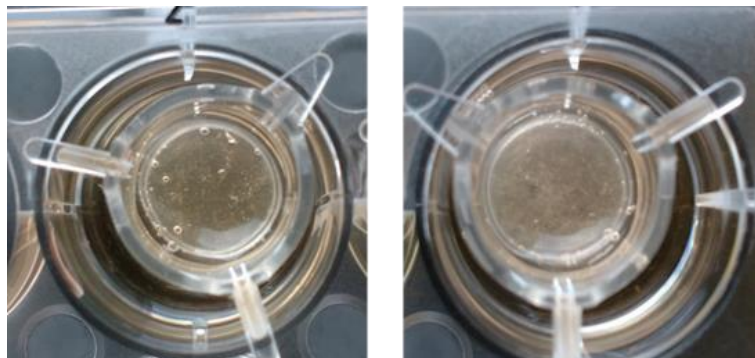


Figure 21. Solubility of Gelatin Particles, Cross-Linked (left) and Uncross-Linked (right), 24 hours after Mixture

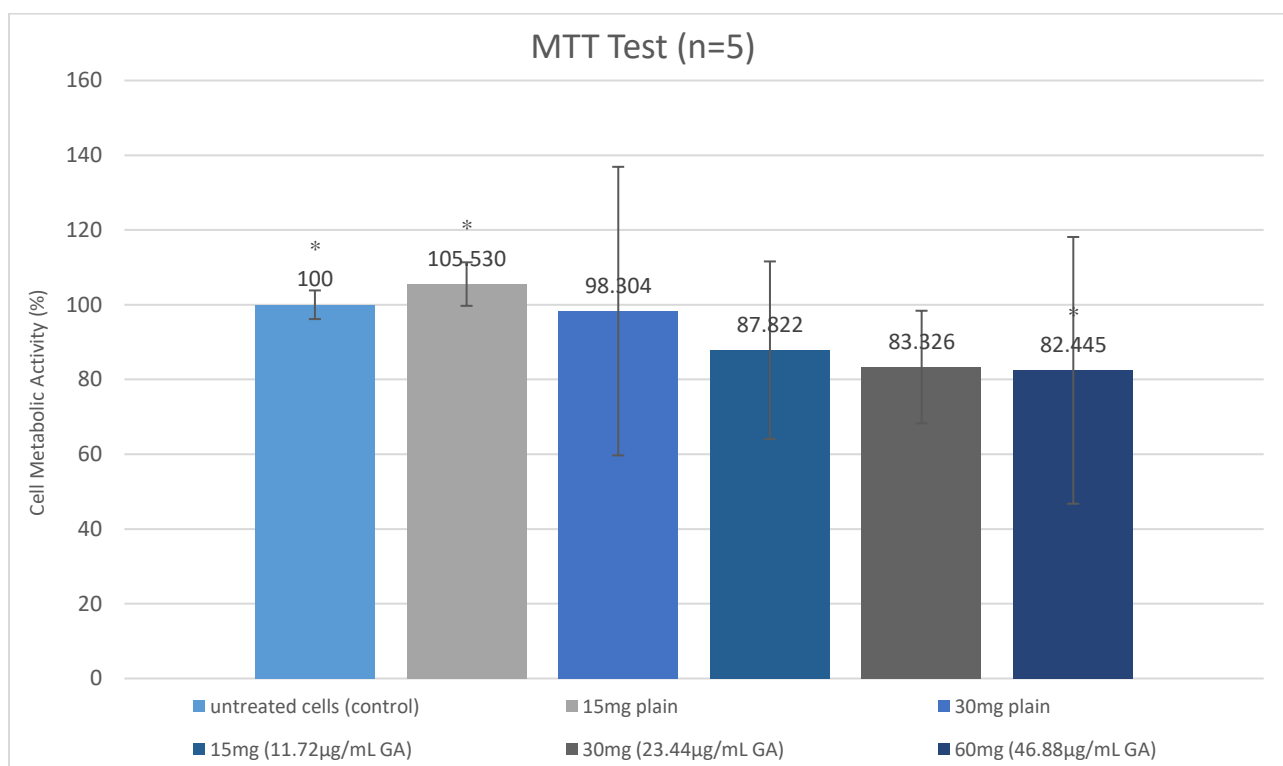


Figure 22. Biocompatibility Test of the Cross-Linked Gelatin Particles (62.5µg/ml GA) in Comparison with Plain Gelatin and Untreated Cells. All the data were checked for normality and groups with asterisk indicated statistical significance at  $p < 0.05$  through Kruskal-Wallis Test

## 5. EGCG Release Rates

Three ( $n=3$ ) independent release experiments were performed under the same conditions. The results are represented in consolidating graphs. Concentration of EGCG was measured using Ferrous Tartrate method and calculated using calibration curves. EGCG release along time is shown in Figure 23 and % cumulative concentration of released EGCG is shown in Figure 24. The remaining EGCG entrapped in HA-pNIPAM by the end of the experiments, is shown in Figure 25 for all samples.

Due to significant standard deviations among experiments, no firm conclusion about the pattern of EGCG release can be made. Trends indicate that release rates of encapsulated EGCG come up to 0.15mM, while both free EGCG with or without hydrogel addition (Control1, Control2) indicate 0.5mM release rates (Figure 22). The % cumulative release rates graph (Figure 24) indicates that encapsulated EGCG is released in a percentage of almost 100% (94.7%), by the end of the experiment ( $t=7d$ ). To the contrary, the total released concentration of EGCG, for Control1 and Control 2 are 124.6% and 122.6% ( $>100\%$ ), respectively. Additionally, the graph of gel residuals (Figure 25) indicated that less than 1.2mM of encapsulated EGCG was released in the 0.9% NaCl medium and more than 3mM of free EGCG was released from Control1 samples. The absorbance values of bare HA-pNIPAM (Control3) were subtracted, in order to have the original values of EGCG absorbance. However, release rate graph (Figure 23) and gel residuals graph (Figure 25) do not



confirm each other. As an alternative method, measurements of UV spectrum were obtained and the respective results are represented in Appendix (Figures 76-78).

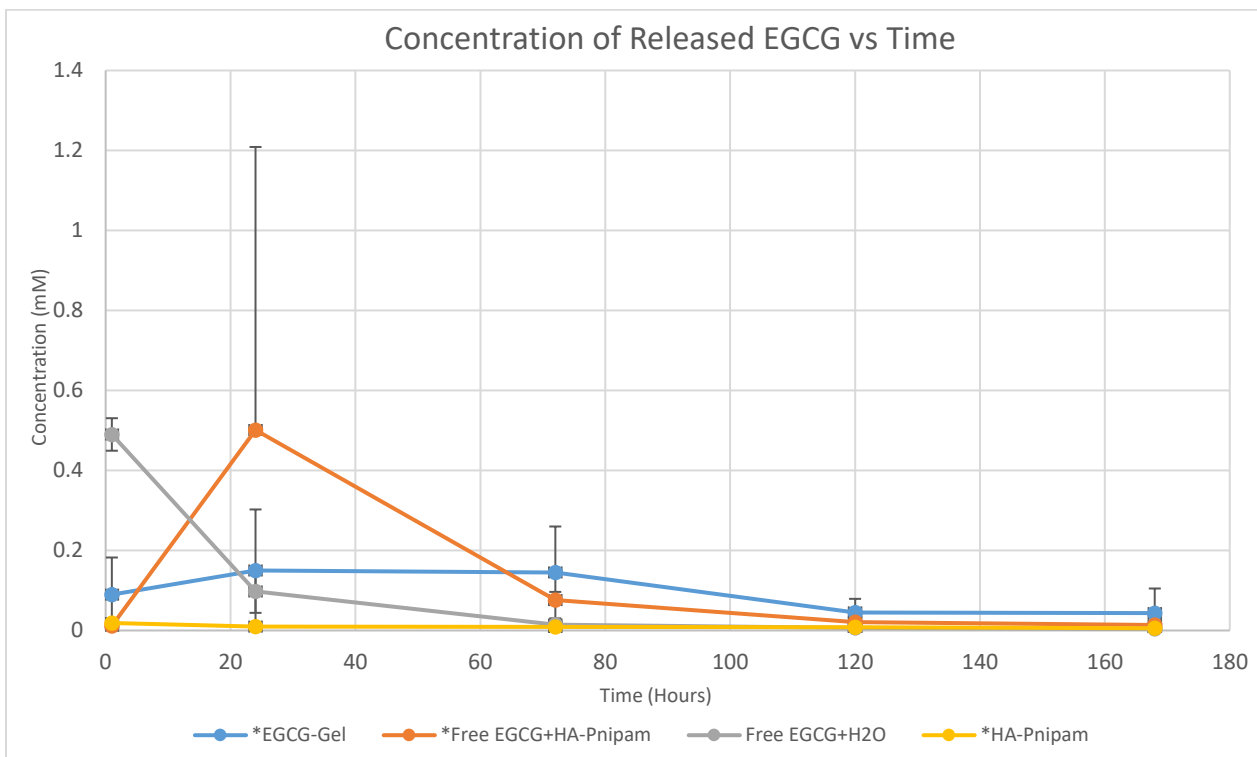


Figure 23. Concentration of Released EGCG in the medium of NaCl 0.9%, Along Time. The respective images of the remaining gels after 1 week of experiment duration. Statistical analysis with Kruskal-Wallis test ( $p=0.1$ ,  $n=3$ ) (Overall Results)

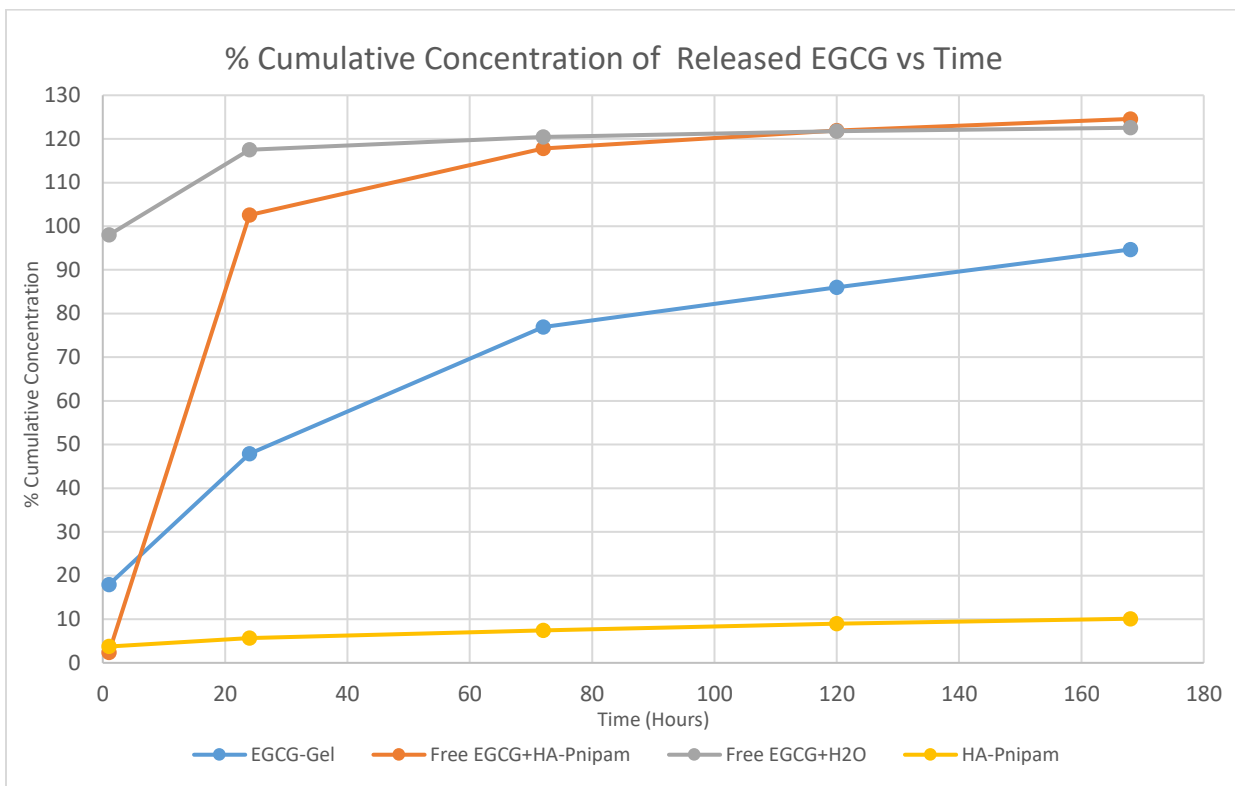


Figure 24. % Cumulative EGCG Release Rates in 0.9% NaCl medium Along Time. The % rates have been estimated in respect of the 0.45mM amount of concentration which is the maximum amount of EGCG that can be released in each sample, as the concentration of EGCG before the addition of 10mL release medium was 5mM. (Overall Results, n=3)

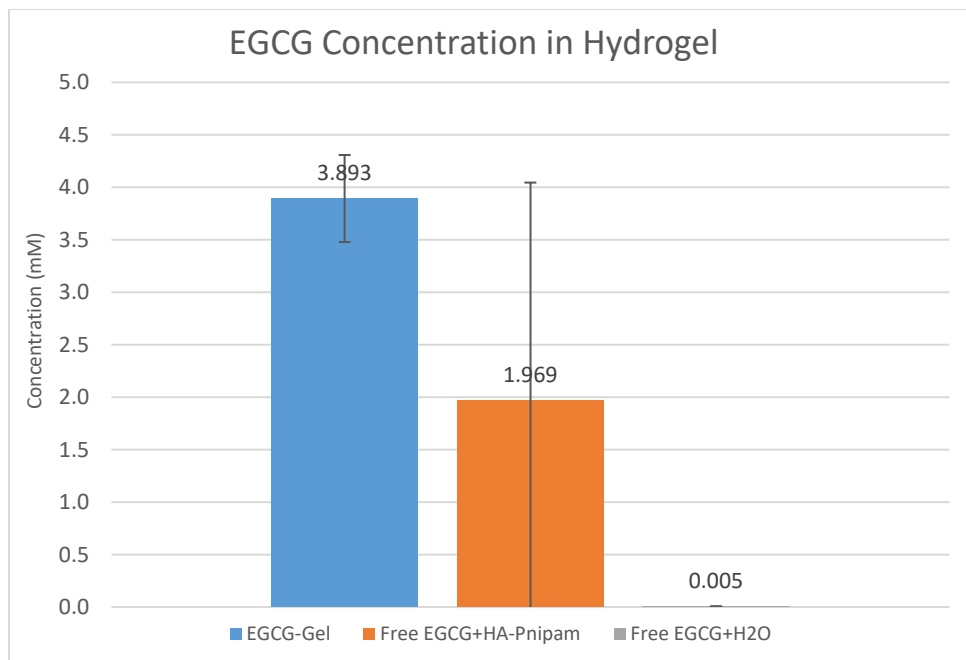


Figure 25. EGCG Concentration Entrapped in Hydrogel by the End of the Experiment. (Overall Results) Statistical analysis with Kruskal-Wallis test ( $p=0.1$ ,  $n=3$ )

## 6. Activity of Released EGCG

In parallel with absorbance measurements of EGCG release, activity measurements of the released EGCG took place, using DPPH Assay. Following the same concept as in release section, activity results are represented in consolidating graphs of normalized and percentage values along time.

EGCG activity was calculated in respect to blank DPPH solution in ethanol (negative control). The results, represented as % Activity in respect of time (graph 25), demonstrated that encapsulated EGCG features limited activity (14%), in comparison with free EGCG mixed with hydrogel (Control1, 30.9%) and free EGCG in water (Control2, 91.4%). All of them decrease gradually towards zero by the end of the experiment, though. However, these activity values are directly related with the respective concentration values of released EGCG. Therefore, the graph of normalized activity in respect of concentration represents a clearer interpretation of EGCG activity (graph 26). Indeed, in this graph the profiles of EGCG activity for encapsulated and free EGCG mixed with HA-pNIPAM seem to strongly coincide.

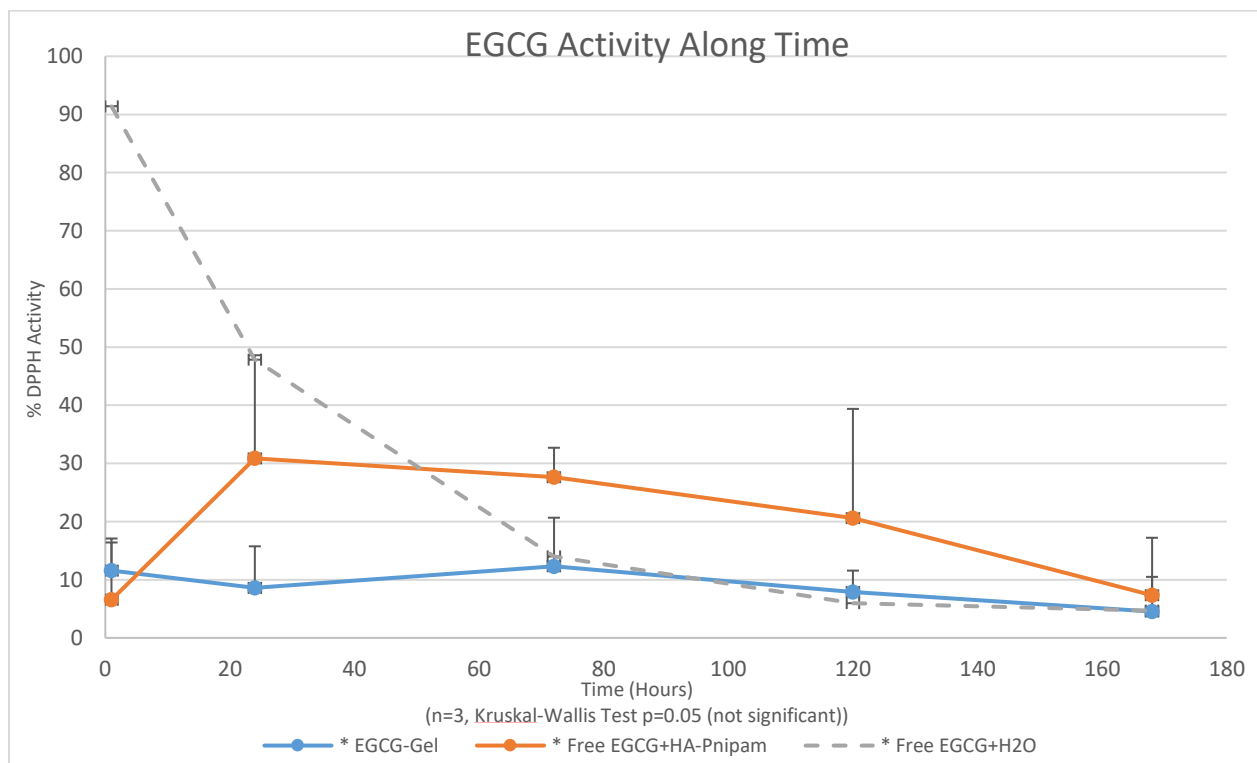


Figure 26. % Activity of Released EGCG as a Function of Time. The respective values of HA-pNIPAM control have been subtracted, to have the original activity of EGCG for Each sample. The calibration curve of L-Ascorbic Acid (Positive Control) has been added as legend on the graph (Consolidating Figure). Statistical analysis with Kruskal-Wallis test ( $p=0.05$ ,  $n=12$ )

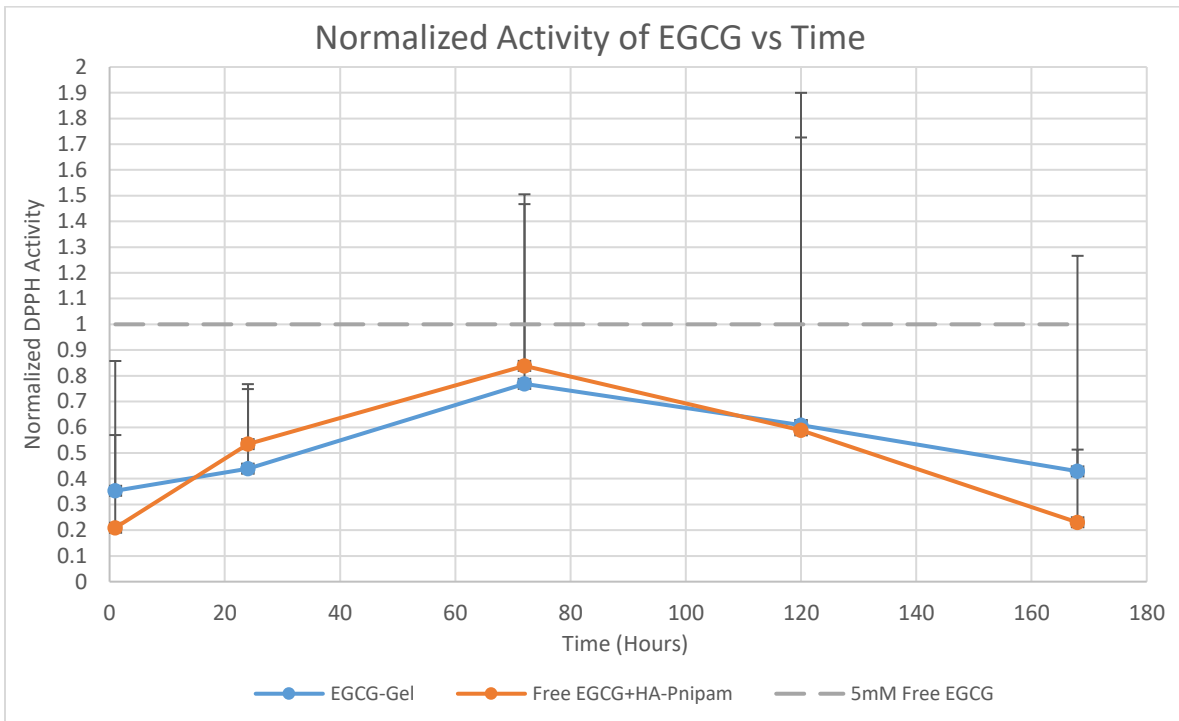


Figure 27. % Activity of Released EGCG as a Function of Time. The normalization has been obtained in respect of concentration. By this, activity profiles of each sample have a different shape (Consolidating Figure).

# D. Discussion

## 1. Synthesis of EGCG Drug Delivery System

The purpose of this project was the synthesis and evaluation of a DSS for EGCG administration against DDD. EGCG had to be encapsulated, control its release and retain its activity. Essentials for this, was the effective creation of gelatin microparticles via electrospraying, the ability of these particles to protect EGCG from burst release and degradation, as well as the effective use of HA-pNIPAM as a supportive carrier of the particles for future injections into degenerative intervertebral discs. Therefore, a protocol for preparation and formation of gelatin microparticles via electrospraying was edited. Those particles were tested for their morphological characteristics, solubility and cytotoxicity. The next step was to incorporate EGCG into gelatin particles and combine the EGCG-Gelatin particles with HA-pNIPAM. Finally, tests of EGCG release rates (Ferrous-Tartrate Assay) and activity (DPPH assay) *in vitro* took place.

During this project, synthesis of gelatin microparticles with proper specifications was the first step to start with the designed DDS creation and was achieved via electrospraying and operational parameters of 2  $\mu\text{L}/\text{min}$  flow rate, 20 kV voltage supply, 37.5  $\mu\text{g}/\text{mL}$  GA for chemical cross-linking of gelatin and 4% gelatin solution. The diameter of the resulting particles was  $661.081 \pm 120.979$  nm. Although the particles' biocompatibility seems admissible, indicating minimum 83% cell metabolic activity, this still must be confirmed with further trials and tests. EGCG encapsulation seems to reduce its release up to 50% of the initial concentration at the first 24 hours, while its activity seems unaffected. However, experiments regarding release and activity of encapsulated EGCG require further optimization.

The first step of this commitment was to determine the most suitable electrospraying operational set of parameters for particle formation. More specifically, some trials obtained for optimal electrospraying parameters determination, revealed broad fiber formation. It has been shown that both electrospinning (fibers) and electrospraying (particles) are based on the same principles and apparatus. However, the critical point of producing fibers or particles depends on the experimental conditions used, especially on polymer solution concentration and then, on voltage and flow rate. [33, 51, 52] An increase in polymer concentration leads to higher viscoelastic forces and thus, to fiber formation. Another factor that could increase the viscoelastic forces is gelatin cross-linking, because gelatin polymer chains get bonded together and change the solution's viscoelastic properties. In our case fiber formation is unfavorable, as the presence of fibers can interrupt the particles' injectability. Fibrous structures in a solution can increase the mixture viscoelasticity and thus the surface tension. [33, 36, 51, 52] A solution with an increased tension and viscosity would require an injection needle with wider diameter. Therefore, we aimed for the set of experimental parameters that would produce spherical particles, without any fibers among them.

The first electrospraying trials of plain gelatin particles indicated that 4  $\mu\text{L}/\text{min}$  flow rate, 21kV voltage and 4%w/v gelatin concentration, are the optimal conditions for particle formation. However, once these conditions were applied for cross-linked gelatin, results were significantly different. With further experiments and trials, it was concluded that the best electrospraying parameters for cross-linked gelatin are 2  $\mu\text{L}/\text{min}$  flow rate, 20kV voltage, 4%w/v gelatin concentration and 37.5  $\mu\text{g}/\text{mL}$  GA.

The formed particles produced by these conditions had an average size of  $669.72 \pm 172.03\text{nm}$ , spherical, dispersed without any fibers among them. Consequently, they were considered appealing for EGCG encapsulation.

The size range of the formatted particles lies between 480-670nm, along with the different electro spraying parameters that were applied. According to statistical analysis that was applied for the particle size in each case, the data were normally distributed in the majority of the trials. This normality stands for the optimal experimental sets selected for plain and cross-linked gelatin particles. Regarding EGCG encapsulation, the selected parameters gave particles with an average size of  $669.72 \pm 172.03\text{nm}$ , despite the size of plain gelatin particles,  $476.23 \pm 125.05\text{nm}$ . However, the bigger the particles would be, the better for our purpose, as the decreased surface to volume ratio would reduce further the release and bioavailability of EGCG. Nevertheless, the attained size of EGCG-gelatin particles,  $661.08 \pm 120.98\text{nm}$ , may fulfil our expectations. Comparing the diameters of the resulting particles for each different experimental electro spraying case through statistical analysis, it seems that in most cases the particle size is not statistically different from the others. In the future, it would be useful to investigate the influence of the electro spraying conditions on the particle size. However, it is known from literature that bigger voltage input during electro spraying leads to smaller particles dimaters. [23, 33, 79]

Drug-encapsulation efficiency is another property of the designed DDS, that its role is important. Generally, it is on the interest of the producer, the encapsulation efficiency to be as high as possible, so that as much pharmaceutical compound as possible to be encapsulated in the carrier. Encapsulation efficiency control means control of release rates of the encapsulated compound. Additionally, through high encapsulation efficiency, smaller amount of particles can be used for the same drug dosage, which also contributes to energy and cost saving. In this project, encapsulation efficiency was not determined successfully (Appendix, Table 5). Most probably, this was due to experimental defect and has to be repeated in future research.

The pH of gelatin solution is considered an important aspect of the designed DDS. According to literature, pH seems to have a strong impact on the electro spraying performance, on particles' formation, the encapsulation efficiency etc. [67] Another aspect that pH seems to influence is the mechanism of the reaction between gelatin and glutaraldehyde and the cross-linking procedure. [57, 62, 68] pH seems to influence also the metabolic activity of cells, either in a direct or indirect way, through its effect on contained GA.

Glutaraldehyde is a common used cross-linking agent, due to the efficiency that it provides and its low cost. Thus, it is widely used in order to react with polymers and create bonds among the polymer chains. [68] It has been found that bonding strength due to glutaraldehyde cross-linking increased up to 5 times. [62] Also, the polymer's bonding strength seems to increase with increasing aldehyde content. A low solution pH can increase the number of protonated groups and thus, the possibility of cross-linking reactions is significantly reduced. Otherwise, cross-linking reactions may follow different reaction mechanisms (Figure 29). [68]

Actually, there is no commonly accepted explanation about the main reactive species that participates in the crosslinking process. [59] According to literature, low pH may result in reduced cross-linking reactions or cross-linking reactions may follow different reaction mechanisms. A decrease in pH leads to an increase of positively charged amino groups, which are unavailable for

crosslinking reaction with glutaraldehyde. [59, 68] On the other hand, neutral to slightly alkaline pH values (sub-acid conditions) are more favorable for gelatin crosslinking. [59] Furthermore, according to chemical rules of redox reactions, aldehydes can be oxidized to carboxylic acid in acetic environment ( $[H^+]$ ), under oxygen presence, while in alkaline conditions aldehydes can be reduced to carboxylic salts. Also, by water addition to reaction with aldehydes, alcohols come out (Figure 28).

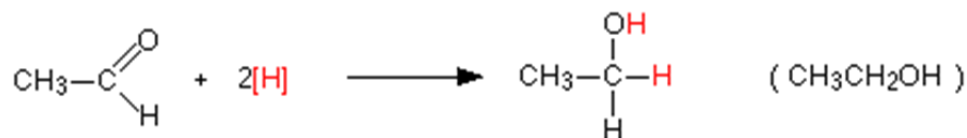


Figure 28. Oxidization of Aldehyde to Carboxylic Acid

In our case, glutaraldehyde acts under acidic acid (Figure 28-30). More specifically, the pH of different gelatin solutions in acetic acid (4% w/v gelatin in 20%v/v acetic acid) was calculated, as well as the pH value of 20%v/v acetic acid itself, both theoretically and experimentally. The results showed that pH of gelatin solutions lies around 2.26, while the solvent of 20%v/v acetic acid has an experimental pH value of 1.47 and a theoretical one of 2.18. Therefore, partial oxidization of glutaraldehyde may be possible, while mixed with the gelatin solution. This results to partial inactivation of glutaraldehyde or limited efficiency of cross-linking reaction. Therefore, cross-linking is not very effective. A reliable way to check the extent and the results of gelatin cross-linking is conduction of FTIR measurements. [28]

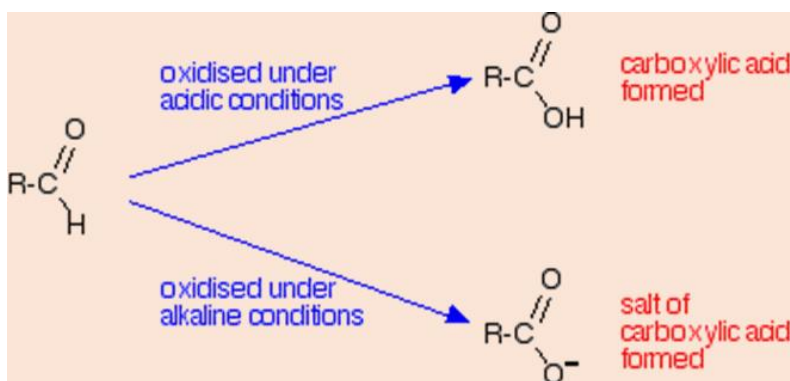


Figure 29. Individual Reactions of an Aldehyde Under Acidic or Alkaline Conditions

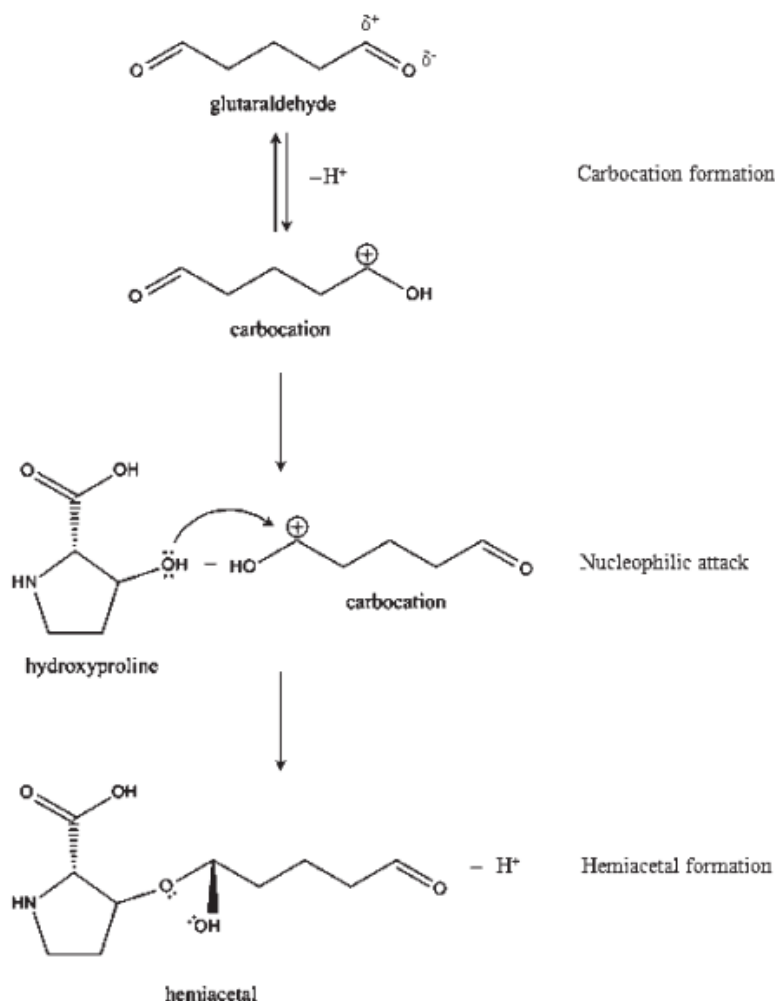


Figure 30. Possible mechanism of the cross-linking reaction between gelatin and glutaraldehyde at acidic pH values. [68]

In order to investigate the extent of the cross-linking reaction between gelatin and GA, it was considered important to check the solubility of the gelatin particles. Along with biocompatibility testing then, optical observations on the solubility of the gelatin microparticles took place. In recent study, gelatin membranes cross-linked with GA and produced via electrospinning, were tested for their biodegradability. [28] Those membranes were embedded to simulated body fluid (SBF) up to 24 hours and the swelling behavior and biodegradability of the membranes were assessed. [28] According to that, a similar way was used for the solubility testing of our gelatin particles (Appendix). In other studies, Fourier Transform Infrared Spectroscopy (FT-IR) analysis, in combination with residual amino group determination, was used to investigate the chemical functional groups involved in the cross-linking reaction between glutaraldehyde and gelatin molecules and the progress of it. [68] Therefore, FTIR spectrometry or Hyp-test can be used in our project to calculate the degradability rates of cross-linked gelatin, compared to plain gelatin.

However, quantitative testing should be applied, to determine gelatin degradability. In the future, the solubility of gelatin will be quantified by other methods, like collagen-concentration



measurements or Hyp-test. This test measures the hydroxylproline (Hyp) levels in a solution. [75] Hyp is a major component of collagen and hence, of gelatin, and its concentration is used as an index for collagen or gelatin concentration. An alternative method would be the detection of gelatin degradability through enzymatic reaction (e.g. proteinase N). [76]

## 2. Evaluation of the EGCG Drug Delivery System

Except of gelatin solubility, the effect of GA on cells was studied through biocompatibility tests. Results indicated that cell metabolic activity ranged to almost normal levels, 82.5-88%, for samples including GA. Other research studies showed that maximum non-toxic GA concentration for fibroblasts tested *in vitro* is 3.4  $\mu\text{L}/\text{mL}$  (63.76 $\mu\text{g}/\text{mL}$ ). [50] More specifically, different concentrations of GA solutions in Dulbecco's Modified Eagle's medium (DMEM) was added in fibroblast cultures and the cell viability was tested via MTT for different time durations. [50] In another method, the GA toxicity levels in aquatic organisms was tested, indicating 73.8 mg/L minimum toxic concentration. [48] Compared to these studies [48-50], the amounts of GA used in this current project were lower, 11.72 – 46.88 $\mu\text{g}/\text{mL}$ . Therefore, cells were likely to indicate normal metabolic activity.

In fact, MTT assay indicated moderate decrease of the cell viability (82.5-88%), in comparison with the control cells (Figure 22). However, more repetitions of biocompatibility tests are recommended to be conducted in future work, because the collected data are not statistically significant and some of the samples displayed high standard deviations. MTT results indicated reduced metabolic activity by the cells treated with 30mg of plain gelatin, in some repetitions. A potential explanation for this, can be possible residuals of acetic acid on the gelatin particles. As gelatin solution before electrospraying were measured to have very low pH (i.e. 2.26) consequently, gelatin particles would have a low pH, too. This can have a significant effect on cell viability. Low pH of particles can also be a reason for the high standard deviations of 30mg plain gelatin samples and 60mg of cross-linked gelatin. Microscope photos (Appendix Figure 43) illustrating the cells during these tests (5 days), confirmed the results of the MTT assay. Therefore, further investigation on cell viability should be obtained, as it is not clearly specified what is the effect of both GA and low particle pH on cells viability, as well as on DDS efficiency. More plain-gelatin-treated samples should be tested and more different doses, as there were less samples of plain gelatin than samples with cross-linked gelatin during the obtained tests and also, there was smaller variability of doses for plain gelatin (15 and 30mg).

Once gelatin particles had been designed, produced and tested properly, EGCG encapsulation and the respective testing of the whole DDS for release and activity rates followed. Research studies have indicated that the beneficially effective, but non-toxic concentration of EGCG *in vitro* ranges between 1-100 $\mu\text{M}$ . Therefore, our aim was to restrict EGCG release via encapsulation and synthesize a DDS that provides an EGCG dose ranging between 1-100 $\mu\text{M}$ , as well as ensure a prolonged deliverance in the suffering tissue for a week or more.

Generally, release takes place mainly via diffusion. Diffusion is a phenomenon, where particles or molecules tend to move from a region of high concentration to a region of low one, either in solid, liquid or gas phase. Usually, the diffusion velocity in each case depends on parameters, such as temperature, initial concentration of the compound, pH, ambient polarity and the medium's properties. [8, 51] More specifically, in case of drug delivery systems, significant role in the diffusion process also play the drug solubility, the physicochemical properties of the carrying material (i.e.

HA-pNIPAM, gelatin), the surface-to-volume ratio of the particles, particle size and morphology, as well as the particles' extent of cross-linking. [18, 51]

EGCG release from biodegradable gelatin particles and HA-pNIPAM structure occurs through a combination of mechanisms. The predominant mechanisms of diffusion in our case of EGCG release are considered, (1) desorption of drug from the surface layer of the particle and (2) drug diffusion through the polymeric matrix and (3) release due to erosion or degradation of the polymer particles. [18, 51] More specifically, water flows through HA-pNIPAM's bulk, where EGCG-gelatin microparticles are entrapped. The microparticles come in touch with the water, swell and start dissolving. Hence, EGCG is released out of gelatin and then out of HA-pNIPAM into the 0.9% NaCl solution. During diffusion, desorption of drug absorbed on the particle's surface leads to burst release, which comes first. After that, the compound which is entrapped in the bulk of the particle is released in a slow and prolonged manner, till it is depleted. [79] Accordingly, in our experiments EGCG release rates indicate a peak at the first 24 hours and then decrease gradually for the rest 4-5 days to zero.

Results obtained by Ferrous Tartrate (and UV spectrum in appendix) and DPPH assays show that these experiments need further optimization. An evidence for this claim can be the significant differences at the results among identical repetitions of the conducted experiment. The main reason for high standard deviations between the individual repetitions can be the fact that the gel collapsed in most of the tested samples (Figure 31). More specifically, in most of the tested samples the hydrogel bulk was partially or completely collapsing and dissolving in the release medium. Therefore, the samples tested via DPPH and Ferrous Tartrate assays included diluted HA-pNIPAM, except of released EGCG. This phenomenon was probably caused by low stability and water resistance of HA-pNIPAM hydrogel, due to poor mechanical properties of the material itself.

HA-pNIPAM is a thermoreversible copolymer synthesized for cell and drug encapsulation. [39, 40] According to recent studies, HA-pNIPAM had been tested *in vitro* and *ex vivo*, as a carrier of human stem cells or NP cells. [9, 77, 78] Although HA-pNIPAM was designed and synthesized to promote cell facilitation, proliferation, differentiation and activity, to be thermoreversible, injectable in disc tissue (22-G needle), with reversible gelling and cytocompatible by-products, its mechanical properties in 37 °C were not sufficient enough. [9, 39, 40, 77, 78] More specifically, in both cases of *in vitro* and *ex vivo* tests the hydrogel indicated poor mechanical stability and loss of its structural cohesion after some time in cell culture or in organ culture model environments. [9, 39, 77, 78] The same type of copolymer was used in all those studies, meaning Hyaluronan (HA) 25% cross-linked with pNIPAM of 20kDa molecular weight. [9, 39, 77, 78] The HA-pNIPAM solution concentration was ranging between 10 or 12% w/v in PBS and 1% w/v in one case. [9, 39, 77, 78] The same defect about HA-pNIPAM mechanical stability is confirmed by our experiments, too. In our experiments, mechanical stability of the material bulk is probably not affected by non-uniform distribution of the mixed material, EGCG-gelatin microparticles or free EGCG, as gel collapsed also in bare HA-pNIPAM (Control3) samples. Gel collapsing and dilution in the release medium lead to rapid release of free EGCG or EGCG-gelatin microparticles.

Activity measurements indicated that EGCG remains active, regardless the encapsulation or not. This reveals that EGCG activity is neither compromised by electrospray processing, nor improved by encapsulation. This indicates that electrospraying may be a good choice for EGCG

encapsulation, however there is still no proof for it. This also suggests that probably EGCG activity is not sustained or enhanced through encapsulation, as it remains the same as that of free EGCG. Another reason that encapsulated EGCG might indicated the same activity as free EGCG in the same conditions, can be the storage conditions of encapsulated EGCG before testing. Encapsulated EGCG was kept in room temperature several hours after electrospinning and then in 4 °C till testing. Also, electrospinning procedure for each sample lasted more than 2 hours and considering that more than 3 samples were produced every day from the same EGCG-gelatin solution, this means that free EGCG was also exposed in room temperature for several hours.

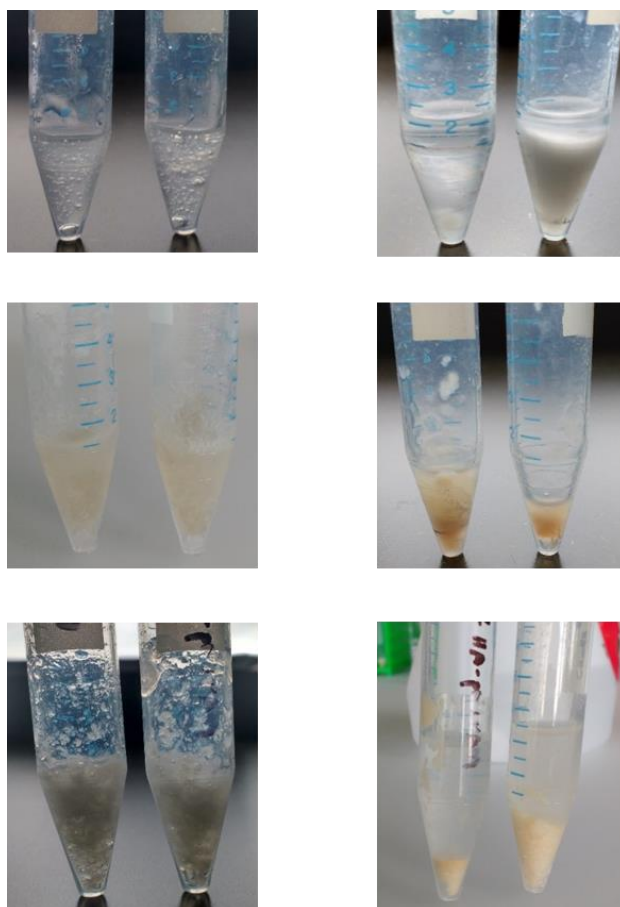


Figure 31. Photographs of HA-pNIPAM samples during DDS evaluation, depicting the hydrogel collapsing during the experiments. The left column represents the gel, either containing EGCG or not, before the release and activity experiments. The right column has the images of the same samples at the end of these experiments. Gel collapsing is obvious in most of them.

On the other hand, the activity of a biomolecule is related to its release rates. [79] Release rates and kinetics of encapsulated compounds are directly related with the diffusion progress. Some parameters that play an important role on diffusion progress are the initial concentration of the encapsulated drug, encapsulation efficiency and method, physicochemical properties of carrying materials (i.e. Gelatin, HA-pNIPAM), the ambient pH and temperature and physicochemical properties of the release medium (i.e. 0.9% NaCl). [79] Another crucial factor that can influence the release rates of a compound is the biodegradability of the encapsulating polymer. [79]

## E. Conclusions

In this project, it was studied whether a drug delivery system of EGCG for local injection in degenerative intervertebral discs can be effectively synthesized. EGCG was encapsulated in gelatin microparticles and followingly those were combined with thermo-reversible hydrogel HA-pNIPAM. Spherical, non-fibrous, dispersed particles of  $669.72 \pm 172.03\text{nm}$  size, were produced with electrospraying, using gelatin as carrier and GA for cross-linking. Cross-linking efficiency was checked only by optical observation upon gelatin dissolution rates, indicating a 24-hour dissolution time for cross-linked gelatin, compared to 2 hours that plain gelatin needs to get completely dissolved. GA content of gelatin microparticles provided non-toxic effects upon IVD cell cultures, although this test requires further repetitions to confirm the result. *In vitro* evaluation of the EGCG DDS took place, indicating that the designed DDS provides prolonged and controlled release of the compound, keeping it active at the same time. Activity tests also indicated that electrospraying and further processing does not compromise the compound's bioactivity. However, HA-pNIPAM revealed loss of its structural cohesion, affecting the experimental outcome.

These findings are quite promising, indicating encapsulated EGCG as a hopeful local DSS against DDD. Considering this outcome in parallel with previously reported anti-inflammatory, anti-oxidative and other beneficial effects of EGCG, the present findings might be further confirmed and used for the development of an optimal novel injectable drug delivery system for DDD treatment.

## F. Suggestions for Future Work

In order to improve this study and considering the derived results, missing parts and aspects that have not been studied yet, a batch of suggestions for further testing and investigation is represented below:

- ❖ The set of experimental parameters used for particle formation and EGCG encapsulation was a very time-consuming process, due to low flow rate ( $2\mu\text{L}/\text{min}$ ). Consequently, particle formation was particularly slow. In order to make the procedure faster and increase the production rates of the particles, optimization of the electrospraying procedure is deemed necessary. However, optimization entails no affection of the particles' morphology or increase of their size. A possible way would be a set of experimental conditions with increased flow rate, in case there is a set of electrospraying parameters (voltage supply, gelatin concentration, needle cross section, distance between needle and collector, ambient temperature and humidity) that can favor production of particles with the desired specifications.
- ❖ An important characteristic that has also to be investigated in future work is the surface charge of the particles. This is an important feature for microparticles produced by electrospraying and helps researchers to comprehend in a better way the features of

microparticles. In our case, surface charge of particles can be determined via zeta ( $\zeta$ ) potential measurements, using a Zeta potential analyzer or through charge detection mass spectrometry. [11, 19, 26, 28, 65] Particle charging possibly takes place either once particles reach the collector plate of the electro spraying apparatus or during electro spraying. Bibliography confirms that the produced particles get charged once electrical field is applied on the needle and the solution that comes through it. [64, 65] The droplets retain their charge once they detach from the needle and even if the solvent evaporates, the charge remains on the particle's surface. [64, 65] This fact was confirmed in our case, as the particles behaved as charged after spraying; the aluminum foil with the deposited particles stacked on the plastic petri plates that are kept, and during collection; the particles hovered and stacked on plastic surfaces.

Therefore, it would be useful to determine the particle surface charge. As the voltage used during electro spraying was positive, the surface charge is positive, too, but it is required to measure its value. According to studies, electro spraying is able to change the zeta potential of the particles from negative to positive or vice versa. [28] This probably happens due to the applied voltage during electro spinning, which may provide surface charge on the material. According to this information, surface charge of the formed electro sprayed particles depends on the voltage mode of the voltage supplier. If electro spraying takes place under negative ion mode, then particles acquire negative charge, while particles have positive surface charge once they are sprayed under positive mode of voltage. [65] Consequently, in our case gelatin particles got positively charged, as we applied positive voltage for electro spraying. It is considered more difficult for positively charged particles to get discharged after electro spraying, as these tend to maintain their charge, comparing to negatively charged particles. [65]

There are indications proving that acidic environment (low pH) improves electro spray quality, but also favors particle charging. [64] For this reason, it seems that several solutions of acids are used as solvents for polymers that will be electro sprayed. More specifically, solution's pH values lower than 4 yielded the best electro spray performance. [64] In our case, the pH of gelatin solutions used for electro spraying was measured equal to 2.26, meaning that the pH value of our gelatin solution favors particle formation, but also intensifies the particle charging.

A possible way to discharge or neutralize the particles could be to leave the electro sprayed particles on the collector plate for some time after electro spraying. If there is no voltage and the collector is grounded, the particles could be gradually, even partially or totally, discharged. Of course, that time should not be long enough to jeopardize EGCG stability. However, this would be even more time consuming. Another alternative could be to change the way that the electro sprayed particles are stored. The plastic petri dishes where the aluminum foil samples containing the electro sprayed particles are stored, favor charge retention. So, gelatin particles keep being charged as far as they are placed into the petri dishes. Once the particles are removed from the plastic petri dishes and stored in glassware, they come in contact with several tools and different materials (metal spatula, glass jar and vials), which enable the particles to transmit part or their total charge on those

objects. It is considered that particles' charge may be partially neutralized, as they do not hover anymore or stick to surfaces less than before (Figure 32.b).

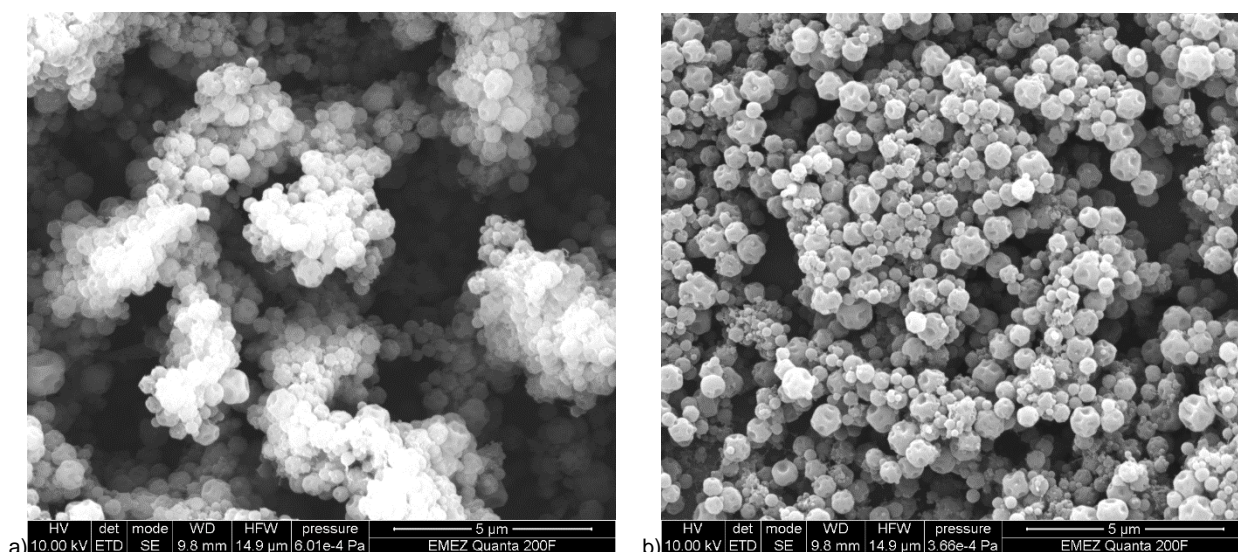


Figure 32. Different regions of the same electrospay sample. In the first picture (a) the particles are organized in clumps, just as they were attached in the collector plate once they were electrospayed. The second one (b) the particles are not aggregated, as they were "interrupted" by metal spatula.

- ❖ Except of charging, aggregation is another characteristic that is occasionally observed on particles via SEM. The produced gelatin particles are deposited on the collector plate in groups (Figure 32.a), like aggregated, and not sparsely or randomly placed on it. However, this phenomenon is opposed to the fact of charging, that was described above. Considering that the particles are charged due to voltage application on gelatin solution, they acquire the same kind of charge, therefore they should repel each other and lie on the collector in a random way. On the contrary, gelatin particles appear to grow in groups on the collector plate, which does not correspond with the incident described above (hover and stuck on plastic) and attributed to charging. These groups however, may be attributed to physical arrangement of the particles once they lay on the electrospaying collector. This means that those outward clumps, stop existing and the particles get dispersed by collection and further implementation. In any case, aggregation (Figure 32.a) is not acceptable, because the formatted clusters would possibly cause problems at the injection ability of the DDS in this particular project. Also, particles must be uniformly dispersed in the bulk of HA-pNIPAM, in order to achieve stable and constant EGCG release in all directions into intervertebral discs. In case particle groups were not a result of physical growth, a possible way to achieve particle dispersion and overcome particle aggregation without gelatin getting dissolved, could be the dilution in a non-polar solvent. Gelatin is insoluble in some alcohols and most organic solvents, which are non-polar. Therefore, an effective particle dispersion can be obtained by using a non-polar solvent, like chloroform, DCM, non-polar alcohols or even ethanol. [69] The particle dispersion could ideally take place before the mixing of the particles with HA-pNIPAM, in order to ensure uniform distribution of the particles into the mixture.

- ❖ The procedure of cross-linking reaction and its effect on gelatin solubility; this can be achieved via FTIR (or HPLC) measurements, as analyzed in Discussion section.
- ❖ Quantitative measurements of gelatin solubility should be obtained. In this way, the dissolution rates of gelatin in medium will be recorded. Proper tests for this aim are measurements of collagen concentration via the Hyp-test. [75]
- ❖ Determination of the particles' EE, is another aspect that should be attempted. Drug encapsulation efficiency can be determined by spectrophotometric estimation (ultraviolet-visible spectrophotometer) [13], HPLC/UV methods [9], or FTIR [14, 19, 23] and formula [19]

$$EE(\%) = \frac{\text{Actual EGCG Content in the Capsules}}{\text{Theoretical EGCG content in the capsules}} \cdot 100\%$$

If encapsulation doesn't work for EGCG stabilization, chemical modification of EGCG is an alternative suggestion, that may protect EGCG from rapid solubility in water and degradation. EGCG molecules contain hydroxyl groups that react with water molecules and trigger autoxidation and epimerization. [12, 74] Therefore, if these groups were prevented from reacting with water, EGCG would not be degraded so rapidly and would acquire enhanced antioxidant properties. There are some chemical applications that could protect EGCG's active groups, such as acetylation, treatment with acetic anhydride and pyridine and further encapsulation in liposomes, esterification with fatty acids, as well as co-crystallization. [63, 74, 80-82]

- ❖ Optimization of release and activity experiments; firstly, improvement can be achieved with application of additional control samples, such as 1) bare gelatin particles in HA-pNIPAM (without EGCG) and 2) EGCG-Gel particles in water (without HA-pNIPAM). These extra control-samples will help us investigate better the release kinetics of encapsulated EGCG. It would be useful to check whether bare gelatin affects Ferrous Tartrate assay or UV absorbance, through bare gelatin particles in HA-pNIPAM. It is also important to compare the release kinetics of encapsulated EGCG with and without HA-pNIPAM, in order to investigate the role of HA-pNIPAM hydrogel on the diffusion and release of EGCG in medium. Encapsulated EGCG in water can additionally be compared with free EGCG in water, to comprehend the effect of encapsulation on solubility, release and activity of EGCG. The correlation of Ferrous Tartrate and UV methods has to be checked, in order to find out whether their results confirm each other. Additionally, statistical analysis of the methods' results should be obtained (regression test). Improvement of HA-pNIPAM hydrogel should be taken into consideration, however without changing its viscoelastic and cytocompatibility properties. In order to optimize its mechanical properties of the material, improve its gelation and avoid its collapsing and dilution in medium again (Figure 31), a 44kDa-molecular-weight pNIPAM type was synthesized in a recent study. [40] Nevertheless, this type has not been tested yet for its injectability and cell-encapsulation facilities. It has been stated that the material's viscoelasticity in gel state, rheological properties, storage modulus ( $G'$ ) and volume changes upon phase transition, depend on its molecular weight. [9, 40] The heavier the pNIPAM it is, the storage modulus becomes bigger, which probably affects the injectability of the material and becomes hostile for the cells and tissue. [9] Although there are no constraints about cell encapsulation and culture in this particular project, it is crucial

to maintain the same viscoelastic properties and injectability of the material. A possible increase of the hydrogel viscosity and an increased storage modulus, may require the use of a wider needle and result to volume shrinkage upon solidifying. <sup>[9, 39, 40]</sup> In future work, it has also to be clarified whether diluted hydrogel affects the occurred absorbance measurements (DPPH, Ferrous Tartrate) and if HA-pNIPAM reacts with light.



# G. References

1. <http://www.spine-health.com/glossary/intervertebral-disc>
2. Spinal Disks. Peter F. Ullrich, Spine-health.com 1999
3. Senescence in human intervertebral discs. S. Roberts, E. H. Evans, D. Kleitas, D. C. Jaffray, S. M. Eisenstein. *Eur Spine J* (2006) 15 (Suppl. 3): S312–S316 DOI 10.1007/s00586-006-0126-
4. Epigallocatechin 3-Gallate Suppresses Interleukin-1 $\beta$ -Induced Inflammatory Responses In Intervertebral Disc Cells In Vitro And Reduces Radiculopathic Pain In Rats. O. Krupkova, M. Sekiguchi, J. Klasen, O. Hausmann, S. Konno, S.J. Ferguson and K. Wuertz-Kozak. *European Cells and Materials* Vol. 28 2014 (pages 372-386)
5. Electrospayed nanoparticles for drug delivery and pharmaceutical applications. Radhakrishnan Sridhar and Seeram Ramakrishna. *Biomatter* 3:3, e24281; July/August/September 2013
6. Enhancing human nucleus pulposus cells for biological treatment approaches of degenerative intervertebral disc diseases: a systematic review. Demissew Shenegelegn Mern, Anja Beierfuß, Claudius Thomé and Aldemar Andres Hegewald. *J Tissue Eng Regen Med* 2014; 8: 925–936.
7. Organ Culture Bioreactors – Platforms to Study Human Intervertebral Disc Degeneration and Regenerative Therapy. Benjamin Gantenbein, Svenja Illien-Jünger, Samantha CW Chan, Jochen Walser, Lisbet Haglund, Stephen J Ferguson, James C Iatridis, and Sibylle Grad. *Curr Stem Cell Res Ther.* 2015 ; 10(4): 339–352
8. Biomaterials For Intervertebral Disc Regeneration: Past Performance And Possible Future Strategies. E.M. Schutgens, M.A. Tryfonidou, T.H. Smit, F. Cumhur Öner, A. Krouwels, K. Ito and L.B. Creemers. *European Cells and Materials* Vol. 30 2015 (pages 210-231)
9. Injectable thermoreversible hyaluronan-based hydrogels for nucleus pulposus cell encapsulation. Marianna Peroglio, Sibylle Grad, Derek Mortisen, Christoph Martin Sprecher, Svenja Illien-Junger, Mauro Alini, David Eglin. *Eur Spine J* (2012) 21 (Suppl 6):S839–S849
10. Intervertebral disc regeneration or repair with biomaterials and stem cell therapy – feasible or fiction? Samantha C.W. Chan, Benjamin Gantenbein-Ritter. *Swiss Med Wkly.* 2012; 142: w13598
11. Application of nanotechnology in improving bioavailability and bioactivity of diet-derived phytochemicals. Shu Wang, Rui Su, Shufang Nie, Ming Sun, Jia Zhang, Dayong Wu, and Naima Moustaid-Moussa
12. Stability of (-)-Epigallocatechin Gallate and its Activity in Liquid Formulations and Delivery Systems. Olga Krupkova, Stephen J Ferguson, Karin Wuertz-Kozak. *Journal of Nutritional Biochemistry* 37 (2016) 1–12
13. Plga-encapsulated tea polyphenols enhance the chemotherapeutic efficacy of cisplatin against human cancer cells and mice bearing Ehrlich ascites carcinoma. Madhulika Singh, Priyanka Bhatnagar, sanjay Mishra, Pradeep Kumar, Yogeshwer Shukla, Kailash chand gupta. *International Journal of Nanomedicine* 2015:10 6789–6809
14. Whey protein capsules obtained through electrospaying for the encapsulation of bioactives. Amparo López-Rubio, Jose M. Lagaron. *Innovative Food Science and Emerging Technologies* 13 (2012) 200–206
15. Introducing Nanochemoprevention as a Novel Approach for Cancer Control: Proof of Principle with Green Tea Polyphenol Epigallocatechin-3-Gallate. Imtiaz A. Siddiqui, Vaqar M. Adhami, Dhruba J. Bharali, Bilal B. Hafeez, Mohammad Asim, Sabih I. Khwaja, Nihal Ahmad, Huadong Cui, Shaker A. Mousa, and Hasan Mukhtar. *Cancer Res.* 2009 March 1; 69(5): 1712–1716
16. Nanochemoprevention: Sustained Release of Bioactive Food Components for Cancer Prevention. Imtiaz A. Siddiqui, Vaqar M. Adhami, Nihal Ahmad, and Hasan Mukhtar. *Nutr Cancer.* 2010 October; 62(7): 883–890
17. Impact of nanotechnology on delivery of natural products for cancer prevention and therapy. Imtiaz A. Siddiqui and Vanna Sanna, 10.1002/mnfr.201600035
18. Recent advances on chitosan-based micro- and nanoparticles in drug delivery. Sunil A. Agnihotri, Nadagouda N. Mallikarjuna, Tejraj M. Aminabhavi. *Journal of Controlled Release* 100 (2004) 5–28
19. Electrospayed gelatin submicroparticles as edible carriers for the encapsulation of polyphenols of interest in functional foods. Laura G. Gomez-Mascaraque, Jose María Lagaron, Amparo Lopez-Rubio. *Food Hydrocolloids* 49 (2015) 42-52
20. Chitosan nanoparticles enhance the intestinal absorption of the green tea catechins (+)-catechin and (-)-epigallocatechin gallate. Admire Dube, Joseph A. Nicolazzo, Ian Larson, *European Journal of Pharmaceutical Sciences* 41 (2010) 219–225

21. Formation of Enriched Black Tea Extract Loaded Chitosan Nanoparticles Via Electrospraying. Samuel James Hammond. Thesis of Graduate School-New Brunswick Rutgers, The State University of New Jersey
22. The Natural Polyphenol Epigallocatechin Gallate Protects Intervertebral Disc Cells from Oxidative Stress. Olga Krupkova, Junichi Handa, Marian Hlavna, Juergen Klasen, Caroline Ospelt, Stephen John Ferguson, and Karin Wuertz-Kozak. *Oxidative Medicine and Cellular Longevity*, Volume 2016, Article ID 7031397, 17 pages, <http://dx.doi.org/10.1155/2016/7031397>
23. An application of nanotechnology for the stability and sustained biological activity of tea polyphenol Kulandaivelu Karikalan and Abul Kalam Azad Mandal
24. <http://www.newobjective.com/electrospray/index.shtml>
25. A nanostructural investigation of glassy gelatin oligomers: molecular organization and interactions with low molecular weight diluents. M Roussenova, J Enrione, P Diaz-Calderon, A J Taylor, J Ubbink and M A Alam. *New Journal of Physics* 14 (2012) 035016 (18pp)
26. Affecting parameters on electrospinning process and characterization of electrospun gelatin nanofibers. Nagihan Okutan, Pinar Terzi, Filiz Altay. *Food Hydrocolloids* 39 (2014) 19-26
27. Aldehydes, Aliphatic, Christian Kohlpaintner, Markus Schulte, Jürgen Falbe, Peter Lappe, Jürgen Weber (2005), *Ullmann's Encyclopedia of Industrial Chemistry*, Weinheim: Wiley-VCH, doi: 10.1002/14356007.a01\_321.pub2
28. Fabrication and Characterization of cross-linked gelatin electro-spun nanofibers. Thi-Hiep Nguyen, Byong-Taek Lee. *J. biomedical science and Engineering*, 2010, 3, 1117-1124
29. Pulses in negative point-to-plane corona. L. B. Loeb; A. F. Kip; G. G. Hudson; W. H. Bennett (1941). *Physical Review*. 60 (10): 714–722. Bibcode:1941PhRv...60.714L. doi:10.1103/PhysRev.60.714
30. McMullan, D. (2006). "Scanning electron microscopy 1928–1965". *Scanning*. 17 (3): 175–185. doi:10.1002/sca.4950170309.
31. Microspheres for Drug Delivery. Kyekyoon "Kevin" Kim and Daniel W. Pack. University of Illinois at Urbana-Champaign
32. Design, fabrication and characterization of drug delivery systems based on lab-on-a-chip technology. Nam-Trung Nguyena, Seyed Ali Mousavi Shaegh, Navid Kashaninejad, Dinh-Tuan Phan
33. Applications of electrospinning/electrospraying in drug delivery, Azin Jahangiri, Khosro Adibkia. *BioImpacts*, 2016, 6(1), 1-2
34. Electrospinning of polymeric nanofibers for drug delivery applications. Xiuli Hu, Shi Liu, Guangyuan Zhou, Yubin Huang, Zhigang Xie, Xiabin Jing - *Journal of Controlled Release* 185 (2014) 12–21
35. Microspheres for Drug Delivery. Kyekyoon "Kevin" Kim and Daniel W. Pack
36. Investigating the particle to fibre transition threshold during electrohydrodynamic atomization of a polymer solution, O. Husain, W. Lau, M. Edirisinghe, M. Parhizkar. *Materials Science and Engineering C* 65 (2016) 240–250
37. Bioactive compounds: Definition and assessment of activity. Hans-Konrad Biesalski, Lars Ove Dragsted, Ibrahim Elmadfa, Rolf Grossklaus, Michael Müller, Dieter Schrenk, Paul Walter and Peter Weber. *Nutrition* 25 (2009) 1202–1205
38. [Medicinenet.com](http://www.medicinenet.com)
39. Tailoring Thermoreversible Hyaluronan Hydrogels by "Click" Chemistry and RAFT Polymerization for Cell and Drug Therapy. Derek Mortisen, Marianna Peroglio, Mauro Alini, and David Eglin, *Biomacromolecules* 2010, 11, 1261–1272
40. Single step synthesis and characterization of thermoresponsive hyaluronan hydrogels. Matteo D'Este \*, Mauro Alini, David Eglin. *Carbohydrate Polymers* 90 (2012) 1378–1385
41. <http://www.nanoscience.com/technology/sem-technology/>
42. Scanning Electron Microscopy. C. W. OATLEY, W. C. NIXON and R. F. W. PEASE, Engineering Department, Cambridge University, Cambridge, England
43. <http://www.scopem.ethz.ch/instruments-services/sample-preparation-for-em.html>
44. Hard gelatin capsules today and tomorrow. Sven Stegemann, Capsugel Bornem
45. DISSOLUTION OF HARD GELATIN CAPSULES I. SIMPLE METHOD FOR CALCULATING THE RATE CONSTANT. ADNAN EL-YAZIGI, *International Journal of Pharmaceutics*, 5 (1980) 79-84
46. <http://www.pbgelatins.com/about-gelatin/physical-and-chemical-properties/solubility/>
47. The shell dissolution of various empty hard capsules. Chiwele I, Jones BE, Podczeczek F *Chem Pharm Bull* (Tokyo). 2000 Jul;48(7):951-6.

48. From sub cellular to community level: Toxicity of glutaraldehyde to several aquatic organisms. Susana P.P. Pereira, Rhaul Oliveira, Sónia Coelho, Carolina Musso, Amadeu M.V.M. Soares, Inês Domingues, António J.A. Nogueira. *Science of the Total Environment* 470–471 (2014) 147–158
49. NTP Technical Report on Toxicity Studies of Glutaraldehyde. Frank W. Kari, National Toxicology Program Toxicity Report Series, Number 25
50. Cytotoxicity of glutaraldehyde and formaldehyde in relation to time of exposure and concentration. Hsiao Wen Sun, Robert J. Feigal, Harold H. Messer, *PEDIATRIC DENTISTRY/Copyright ©1990 by The American Academy of Pediatric Dentistry* Volume 12, Number 5
51. Application of electrospraying as a one-step method for the fabrication of triamcinolone acetonide-PLGA nanofibers and nanobeads, Azin Jahangiri, Soodabeh Davaran, Behnam Fayyazi, Ali Tanhaei, Shahriar Payab, Khosro Adibkia. *Colloids and Surfaces B: Biointerfaces* 123 (2014) 219–224
52. Beaded nanofibers formed during electrospinning, H. Fong, I. Chun, D.H. Reneker. *Polymer* 40 (1999) 4585–4592
53. *Drug Delivery*. Mitra, A. K.; Kwatra, D.; Vadlapudi, A. D. Jones & Bartlett Learning: Burlington, Massachusetts, 2015
54. TheFreeDictionary.com > route of administration Citing: Jonas: *Mosby's Dictionary of Complementary and Alternative Medicine*. 2005, Elsevier
55. Protein delivery: from conventional drug delivery carriers to polymeric nanoreactors. V Balasubramanian, Ozana Onaca, Ramona Enea, David W Hughes & Cornelia G Palivan. 1742-5247 (Print) 1744-7593
56. <http://www.paincommunitycentre.org/article/low-back-pain-problem>
57. Glutaraldehyde as a crosslinking agent for collagen-based biomaterials. L. H. H. OLDE DAMINK, P. J. DIJKSTRA, M. J. A. VAN LUYN, P. B. VAN WACHEM, P. N I E U W E N H U I S, J. FEIJEN. *Journal of Materials Science: Materials in Medicine* 6 (1995) 460-472
58. How to cross-link proteins. M. Kapoor, University of Calgary
59. Glutaraldehyde: behavior in aqueous solution, reaction with proteins, and application to enzyme crosslinking: Isabelle Migneault, Catherine Dartiguenave, Michel J. Bertrand, and Karen C. Waldron
60. [https://pubchem.ncbi.nlm.nih.gov/compound/acetic\\_acid](https://pubchem.ncbi.nlm.nih.gov/compound/acetic_acid)
61. Electrospinning of gelatin fibers using solutions with low acetic acid concentration: effect of solvent composition on both diameter of electrospun fibers and cytotoxicity. Marisa Erenca, Francisco Cano, Jose A. Tornero, Margarida M. Fernandes, Tzanko Tzanov, Jorge Macanás, Fernando Carrillo.
62. Bioadhesion of gelatin films crosslinked with glutaraldehyde. Shojiro Matsuda, Hiroo Iwata, Naomi Se, Yoshito Ikada, 1998
63. Lipophilised epigallocatechin gallate (EGCG) derivatives and their antioxidant potential in food and biological systems. Y. Zhong, F. Shahidi, *Food chemistry*, 131 (2012) 22-30
64. “Electrospray charging of minerals and ices for hypervelocity impact research.” R. Terik Daly, Jonathan D. Kerby, Daniel E. Austin. *Planetary and Space Science* 75 (2013) 182–187
65. “Correlation between the Charge of Polymer Particles in Solution and in the Gas Phase Investigated by Zeta-Potential Measurements and Electrospray Ionization Mass Spectrometry.” Nesrine Ouadah, Tristan Doussineau Thomas Hamada, Philippe Dugourd, Claire Bordes and Rodolphe Antoine
66. Advantages and challenges of the spray-drying technology for the production of pure drug particles and drug-loaded polymeric carriers. Alejandro Sosnik, Katia P. Seremeta. *Advances in Colloid and Interface Science* 223 (2015) 40–54
67. Electrospinning, a Reproducible Method for Production of Polymeric Microspheres for Biomedical Applications, Nathalie Bock, Maria A. Woodruff, Dietmar W. Hutmacher and Tim R. Dargaville. *Polymers* 2011, 3, 131-149; doi:10.3390/polym3010131
68. Alternative Reaction Mechanism for the Cross-Linking of Gelatin with Glutaraldehyde”, Stefano Farris, Jianhui Song, Qingrong Huang. *J. Agric. Food Chem.* 2010, 58, 998–1003
69. *GELATIN HANDBOOK*. Gelatin Manufacturers Institute of America, 2012
70. MTT assay for cell viability: Intracellular localization of the formazan product is in lipid droplets. Juan C. Stockerta, Alfonso Blázquez-Castroa, Magdalena Cañetea, Richard W. Horobinb, Ángeles Villanuevaa. *Volume 114, Issue 8, December 2012, Pages 785–796*
71. Tetrazolium dyes as tools in cell biology: new insights into their cellular reduction. Berridge MV, Herst PM, and Tan AS. *Biotechnology Annual Review*, 11: 127-152 (2005)

72. Freeze-drying of nanoparticles: Formulation, process and storage considerations. Wassim Abdelwahed, Ghania Degobert, Serge Stainmesse, Hatem Fessi. *Advanced Drug Delivery Reviews* 58 (2006) 1688–1713
73. Effects of extraction solvents on concentration and antioxidant activity of black and black mate tea polyphenols determined by ferrous tartrate and Folin–Ciocalteu methods. Nihal Turkmen, Ferda Sari, Y. Sedat Velioglu. *Food Chemistry* 99 (2006) 835–841
74. Activity and controlled delivery of epigallocatechin 3-gallate in the treatment of degenerative disc disease. PhD Thesis, Olga Krupkova. 2016
75. Hydroxyproline Assay Kit. Technical Bulletin. Catalog Number MAK008. Sigma-Aldrich
76. Effect of transglutaminase and EDC on biodegradation of fish gelatin and gelatin-chitosan films. Katarzyna Sztuka, Ilona Kołodziejka. *Eur Food Res Technol* (2008) 226:1127–1133. DOI 10.1007/s00217-007-0641-9
77. Thermoreversible hyaluronan-based hydrogel supports in vitro and ex vivo disc-like differentiation of human mesenchymal stem cells. Marianna Peroglio, David Eglin, Lorin M. Benneker, Mauro Alini, Sibylle Grad. *The Spine Journal* 13 (2013) 1627–1639
78. A papain-induced disc degeneration model for the assessment of thermo-reversible hydrogel–cells therapeutic approach. C. Malonzo, S. C. W. Chan, A. Kabiri, D. Eglin, S. Grad, H. M. Bonél, L. M. Benneker and B. Gantenbein-Ritter. *J Tissue Eng Regen Med* 2015; 9: E167–E176. Published online 9 January 2013 in Wiley Online Library (wileyonlinelibrary.com) DOI: 10.1002/term.1667
79. ENCAPSULATION OF CATECHIN AND EPICATECHIN ON BSA NPS IMPROVED THEIR STABILITY AND ANTIOXIDANT POTENTIAL. Ramdhan Yadav, Dharmesh Kumar, Avnesh Kumari, Sudesh Kumar Yadav. *EXCLI Journal* 2014;13:331-346 – ISSN 1611-2156
80. Formulation and characterization of polyphenol-loaded lipid nanocapsules. A. Barras, A. Mezzetti, A. Richard, S. Lazzaroni, S. Roux, P. Melnyk, D. Betbeder, N. Monfilliette-Dupont, *International journal of pharmaceutics*, 379 (2009) 270-277.
81. Lipase-catalyzed synthesis of acetylated EGCG and antioxidant properties of the acetylated derivatives S. Zhu, Y. Li, Z. Li, C.Y. Ma, Z.X. Lou, W. Yokoyama, H.X. Wang, *Food Res Int*, 56 (2014) 279-286.
82. Anti-inflammatory activity of lipophilic epigallocatechin gallate (EGCG) derivatives in LPS-stimulated murine macrophages. Y. Zhong, Y.S. Chiou, M.H. Pan, F. Shahidi, *Food chemistry*, 134 (2012) 742-748.

# H. Appendix

## 1. SEM

SEM acquirement of plain gelatin particles for different setups and experimental conditions represented in Table 1, are hereby represented in sharper resolution (Figures 33-37):

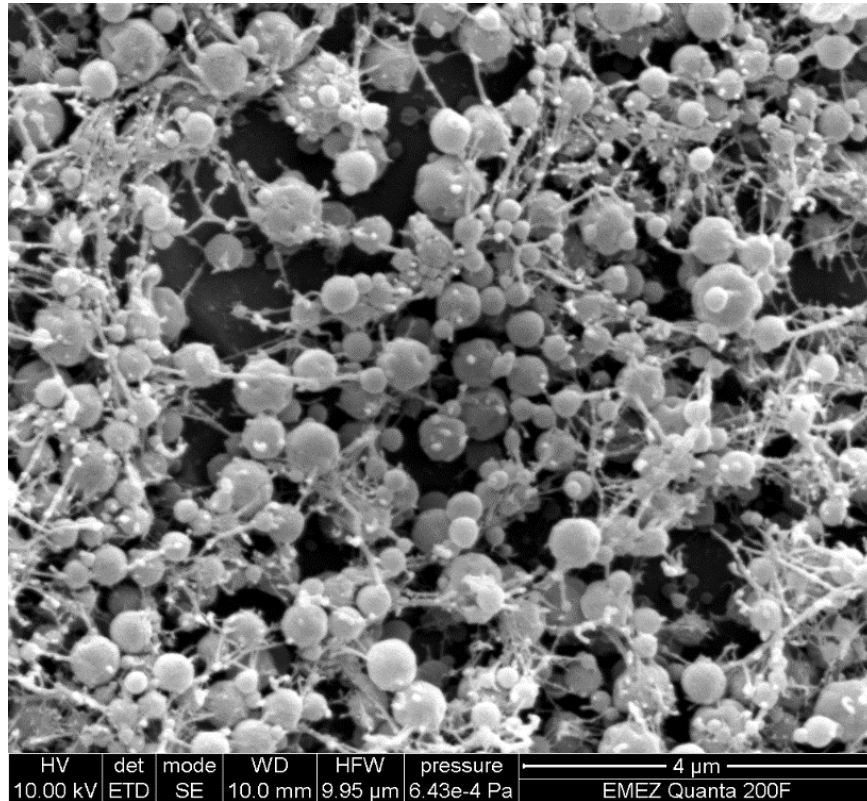


Figure 33. SEM Acquisition for Plain Gelatin sprayed with 2 μL/min flow rate, 17kV voltage and 6% solution concentration

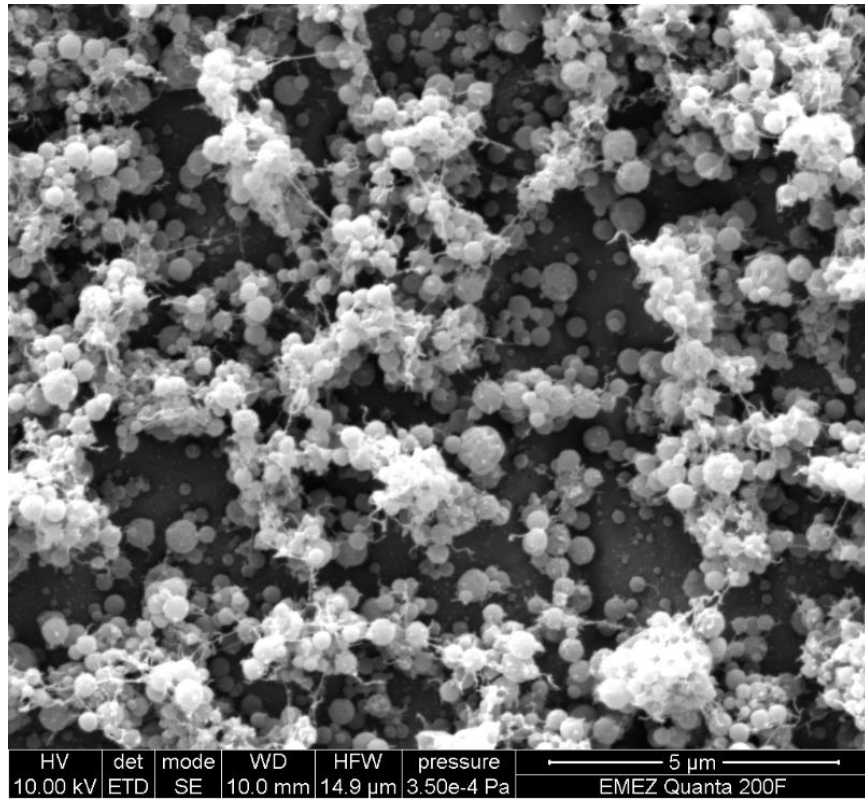


Figure 34. SEM Acquisition for Plain Gelatin sprayed with 4 µL/min flow rate, 21kV voltage and 4% solution concentration

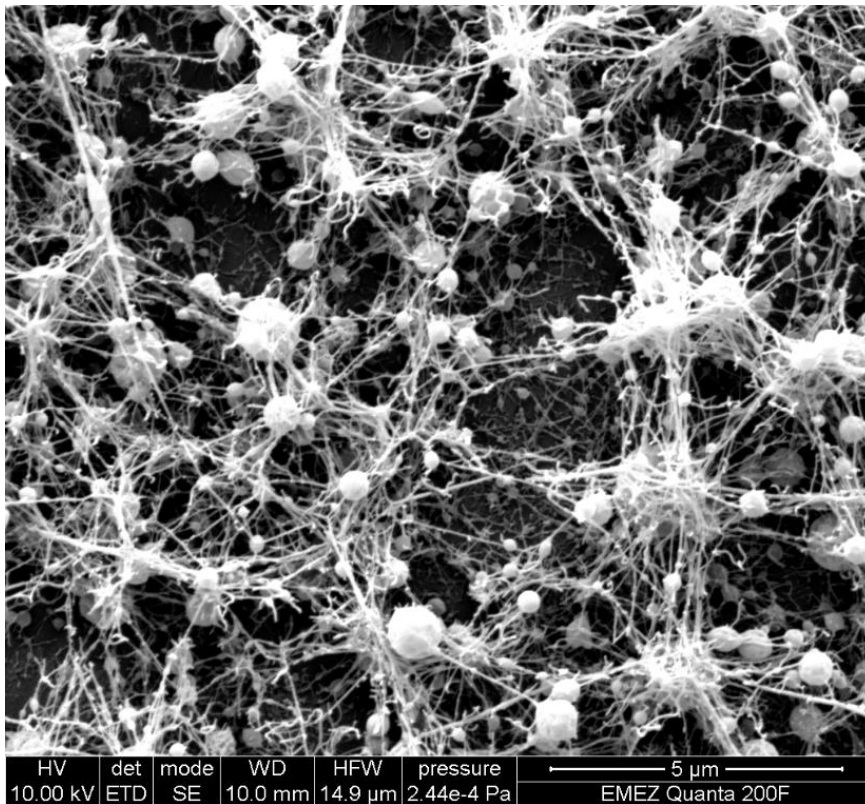


Figure 35. SEM Acquisition for Plain Gelatin sprayed with 4 µL/min flow rate, 22kV voltage and 6% solution concentration

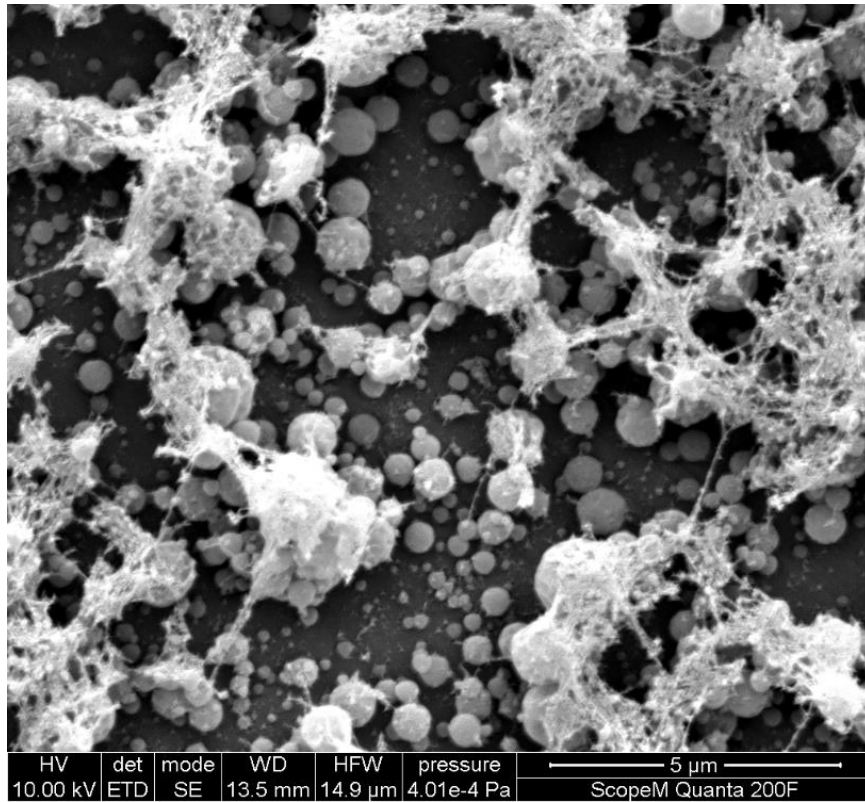


Figure 36. SEM Acquisition for Plain Gelatin sprayed with 2 µL/min flow rate, 22kV voltage and 4% solution concentration

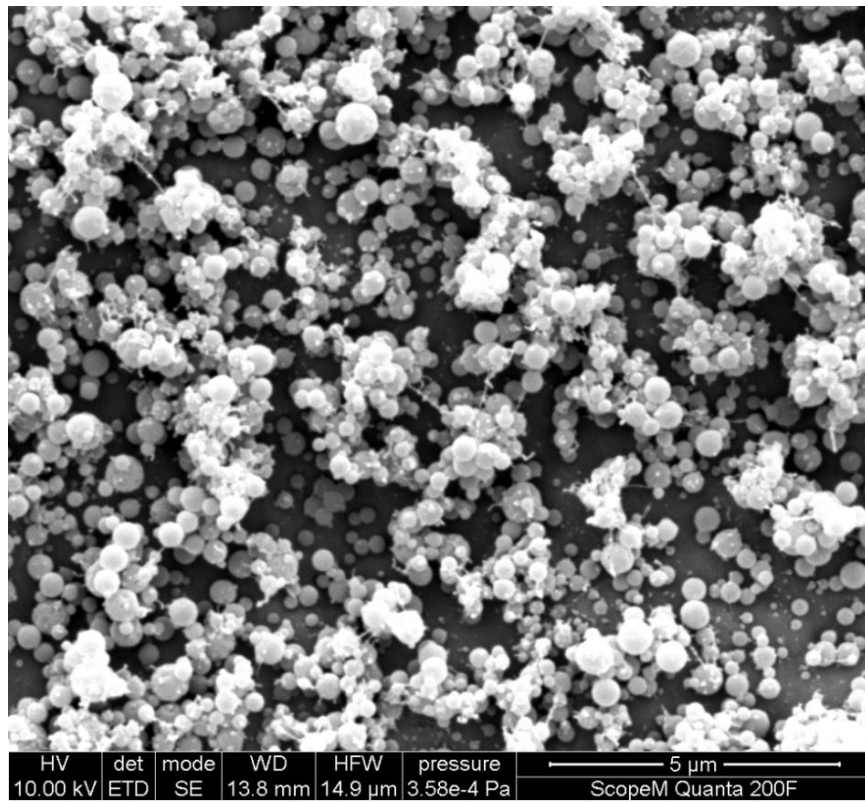


Figure 37. SEM Acquisition for Plain Gelatin sprayed with 2 µL/min flow rate, 20kV voltage and 6% solution concentration

SEM images of most optimal results achieved for the gelatin nano-particles, either uncross-linked or cross-linked, that are included in Table 3. of results section, are represented in full size below (Figures 38-41):

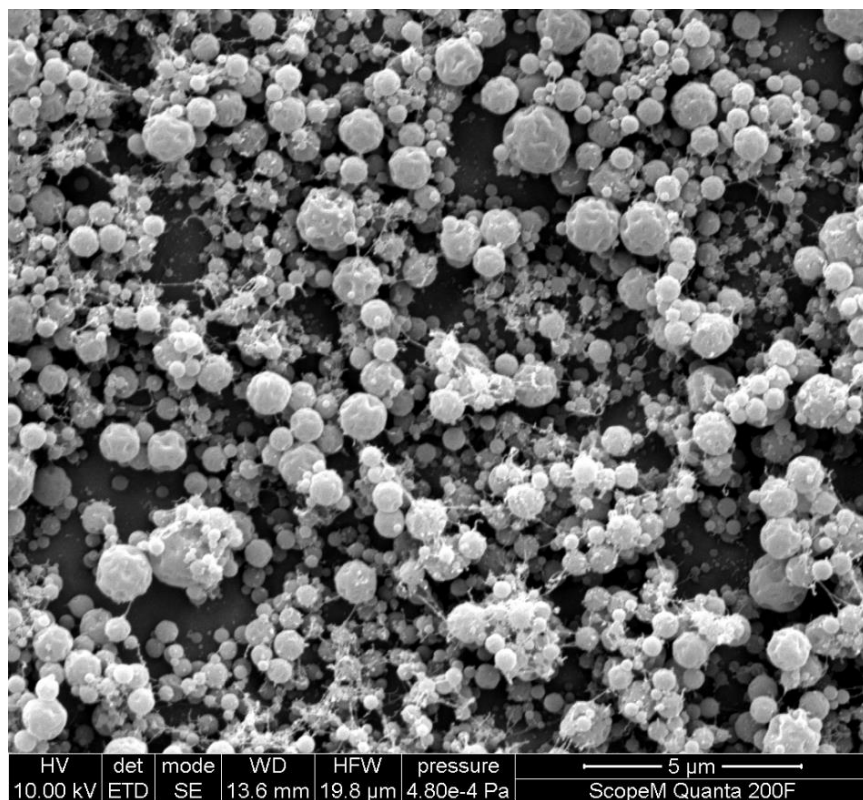


Figure 38. SEM Acquisition for Cross-Linked Gelatin (37.5mg/mL GA) sprayed with 2 µL/min flow rate, 21kV voltage and 4 or 6% solution concentration



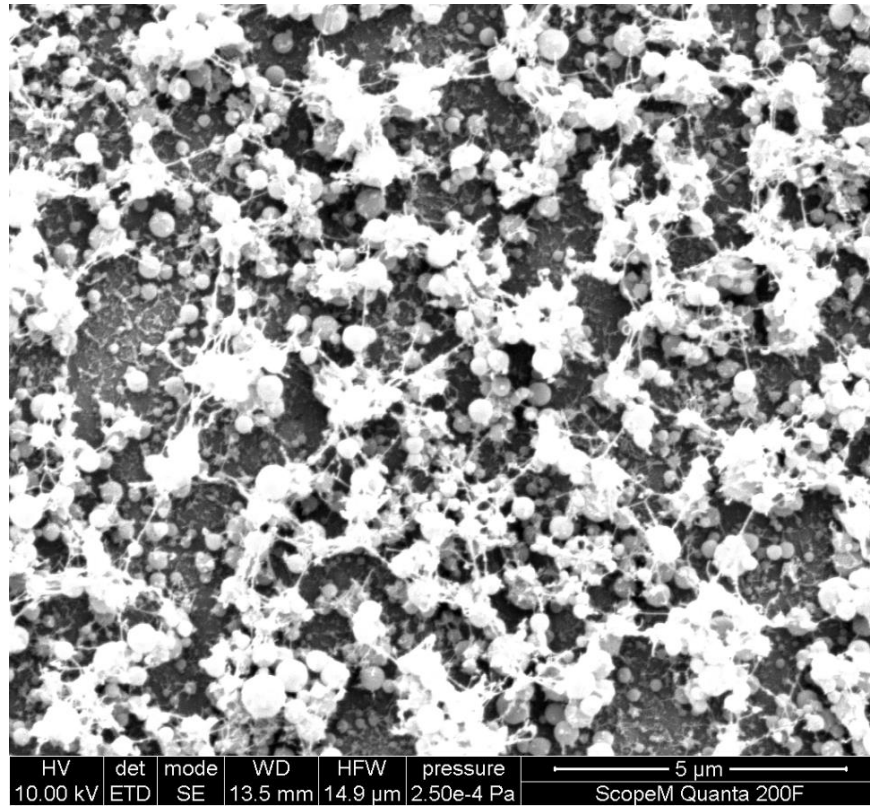


Figure 39. SEM Acquisition for Cross-Linked Gelatin (62.5mg/mL GA) sprayed with 2  $\mu$ L/min flow rate, 21kV voltage and 4% solution concentration

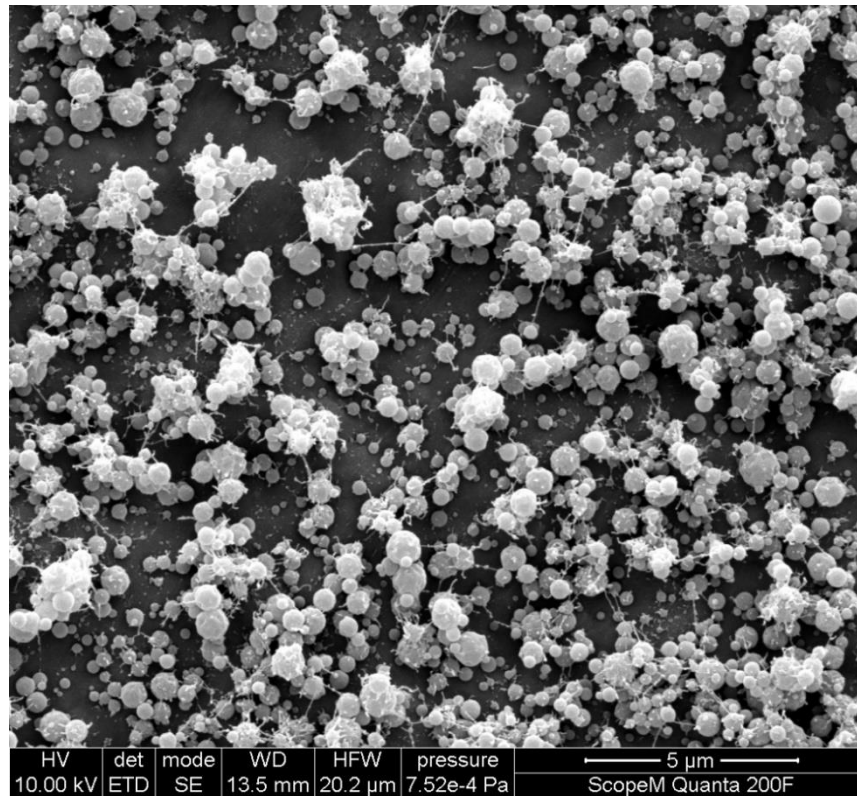


Figure 40. SEM Acquisition for Cross-Linked Gelatin (87.5mg/mL GA) sprayed with 2  $\mu$ L/min flow rate, 21kV voltage and 4% solution concentration

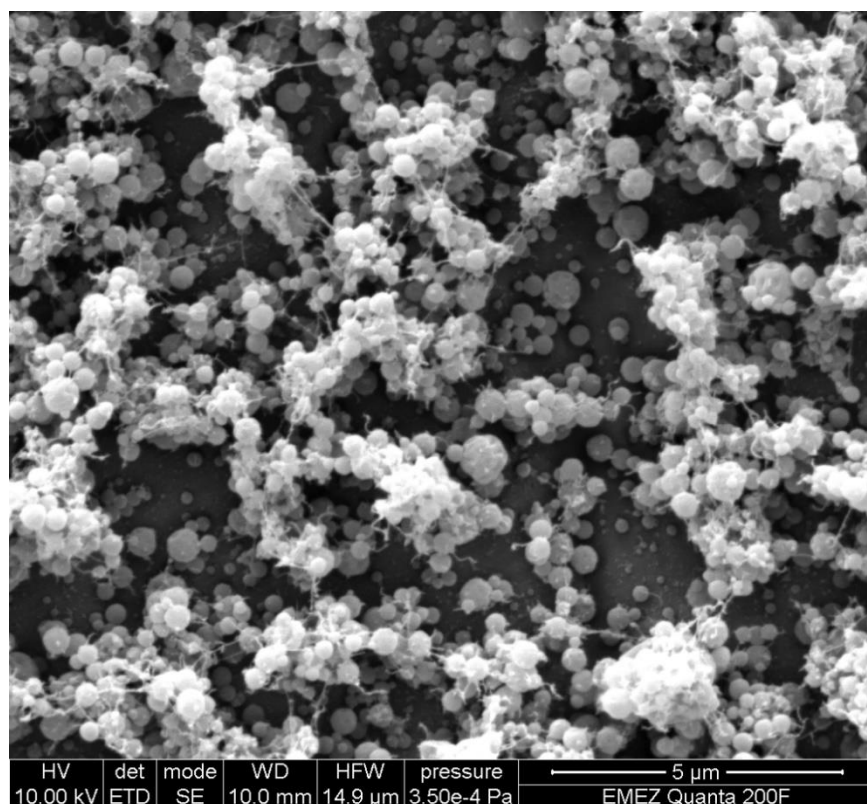


Figure 41. SEM Acquisition of Plain Gelatin sprayed with 4 μL/min flow rate, 21kV voltage and 4% solution concentration

## 2. Encapsulation Efficiency

Table 5. Table of Calculated and measured (Ferrous Tartrate) concentrations of samples and control solution, for Encapsulation Efficiency Calculation

Samples	EGCG-Gelatin Solution (Control)	EGCG-Gelatin Particles in Acetic Acid
Absorbance Measurement No.1	0.0457	0.1987
Absorbance Measurement No.2	0.0512	0.1971
Absorbance Measurement No.3	0.047	0.1984
Absorbance Measurement No.4	0.0544	0.1953
Absorbance Measurement No.5	0.0458	0.2145
Absorbance Measurement No.6	0.0516	0.2184
Absorbance Measurement No.7	0.0454	0.2171
Absorbance Measurement No.8	0.0557	0.1802
<b>Average Value</b>	<b>0.0496</b>	<b>0.2025</b>

Standard Deviation	0.0042	0.0132
Estimated Concentration	5mM	100µM
Measured Concentration (Ferrous Tartrate)	1mM	0mM

### 3. Biocompatibility Test - MTT Assays

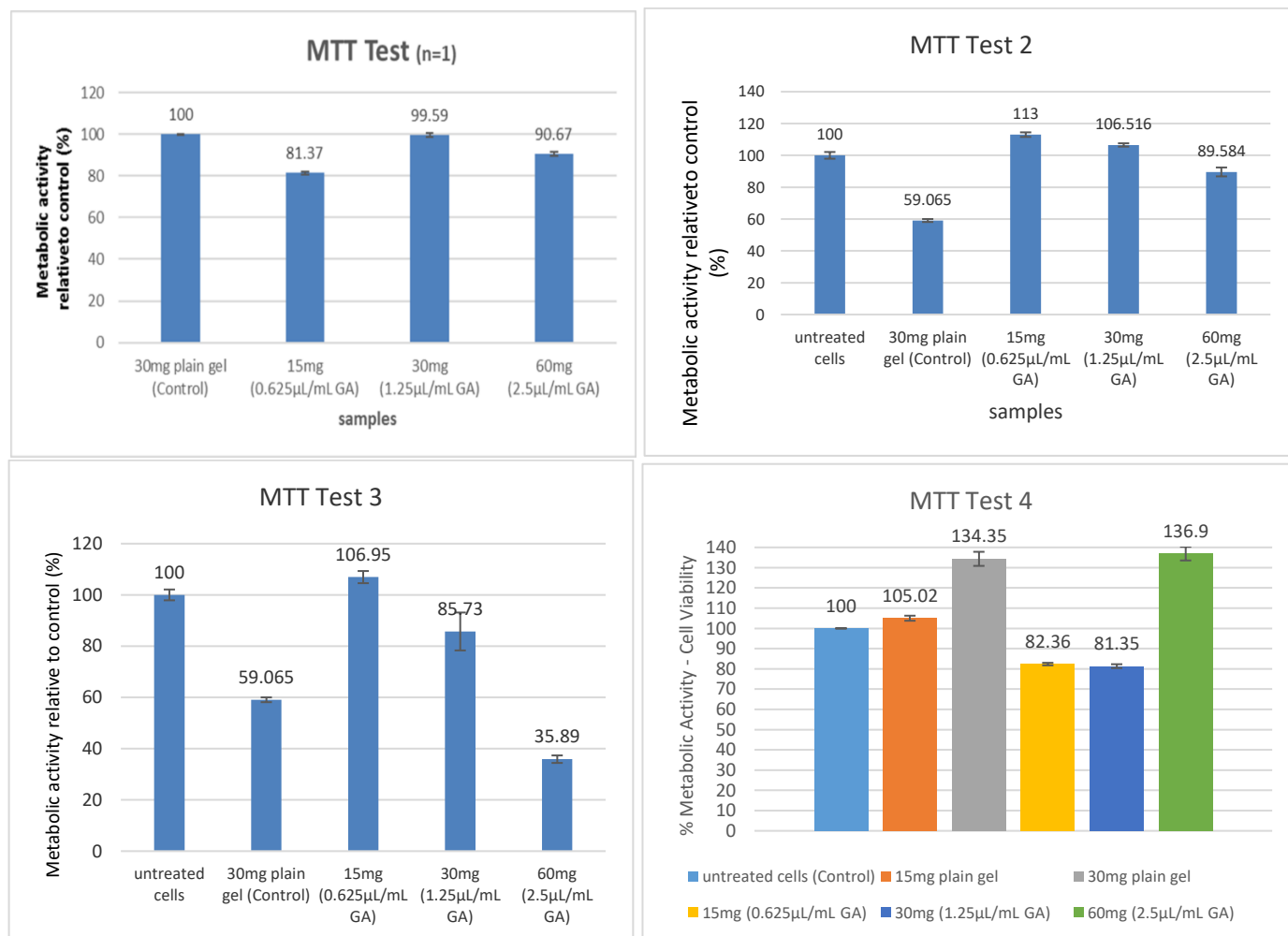


Figure 42. Individual MTT Assays for Biocompatibility Testing of Gelatin Microparticles

The individual repetitions of the biocompatibility experiments are represented in Figure 42. In order to monitor the cell's behavior and progress, as well as predict their outcome regarding the particle's biocompatibility, photos of the cells were taken in daily basis, through the microscope (Figure 43). Indeed, the look and the shape of the cells confirm their metabolic activity. For example, in case of cells treated with 60mg of cross-linked gelatin, where the viability proved to be below 90%, there was reduced number of cells lying in the well. The remaining cells in the well indicated reduced adhesion on the well bottom (Figure 43.c). This was also

confirmed during MTT Assay, where the color shades of each sample differ from each other, depending on the cells' viability (Figure 44).

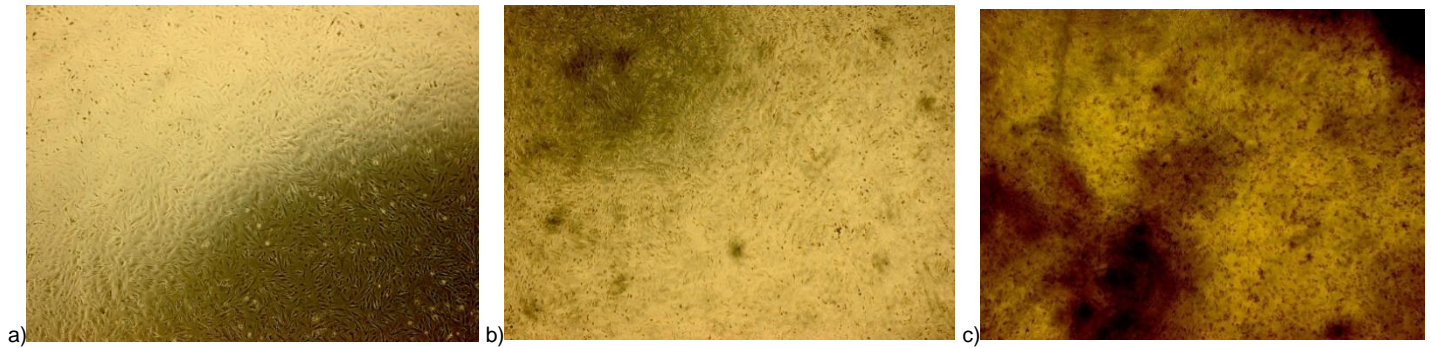


Figure 43. Cells a) Right After Treatment with 30mg of Plain Gelatin, b) 5days after Treatment with 30mg of Plain Gelatin and c) 5days after Treatment with 60mg of Cross-Linked Gelatin



Figure 44. MTT Test Samples of 15 (1), 30(2), 60mg (3) of Cross-Linked Gelatin and 30mg of Plain Gelatin (4)

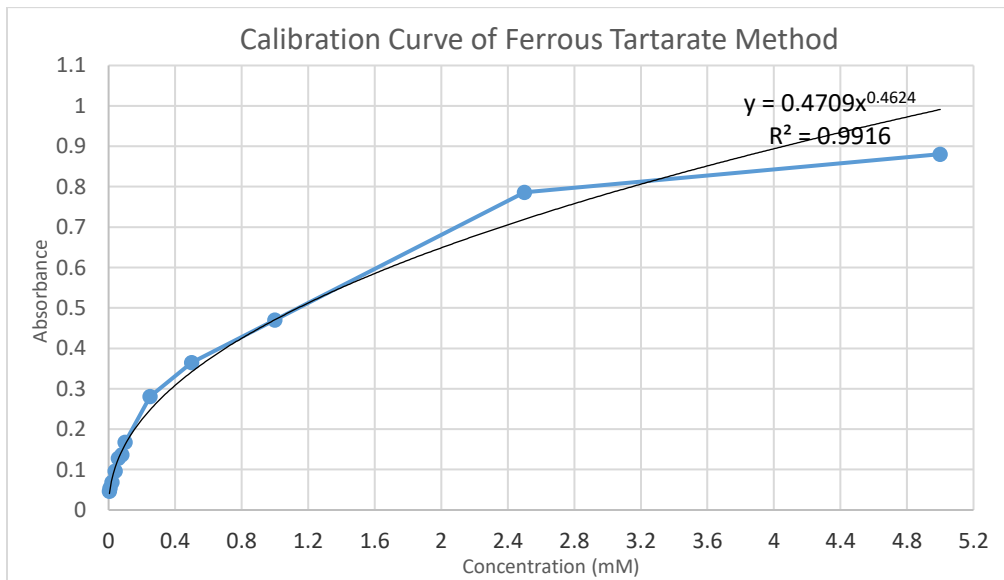


Figure 45. Calibration Curve for Ferrous Tartrate Method (Experiment No.1)

#### 4. EGCG Release (Ferrous Tartrate Method and UV Spectrum)

In this part, the individual repetitions of the release experiments are represented separately, in order to comprehend the effect of gel collapsing and its effect upon the release trends.

❖ Experiment No. 1

The images of the remaining hydrogel-microparticles mixture have been matched with the respective EGCG release profile (Figure 46). It is considered that gel collapsing, which takes place in some cases, may misrepresent the absorbance measurements and thus, the calculated EGCG concentrations. Therefore, in one of Control1 samples (1/2) gel collapsing takes place, where release rates of EGCG reach 0.165mM (t=24hrs). In case the gel was not collapsing and diluting in the medium, may the EGCG release values would be estimated lower. For encapsulated EGCG samples, release rates reach 0.013mM (t=24hrs). The initial concentration of free EGCG in H<sub>2</sub>O (Control2) samples is 0.5mM, which corresponds to the expected concentration, according the dilution law ( $C_1V_1=C_2V_2$ )<sup>9</sup>. However, the detected EGCG concentration decreases rapidly by the first day of the experiment. Regarding Control3 samples of bare HA-pNIPAM, although the absorption rates indicate concentration rates lower than 0.009mM, there is partial gel collapse in both cases.

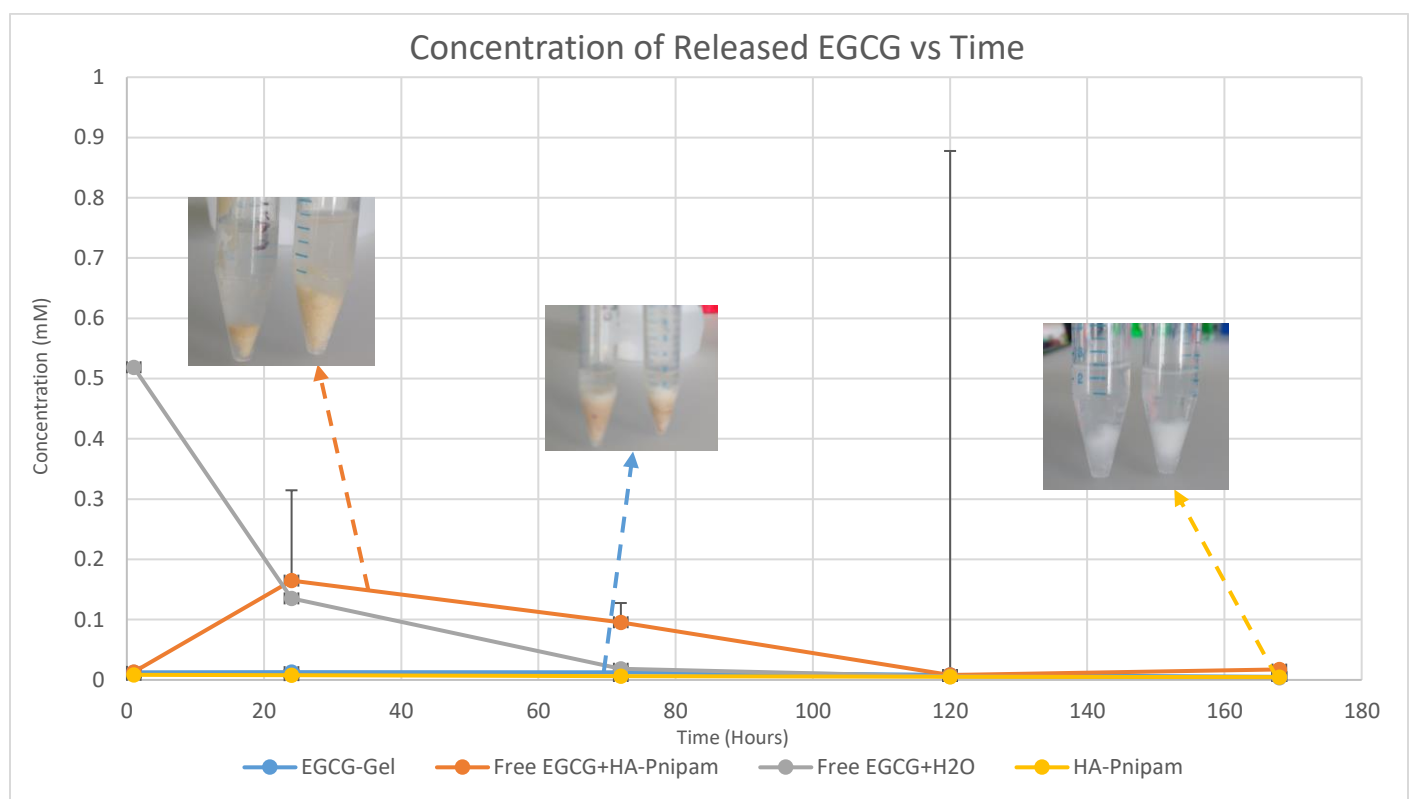


Figure 46. Concentration of Released EGCG in the medium of NaCl 0.9%, Along Time. The respective images of the remaining gels after 1 week of experiment duration. (Experiment No.1)

The cumulative and % cumulative release rates graphs (Figure 47, 48) of this experiment indicate in a clearer way, that encapsulated EGCG is released significantly less than free EGCG, either in hydrogel or water. More specifically, the total released concentration of EGCG is 0.05mM for the case of EGCG-Gelatin particles in hydrogel, while the totally released amounts for free EGCG in hydrogel (Control1) and free EGCG in water (Control2) are 0.3mM and 0.68mM, respectively, by

<sup>9</sup> Before, the addition of the release medium in the tube, there was 1mL of 5mM mixture of free EGCG in water. Then, 10mL of release medium is added. So, the initial concentration (t=1hr) of these samples should be 0.45Mm.

the end of the experiment. According to Figure 48, the total released concentration of EGCG is 10.23% of the initial EGCG amount in the tube for the case of EGCG-Gelatin particles in hydrogel, while the totally released amounts for free EGCG in hydrogel and free EGCG in water are 59.8% and 100%, respectively, by the end of the experiment. There is a general trend that applies for all the different samples, which indicates the increasing of the released EGCG at the first hours of the experiment and then the stabilization of the released amount by the third day of the experiment. Additionally, the gel residuals were diluted and measured with Ferrous Tartrate by the end of the experiment, to detect the EGCG concentration still carried in the hydrogel (Figure 49). The absorbance values of bare HA-pNIPAM control were subtracted, to have the original values of EGCG absorbance. For these graphs (Figures 46-48), the matching between the absorbance and the respective concentration values takes place, based on the calibration curve of Figure 45.

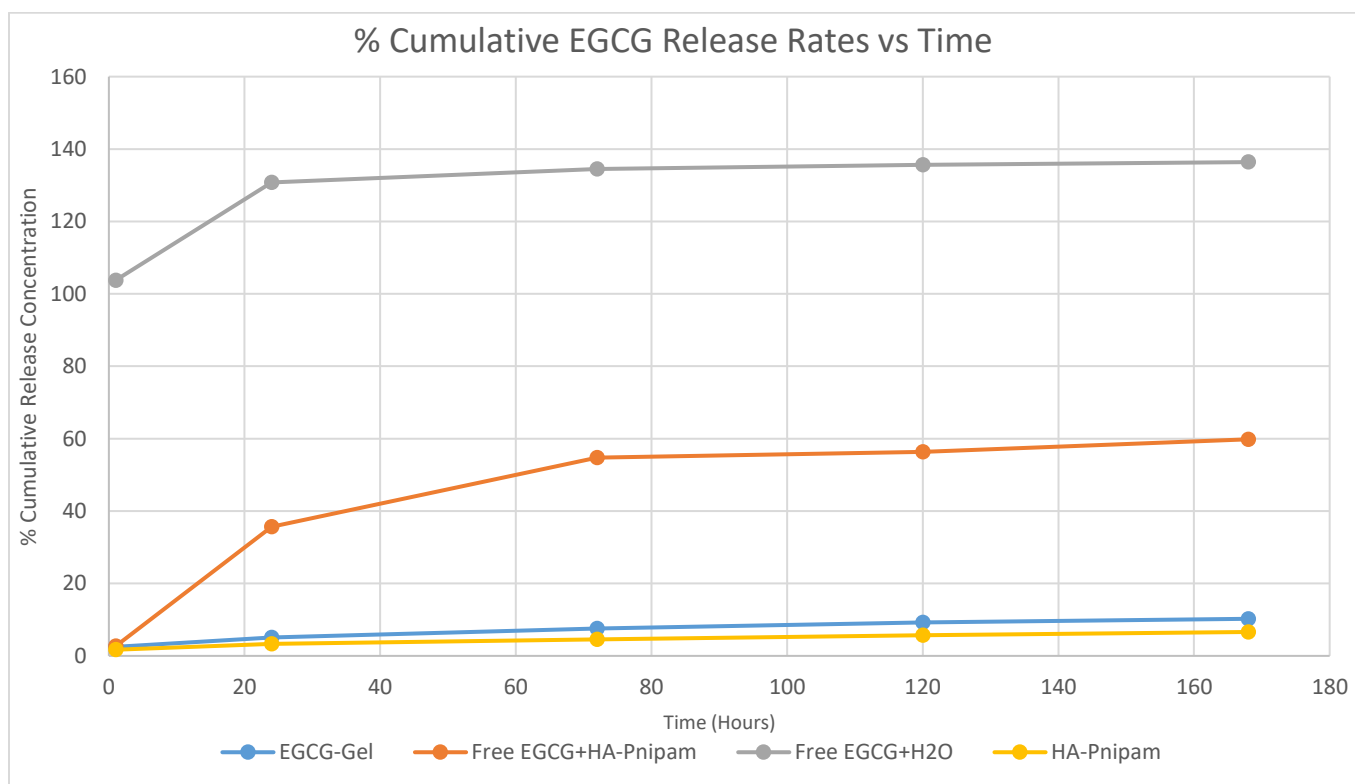


Figure 47. % Cumulative EGCG Release Rates in 0.9% NaCl medium Along Time. The % rates have been estimated in respect of the 0.5mM amount of concentration which is the maximum amount of EGCG that can be released in each sample, as the concentration of EGCG before the addition of 10mL release medium was 5mM. (Experiment No.1)

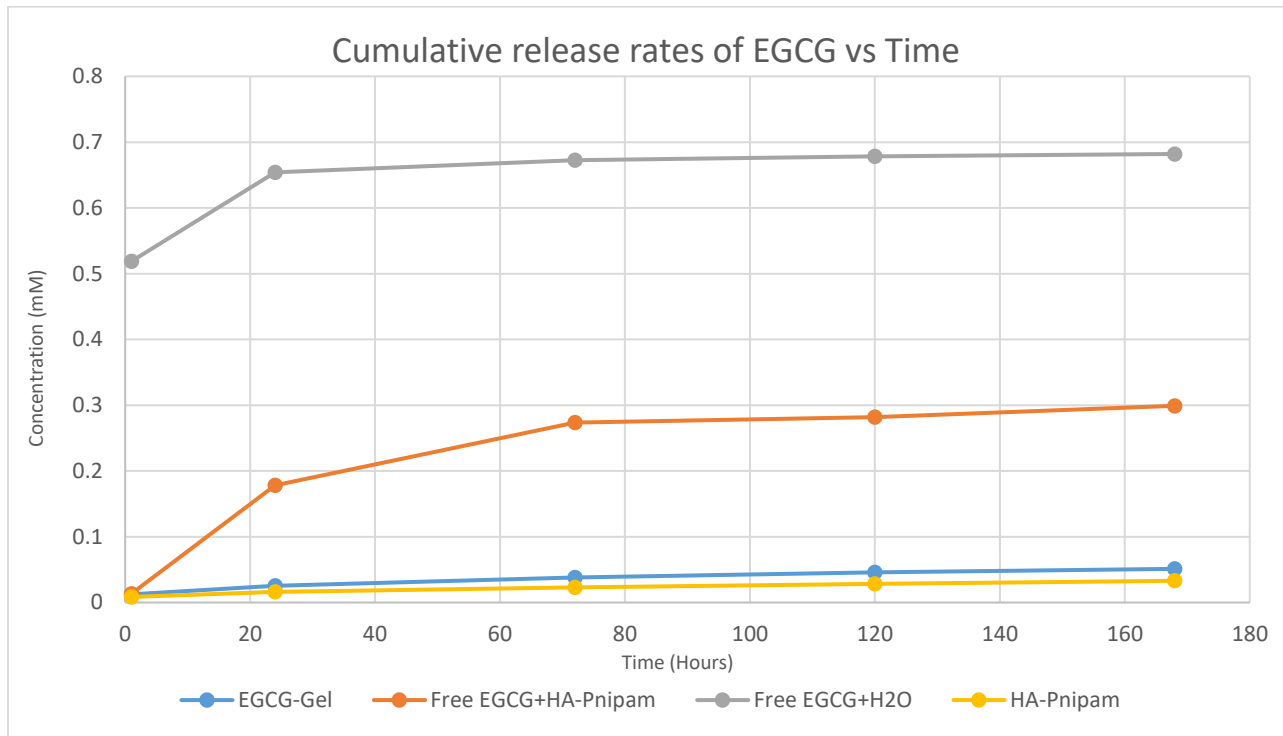


Figure 48. Cumulative Concentration of Released EGCG in the medium of NaCl 0.9%, Along Time. The release rates of the encapsulated EGCG is much lower (0.075mM), than free EGCG in hydrogel (0.45mM) and free EGCG in water (0.615mM). (Experiment No.1)

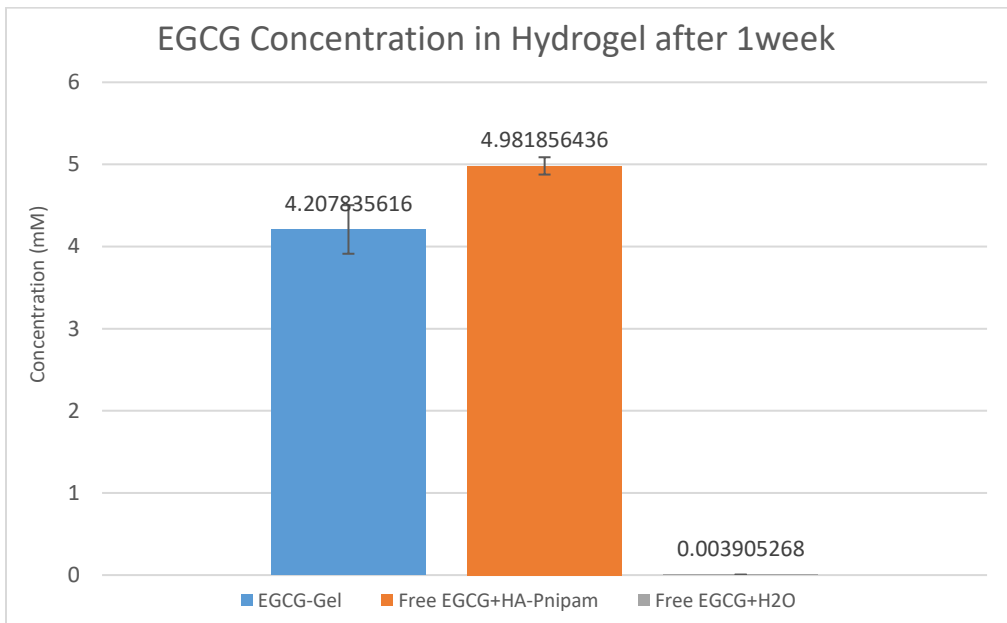


Figure 49. EGCG Concentration Entrapped in Hydrogel by the End of the Experiment (Experiment No.1). Statistical analysis with Kruskal-Wallis test ( $p=0.05$ ,  $n=4$ )

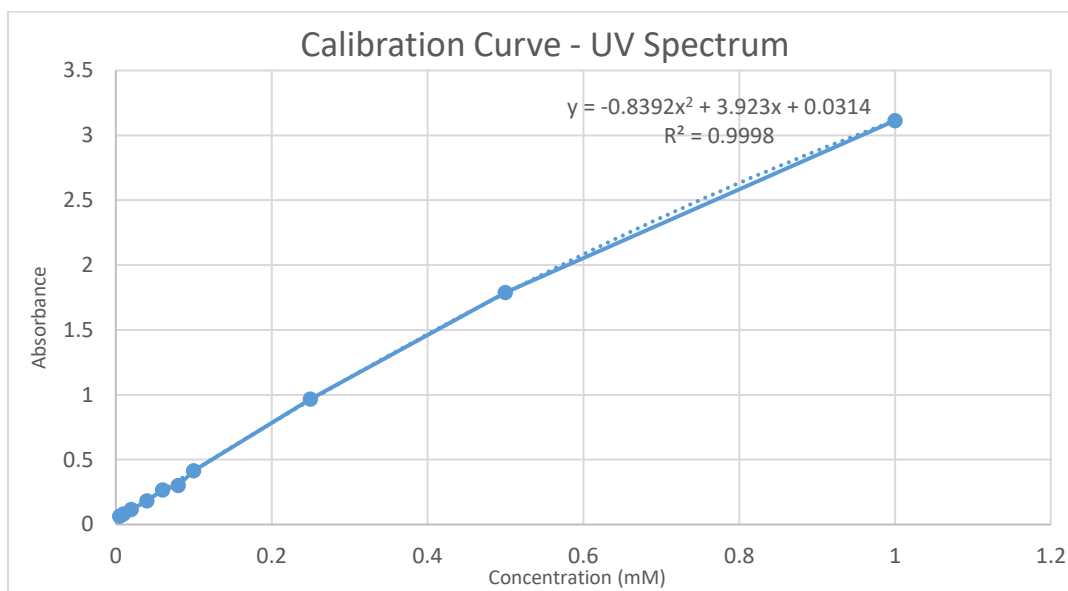


Figure 50. Calibration Curve for UV Measurements (Experiment No.1)

UV measurements were obtained for the same experiments. The respective results are derived by Figure 50 and represented on the following graphs (Figures 51-54). There is gel collapsing in one of Control2 samples, which may affect the absorbance measurements. Indeed, this is obvious in Figure 51, as the release trend of free EGCG mixed with hydrogel samples does not coincide with the trend established by Ferrous Tartrate method. This may be due to gel dilution in the release medium and interaction with UV radiation. The EGCG release rates for these samples reach 0.35mM (t=120hr), which do not agree with the respective values by Ferrous Tartrate method (0.165mM, t=72hr). In case the gel was not collapsing and diluting in the medium, may EGCG release would be lower. For Control2 samples (Free EGCG in H<sub>2</sub>O), the initial concentration is almost 0.82mM, which doesn't correspond to the expected one (0.45mM) and the respective value obtained by Ferrous Tartrate method. The release rates of EGCG for the DDS samples reach 0.08mM according to UV measurements, while for Ferrous Tartrate the value is 0.013mM. Overall, the determined release concentration values of UV measurements don't agree with concentration values of colorimetric method in Experiment No.1



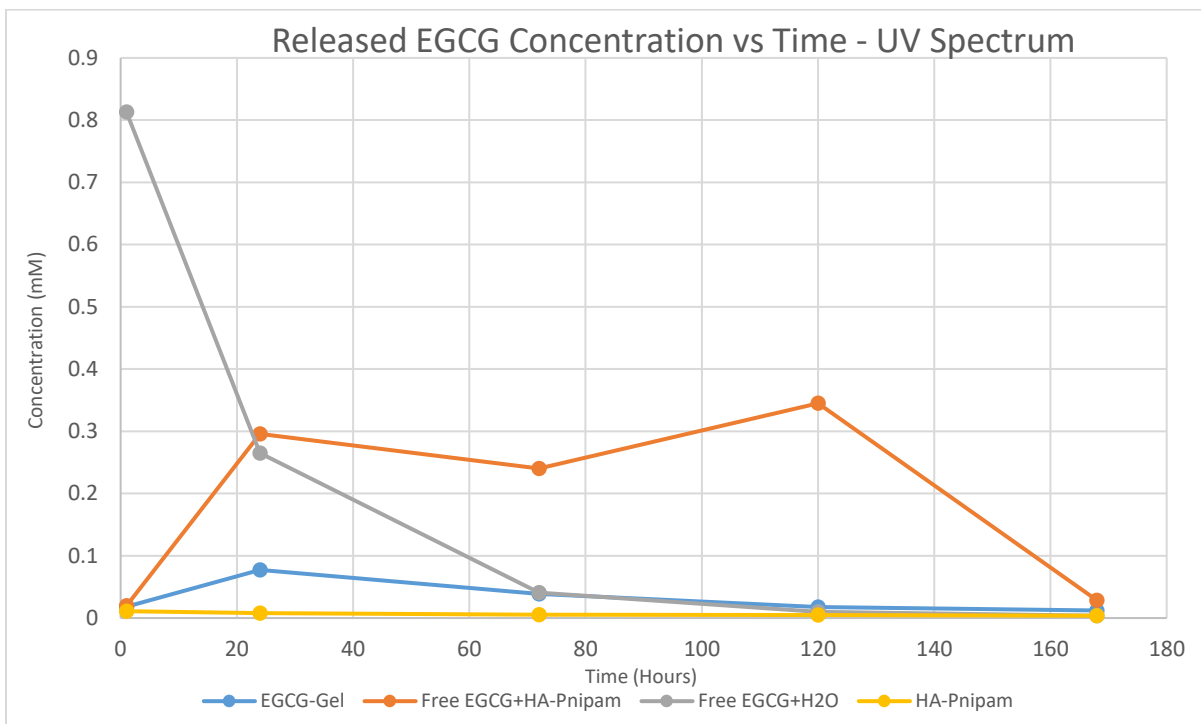


Figure 51. Concentration of Released EGCG Along Time through UV Measurements (Experiment No.1)

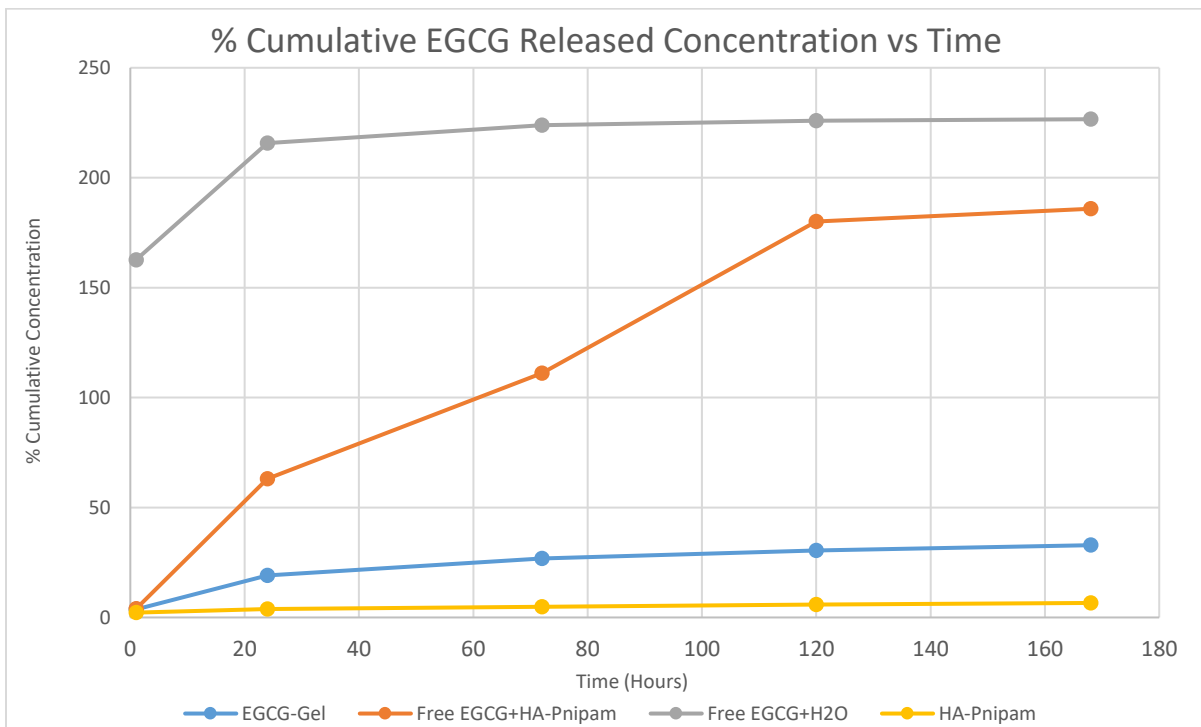


Figure 52. % Cumulative Release Rates of EGCG Along Time through UV Measurements (Experiment No.1)

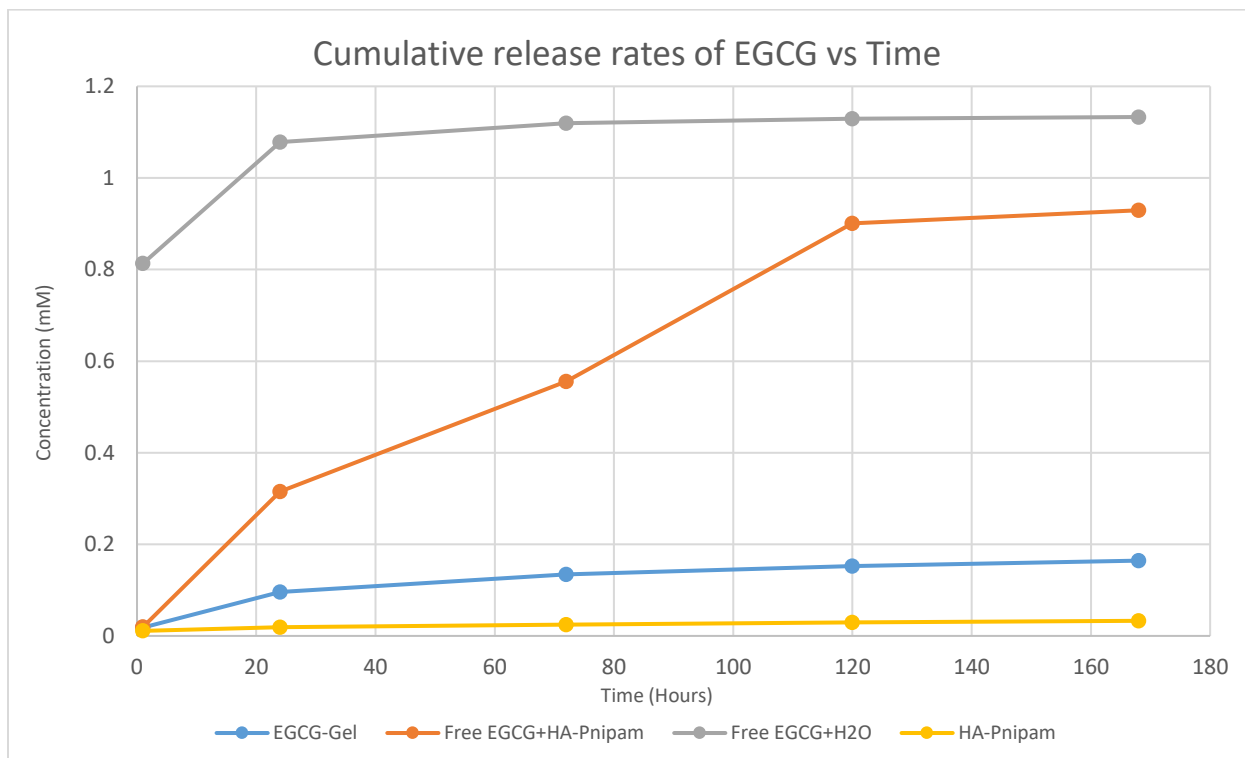


Figure 53. Cumulative Release Rates of EGCG Along Time through UV Measurements (Experiment No.1)

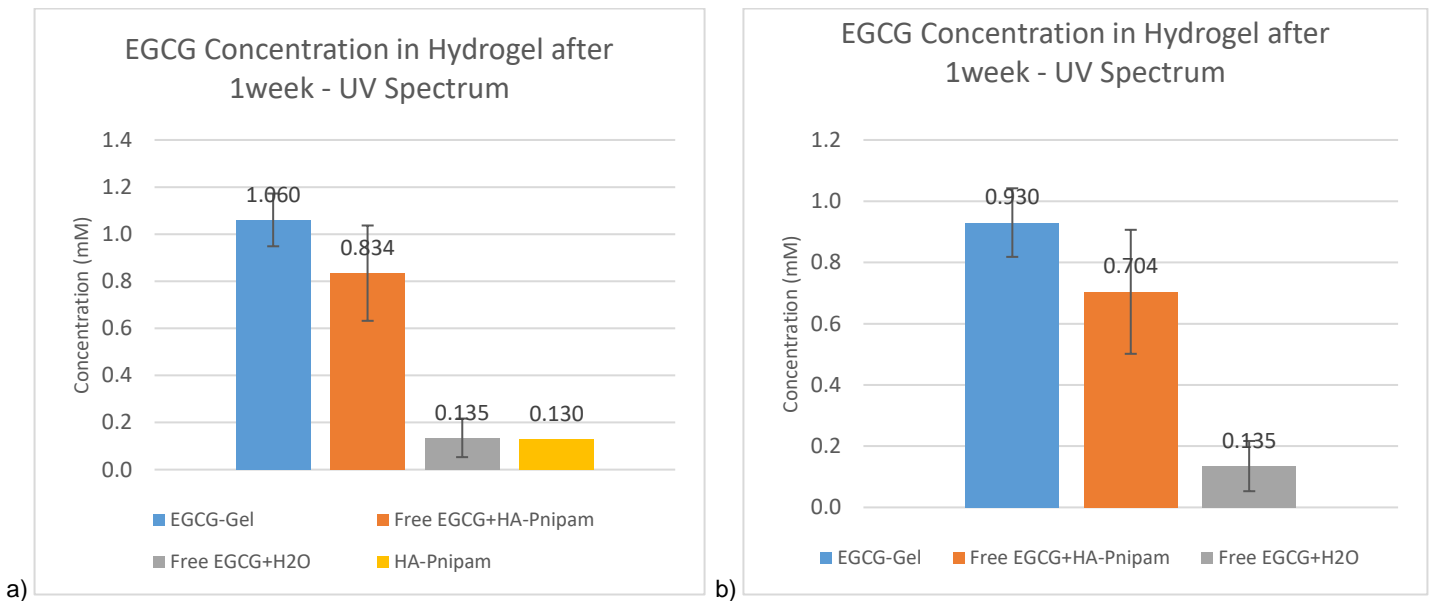


Figure 54. EGCG Concentration Contained in the Remaining Hydrogel (if stated) by the end of the Experiment (Experiment No.1). In graph (b) the absorbance rate of bare HA-pNIPAM has been subtracted in contrast with graph (a) (Experiment No.1). Statistical analysis with Kruskal-Wallis test ( $p=0.05$ ,  $n=12$ )

## ❖ Experiment No.2

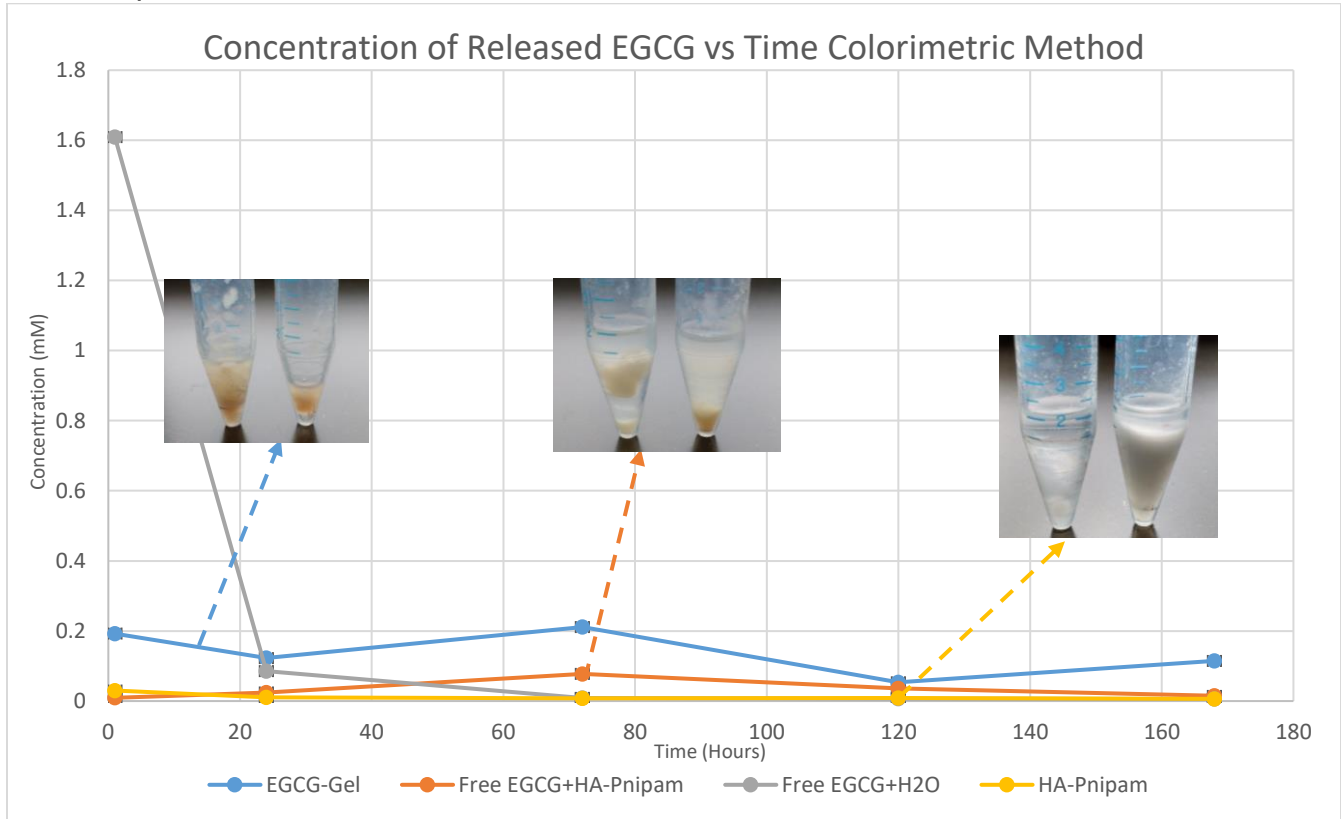


Figure 55. Concentration of Released EGCG in the medium of NaCl 0.9%, Along Time. The respective images of the remaining gels after 1 week of experiment duration. (Experiment No.2)

During the second repetition of the release experiments, there is gel collapsing in one of EGCG-Gelatin particles with HA-pNIPAM samples (Figure 55), where release rates of EGCG reach 0.21mM at  $t=3$  days. For free EGCG in HA-pNIPAM samples, gel collapsing takes place in both samples, where release rates of EGCG reach 0.08mM. In case the gel was not collapsing and diluting in the medium, may the EGCG release would be lower than the values provided in this graph. For the case of free EGCG in water the initial concentration was estimated to be almost 1.6mM, which doesn't correspond to the expected one (0.45mM). This might be due to experimental fault. Experimental fault is also considered by the fact that release of free EGCG carried by hydrogel appears to be more limited than release of encapsulated EGCG. Finally, gel collapse also takes place in one of bare HA-pNIPAM control samples.

The % cumulative release rates graph (figure 57) indicates that encapsulated EGCG is released in a percentage above 100% (133.2%), while the total released concentration of EGCG for free EGCG in hydrogel and free EGCG in water are 32.4% and 343%, respectively. The percentage values of cumulative concentration have been calculated in respect of 0.5mM, because this is the total EGCG amount that can be released in the medium. However, because of possible experimental fault described above, the determined percentages are not realistic (>100%). Nevertheless, the same general trend that stands for the first repetition and applies for

all the different samples, is present here too. This general profile indicates the increasing of the released EGCG at the first hours of the experiment and then the stabilization of the released amount by the third day of the experiment. The cumulative release rates of this experiment are represented below in Figure 56, generally confirming what was stated for % cumulative release in results.

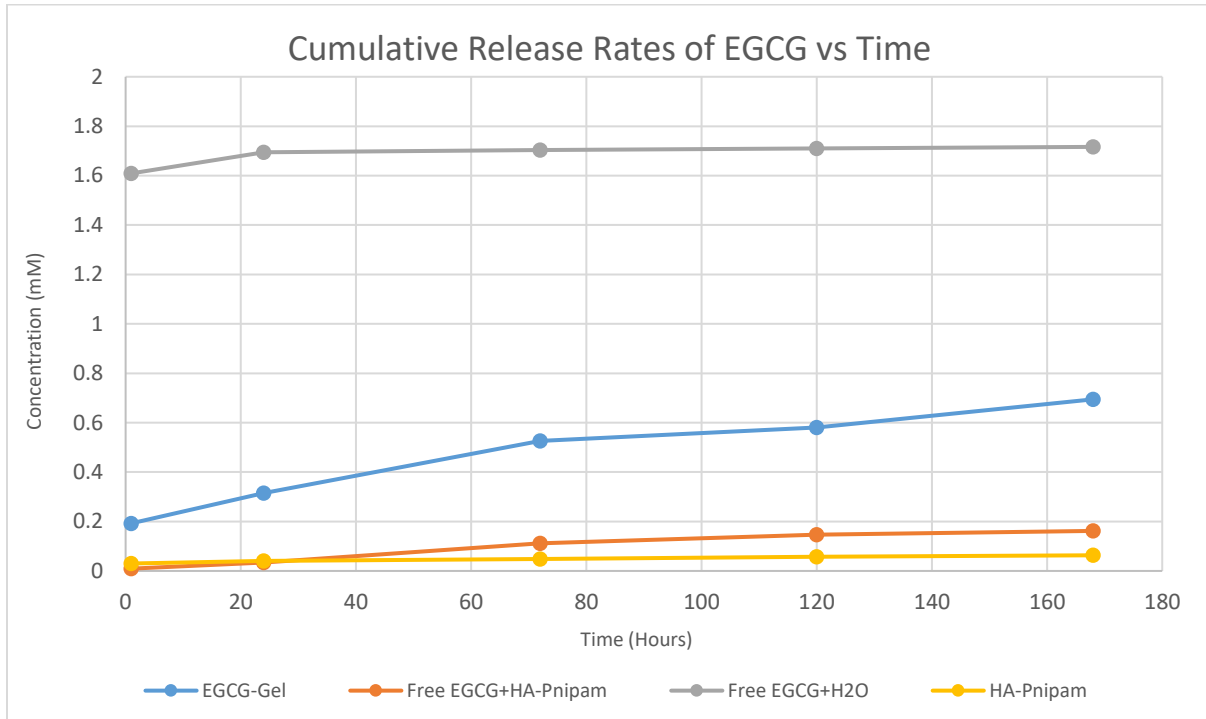


Figure 56. Cumulative Concentration of Released EGCG in the medium of NaCl 0.9%, Along Time. (Experiment No.2)

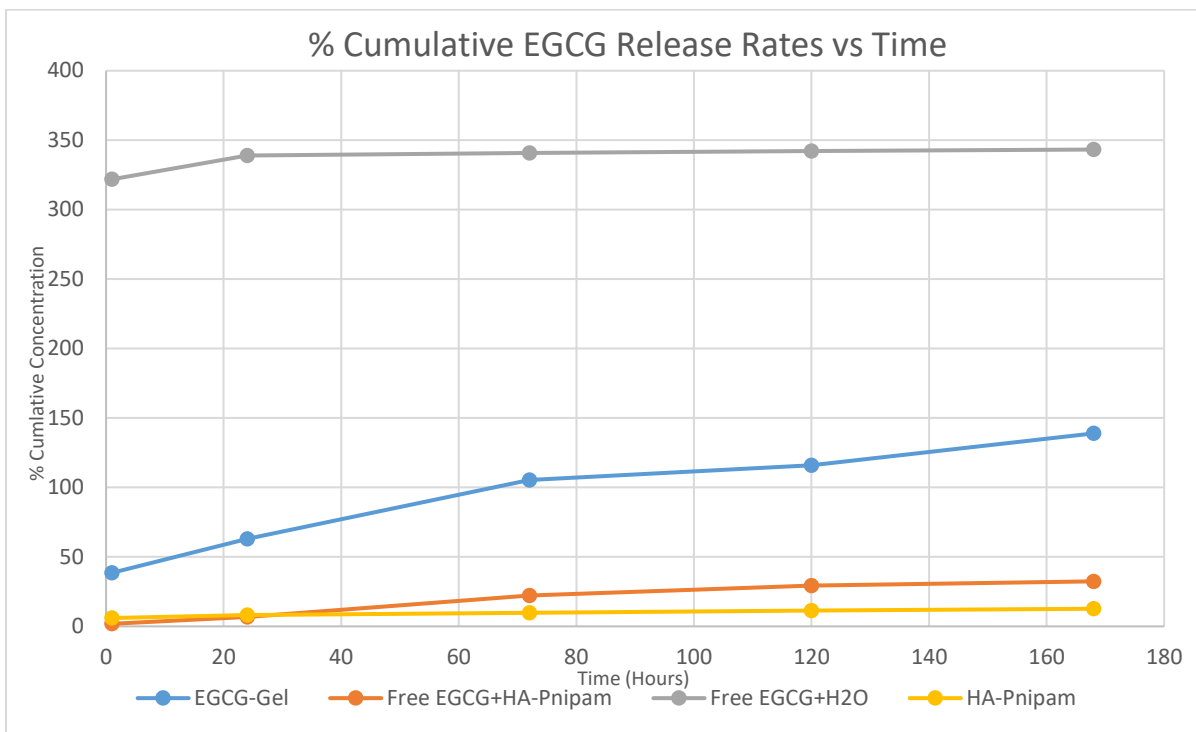


Figure 57. % Cumulative EGCG Release Rates in 0.9% NaCl medium Along Time. The % rates have been estimated in respect of the 0.45mM amount of concentration which is the maximum amount of EGCG that can be released in each sample, as the concentration of EGCG before the addition of 10mL release medium was 5mM. (Experiment No.2)

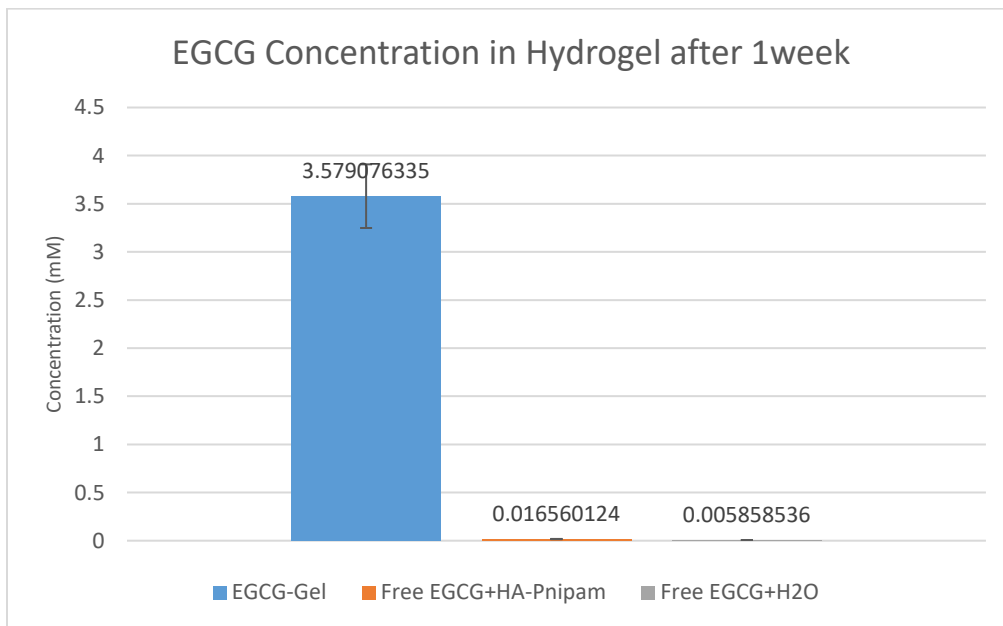


Figure 58. EGCG Concentration Entrapped in Hydrogel by the End of the Experiment (Experiment No.2). Statistical analysis with Kruskal-Wallis test ( $p=0.05$ ,  $n=4$ )

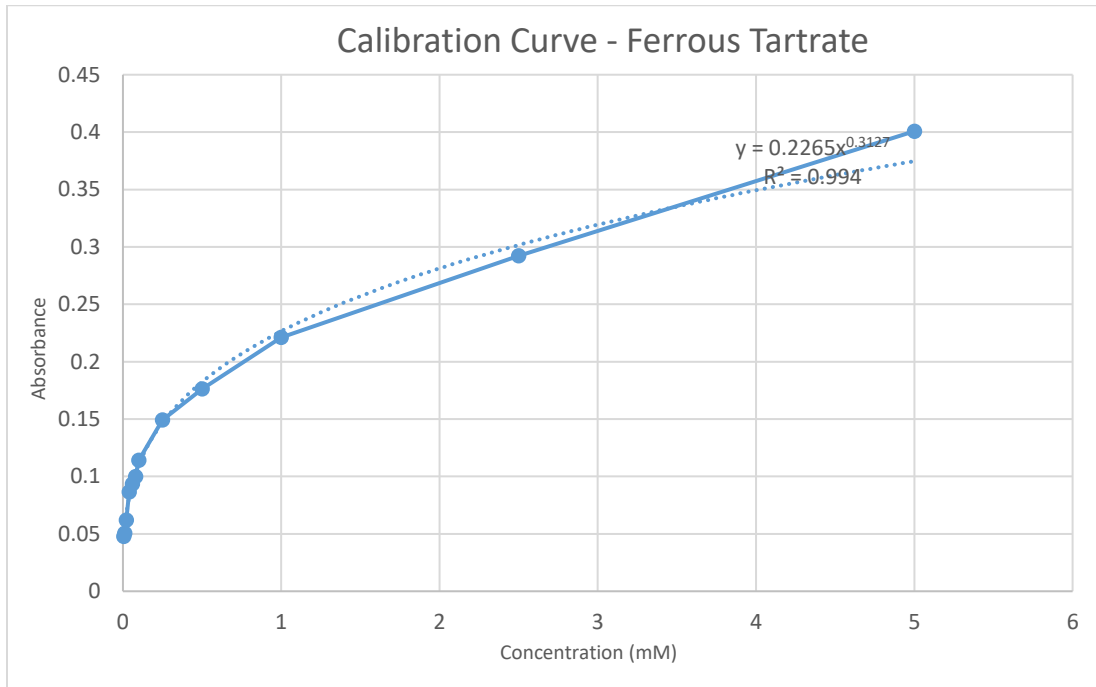


Figure 59. Calibration Curve for Ferrous Tartrate Method (Experiment No.2)

Additionally, the gel residuals were diluted and measured with Ferrous Tartrate by the end of the experiment, to detect the EGCG concentration still carried in the hydrogel (Figure 58). The absorbance values of bare HA-pNIPAM (Control3) were subtracted, in order to have the original values of EGCG absorbance. Based on the calibration curve (Figure 59), the matching between the absorbance and the respective concentration values was obtained for experiment No.2 and graphs 55-58.

UV measurements were obtained for the same experiments. The respective results are represented on the following graphs.

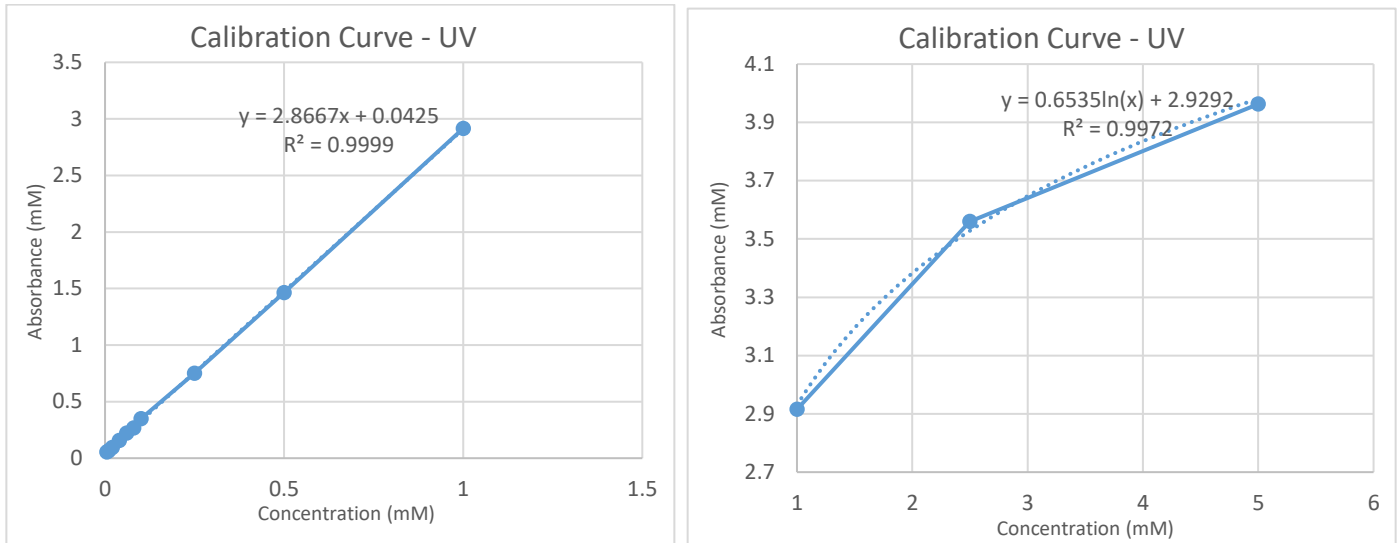


Figure 60. Calibration Curve for UV Measurements (Experiment No.2)

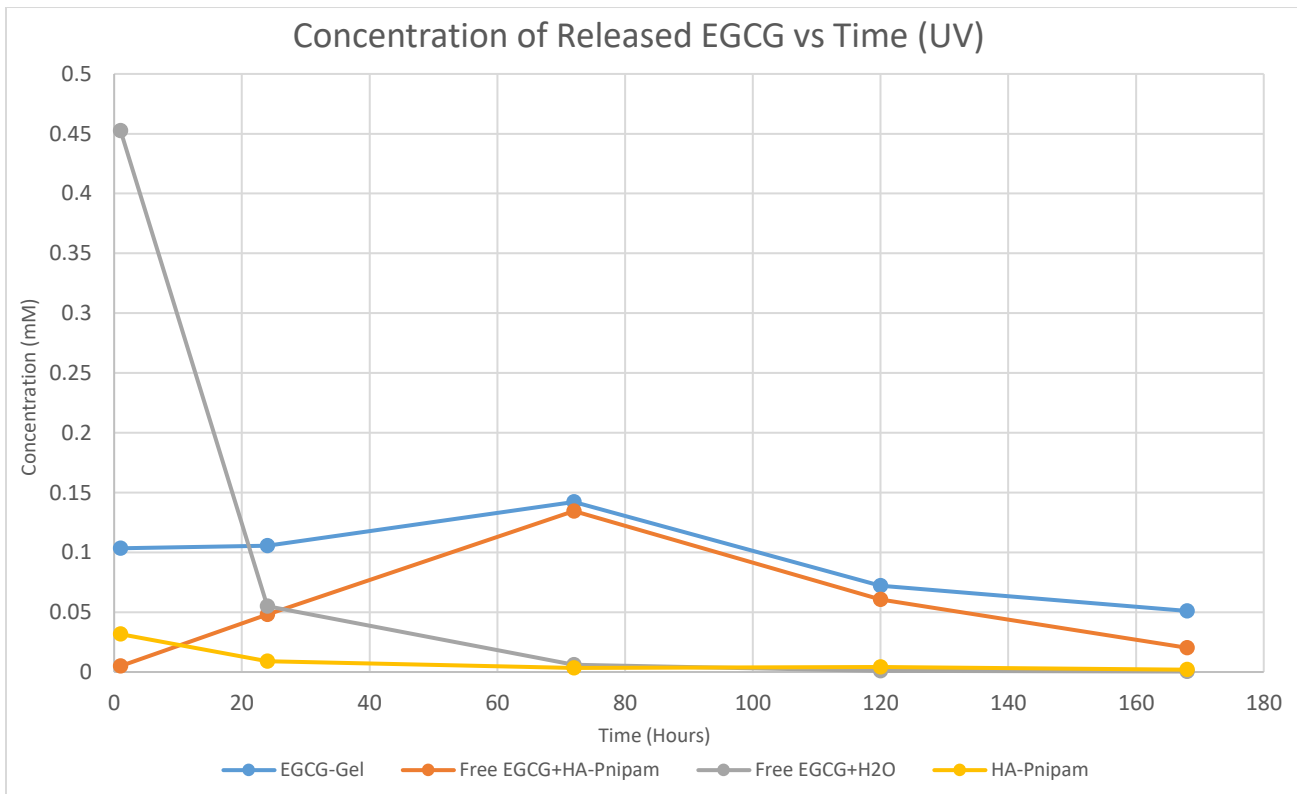


Figure 61. Concentration of Released EGCG Along Time through UV Measurements (Experiment No.2)

As mentioned in the results, there is gel collapsing in one of the DDS samples, which may affect the absorbance measurements. Indeed, this is obvious in Figure 60, as the release rates of EGCG in these samples is larger than in previous repetition. As in experiment No.1, measurements made through Ferrous Tartrate assay appear to have some differences with

results of UV Spectrum. However, in this case UV measurements seem to correspond better in reality, as EGCG's initial concentration in "Free EGCG with water" (Control2) samples are given to have 0.45mM. For cases of encapsulated and free EGCG mixed with hydrogel, the release concentrations reach 0.142mM and 0.135Mm, respectively. The same stands for cumulative and % cumulative release graphs (Figures 62, 63), were encapsulated EGCG seems to be released up to 91.4% and free EGCG mixed with hydrogel (Control3) up to 49.9%. Overall, the determined release concentration values of UV measurements don't agree with concentration values of colorimetric method in Experiment No.2, but the general profiles are alike. As in previous experiment, also here, the total of the released and the entrapped into the gels EGCG concentration is not equal to 5mM, according to absorption measurements (Figure 64).

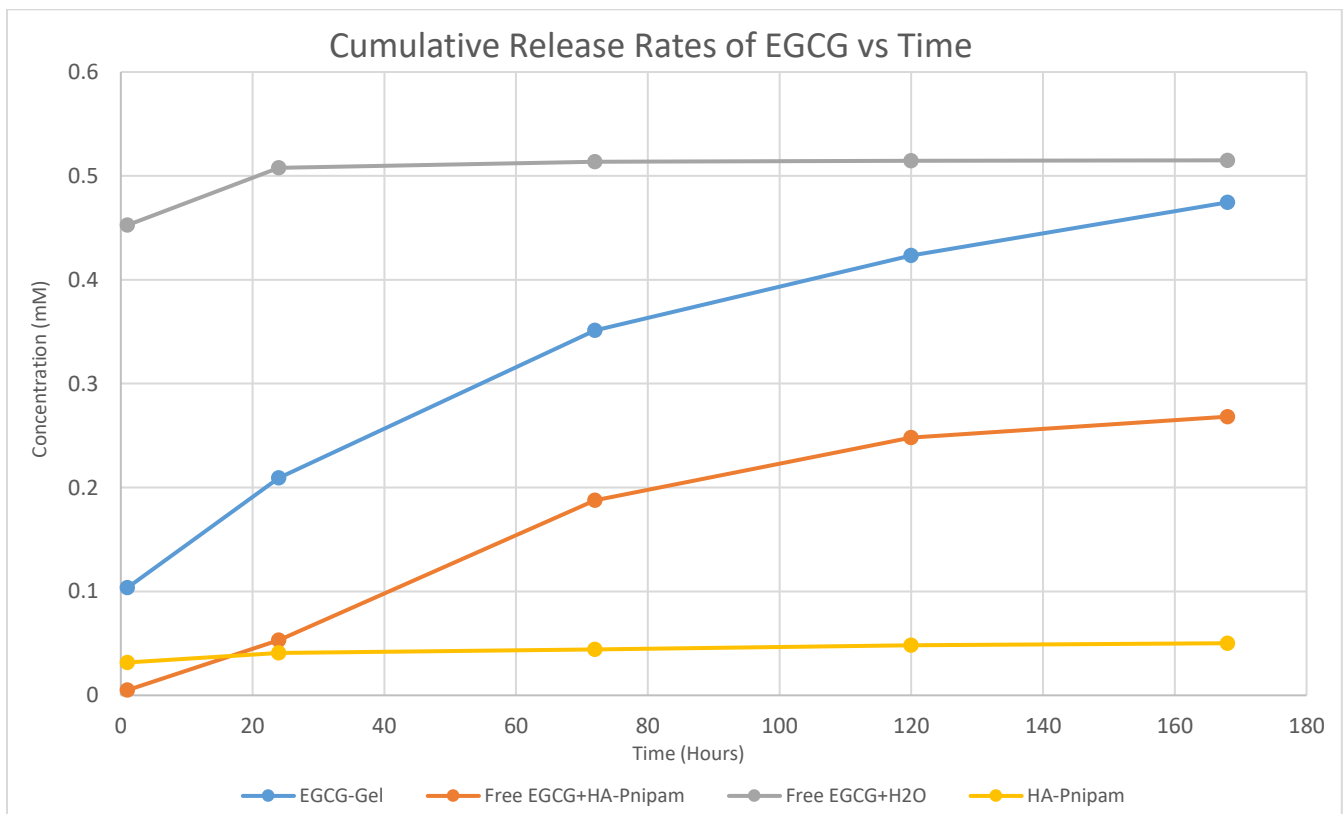


Figure 62. Cumulative Release Rates of EGCG Along Time through UV Measurements (Experiment No.2)



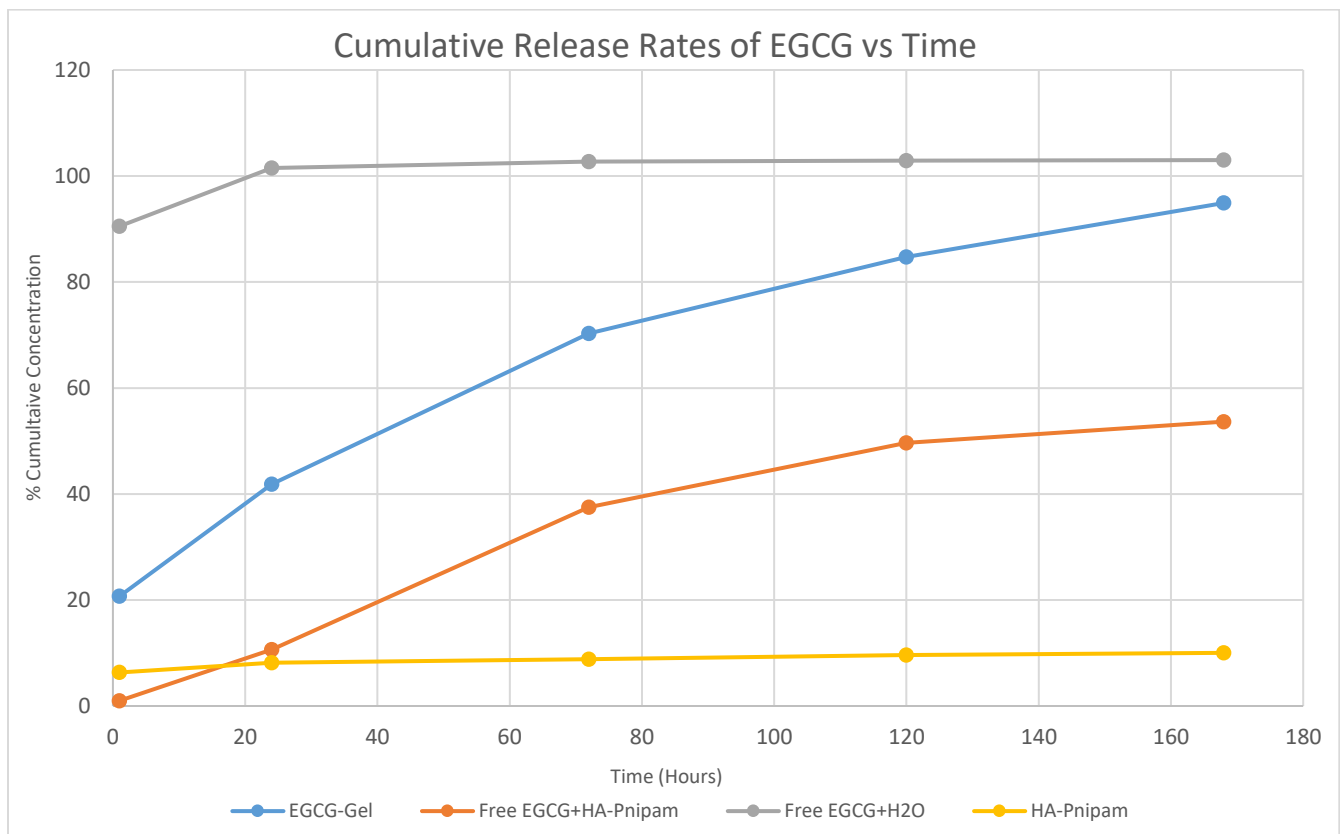


Figure 63. % Cumulative Release Rates of EGCG Along Time through UV Measurements (Experiment No.2)

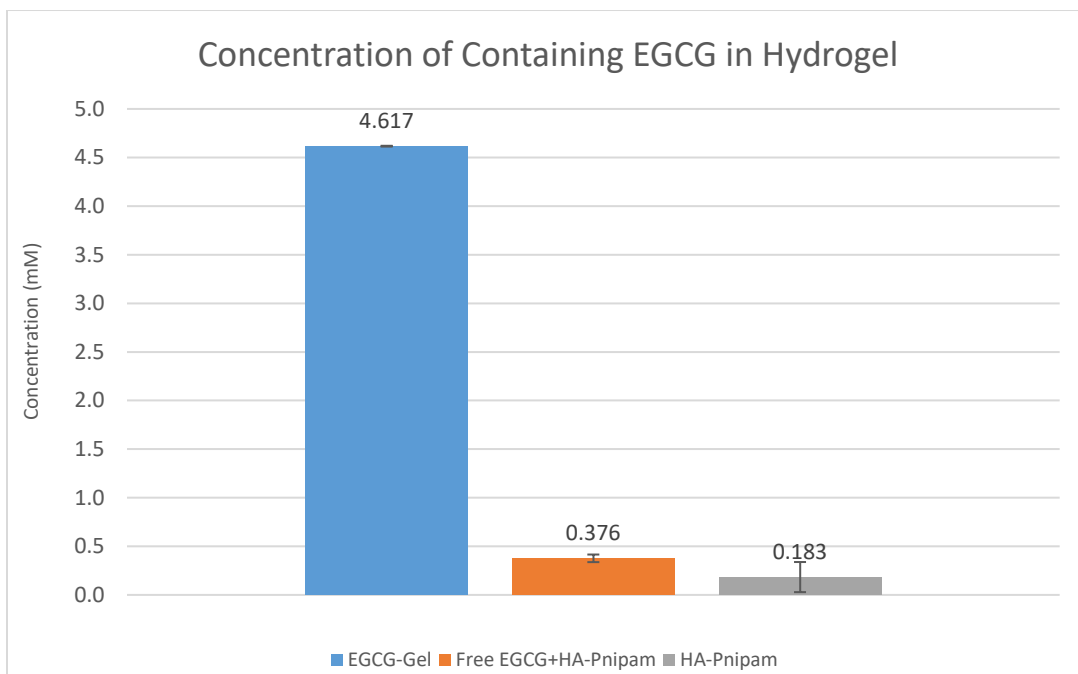


Figure 64. EGCG Concentration Contained in the Remaining Hydrogel (if stated) by the end of the Experiment (Experiment No.2). Statistical analysis with Kruskal-Wallis test ( $p=0.1$ ,  $n=12$ )

### ❖ Experiment No.3

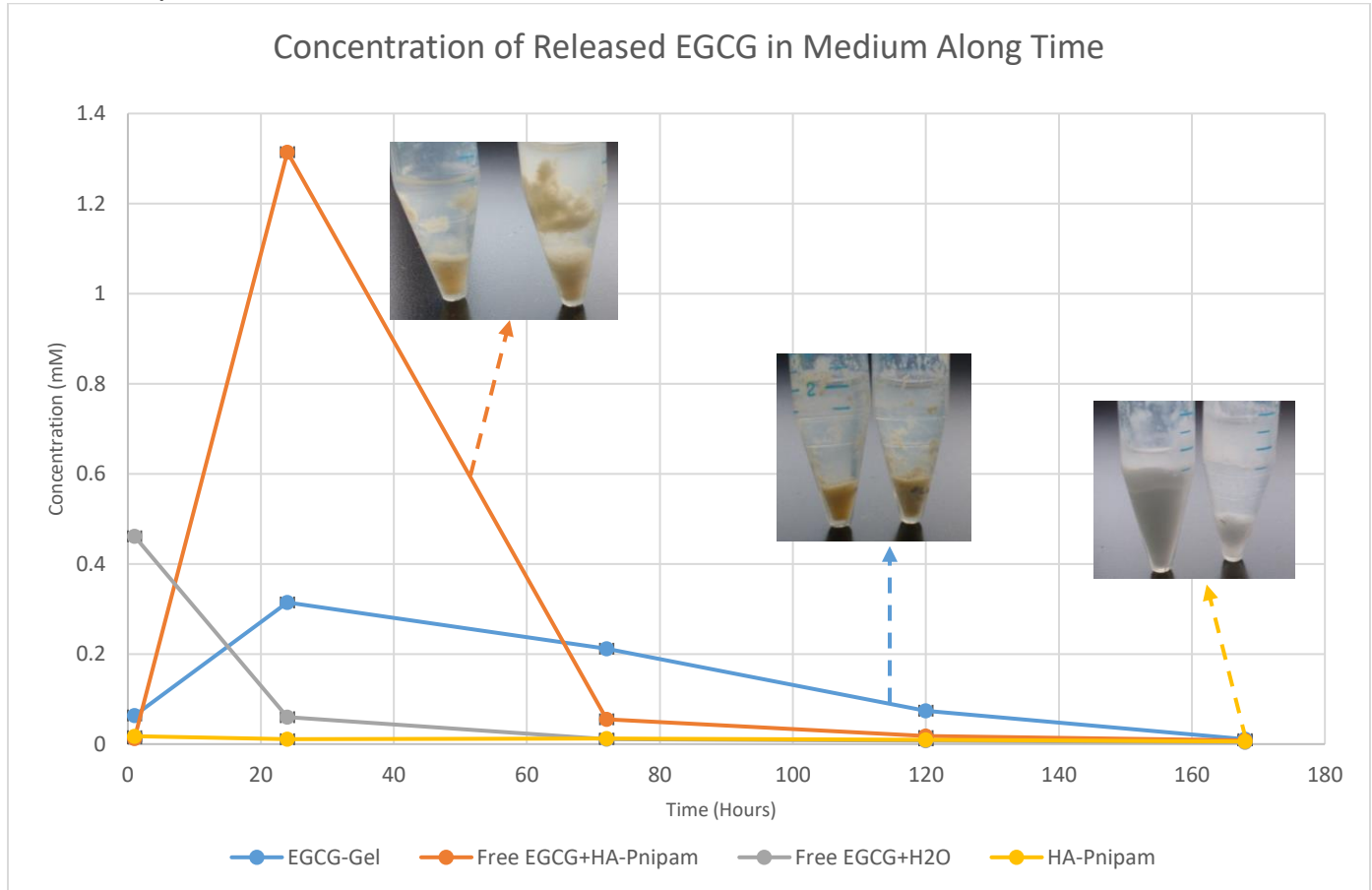


Figure 65. Concentration of Released EGCG in the medium of NaCl 0.9%, Along Time. The respective images of the remaining gels after 1 week of experiment duration. (Experiment No.3)

These are the results of the third repetition of the release experiments. In this case, there is gel collapsing in both DDS samples (Figure 65), where release rates of EGCG reach 0.31mM at  $t=1$  day. For free EGCG in HA-pNIPAM samples, gel collapsing takes place in both samples, where release rates of EGCG reach 1.3mM. In the case of free EGCG in water the initial concentration was estimated to be 0.46mM, which corresponds to the expected one, according to dilution law ( $C_1V_1=C_2V_2$ ). Finally, gel collapse also takes place in one of Control3 samples.

The cumulative release rates (graph 65) of this experiment is represented above, indicating the total amount of EGCG that was released in each case. The % cumulative release rates graph (figure 67) indicates that encapsulated EGCG is released in a percentage above 100% (135%), while the total released concentration of EGCG for Control1 and Control2 are 281% and 108%, respectively. As in previous cases, the percentage values of cumulative concentration have been calculated in respect of 0.5mM, because this is the total EGCG amount that can be released in the medium. However, for encapsulated and free EGCG mixed with hydrogel samples it seems that the total released EGCG amount exceeds 0.5mM. This is probably caused by gel collapsing that takes place for both samples.

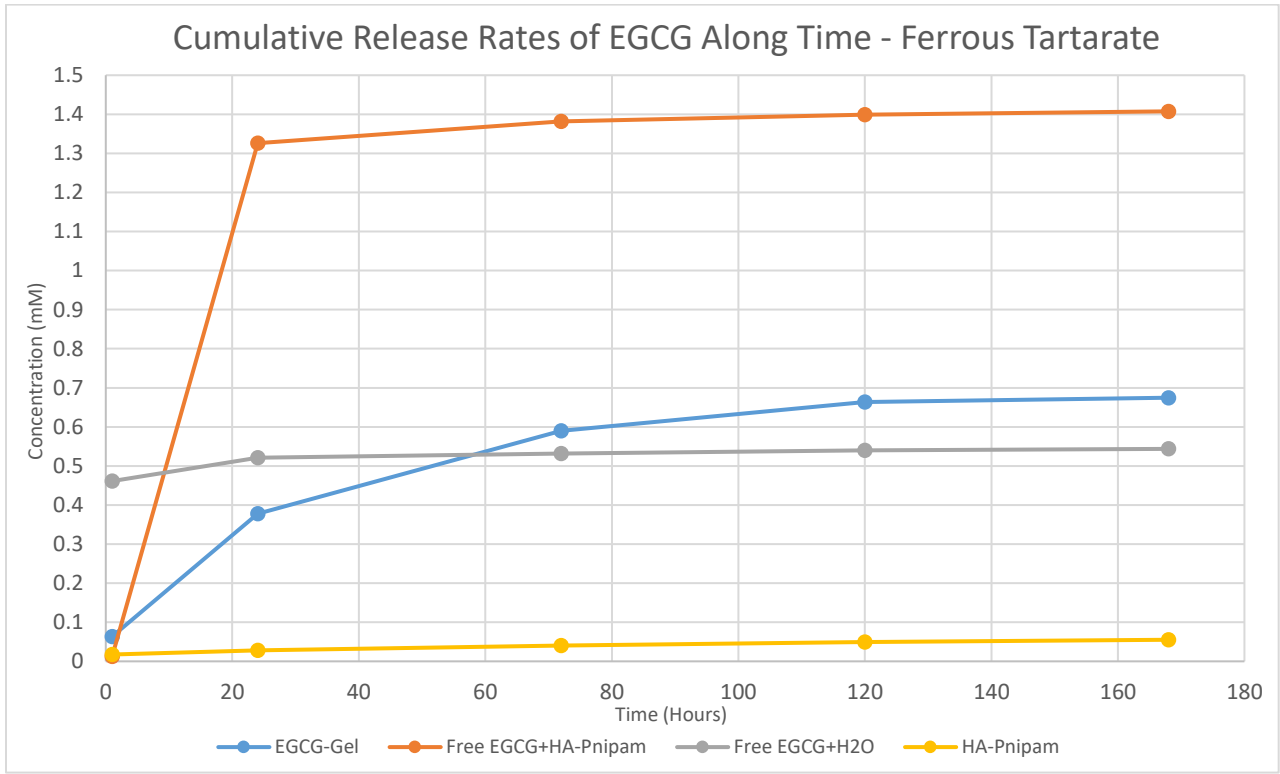


Figure 66. Cumulative Concentration of Released EGCG in the medium of NaCl 0.9%, Along Time. (Experiment No.3)

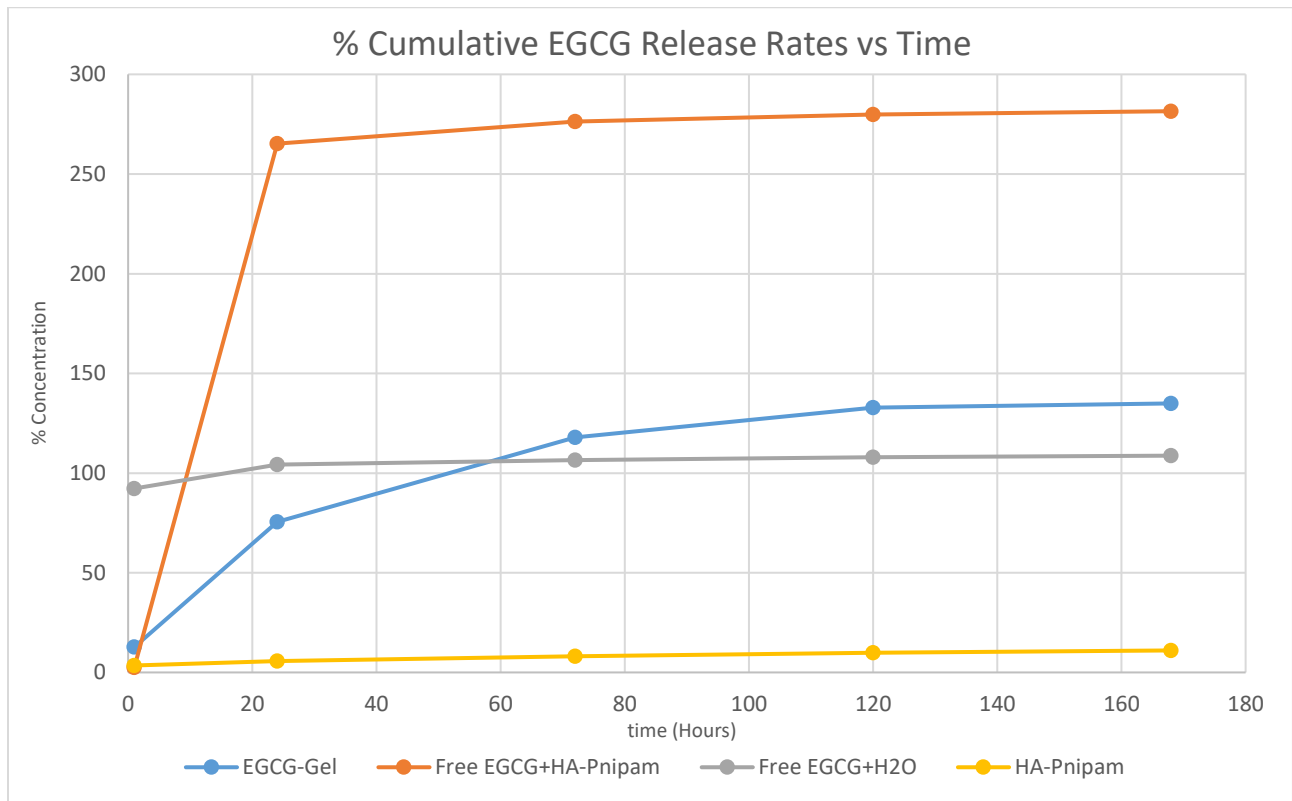


Figure 67. % Cumulative EGCG Release Rates in 0.9% NaCl medium Along Time. The % rates have been estimated in respect of the 0.45mM amount of concentration which is the maximum amount of EGCG that can be released in each sample, as the concentration of EGCG before the addition of 10mL release medium was 5mM. (Experiment No.3)

Additionally, the graph for the gel residuals (Figure 68) indicated that less than 1.2mM of encapsulated EGCG has been released in the 0.9% NaCl medium and more than 4.1mM of free EGCG has been released from free EGCG with HA-Pnipam (Control1) samples. The absorbance values of bare HA-pNIPAM control were subtracted, in order to have the original values of EGCG absorbance. However, this graph is not consistent with figures 65 and 66. This kind of inconsistency may be caused by gel collapsing, as diluted gel in the release medium can probably compromise the reaction between EGCG and Ferrous Tartrate assay and the absorbance measurements.

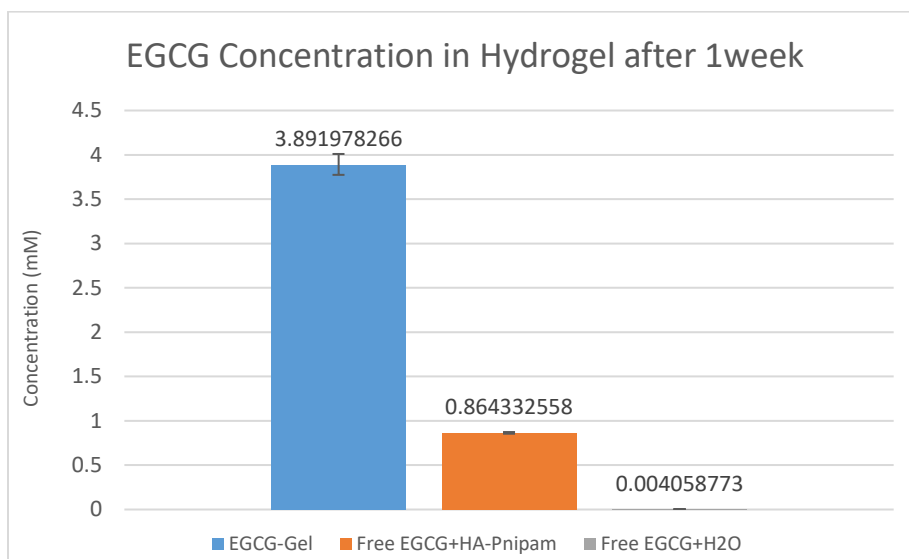


Figure 68. EGCG Concentration Entrapped in Hydrogel by the End of the Experiment (Experiment No.3). Statistical analysis with Kruskal-Wallis test ( $p=0.05$ ,  $n=4$ )

Based on the following calibration curve (Figure 69), the matching between the absorbance and the respective concentration values was obtained for experiment No.3.

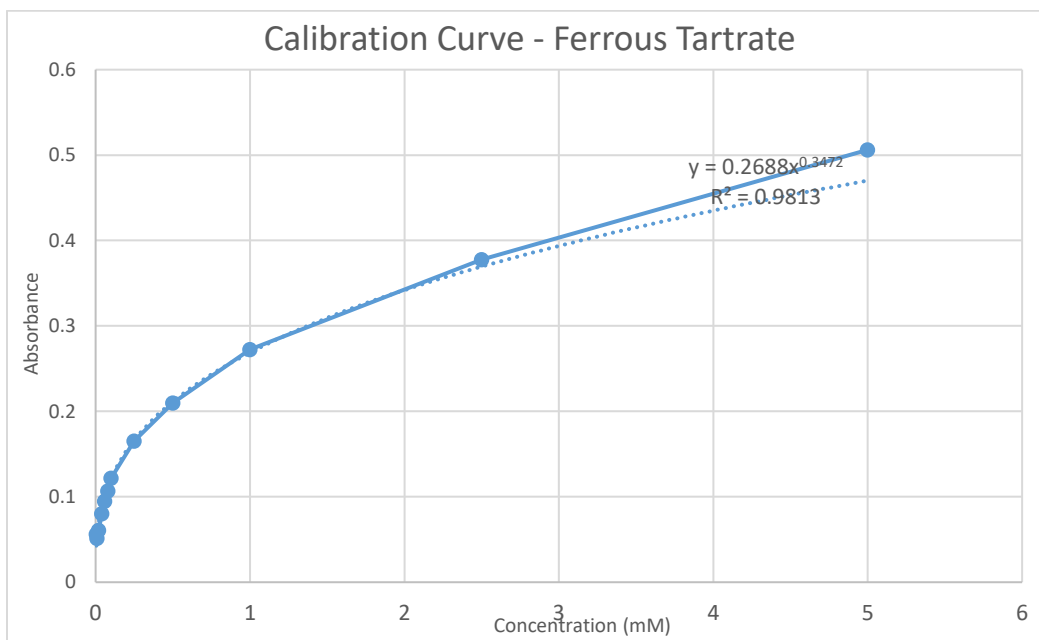


Figure 69. Calibration Curve for Ferrous Tartrate Method (Experiment No.3)

The respective results indicated by absorbance in UV spectrum are represented on the following graphs.

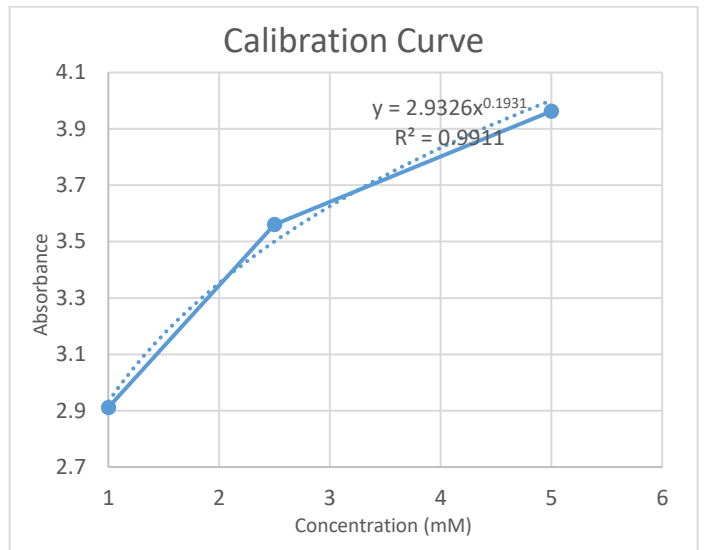
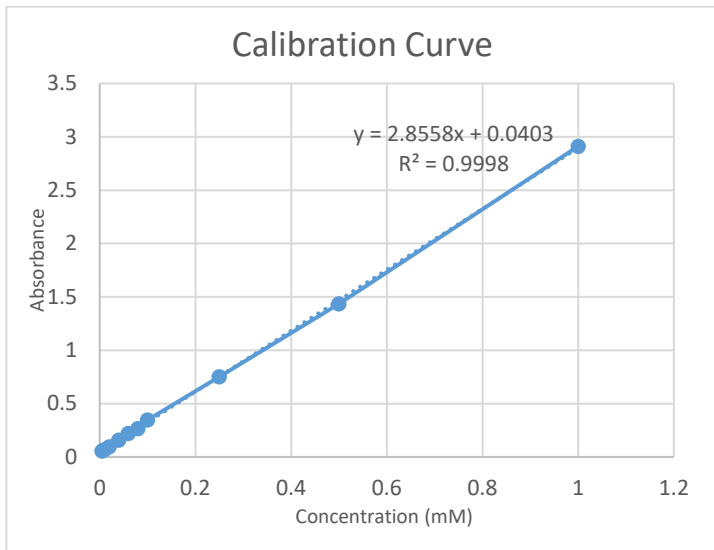


Figure 70. Calibration Curve for UV Measurements (Experiment No.3)

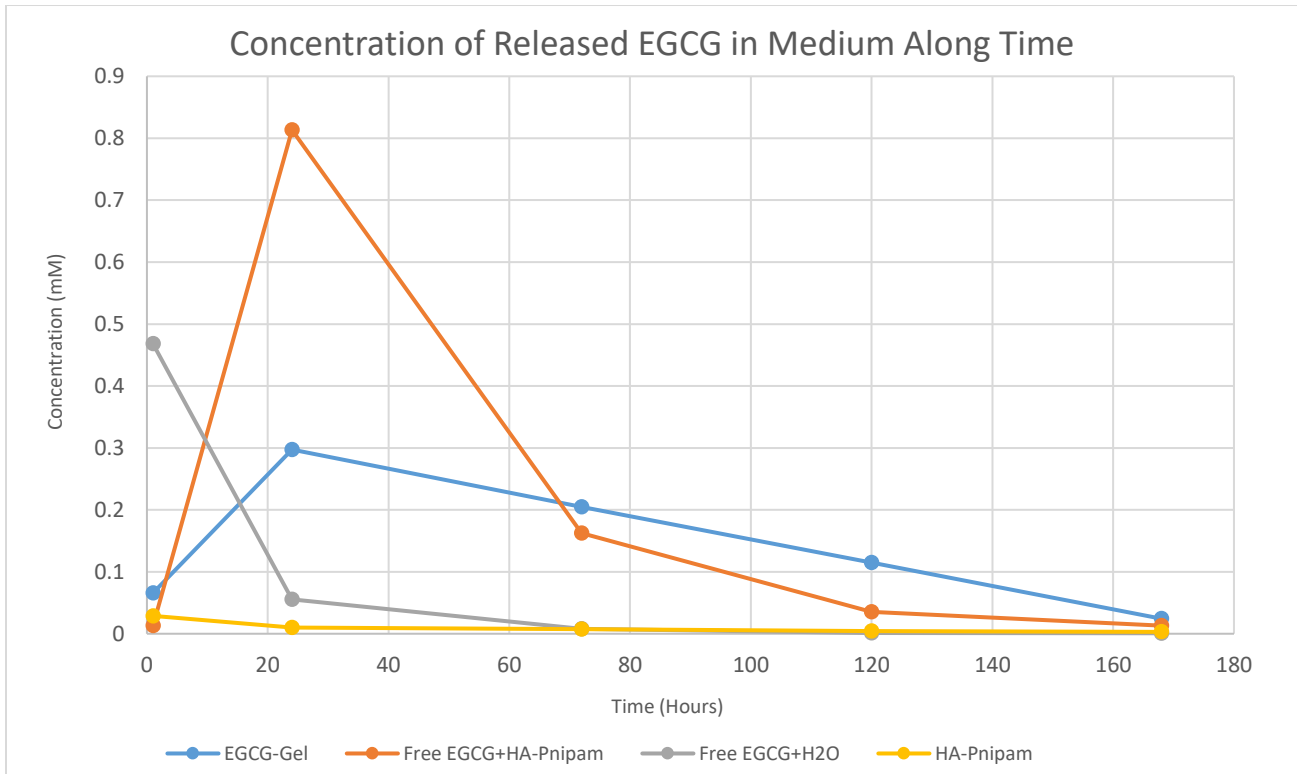


Figure 71. Concentration of Released EGCG Along Time through UV Measurements (Experiment No.3)

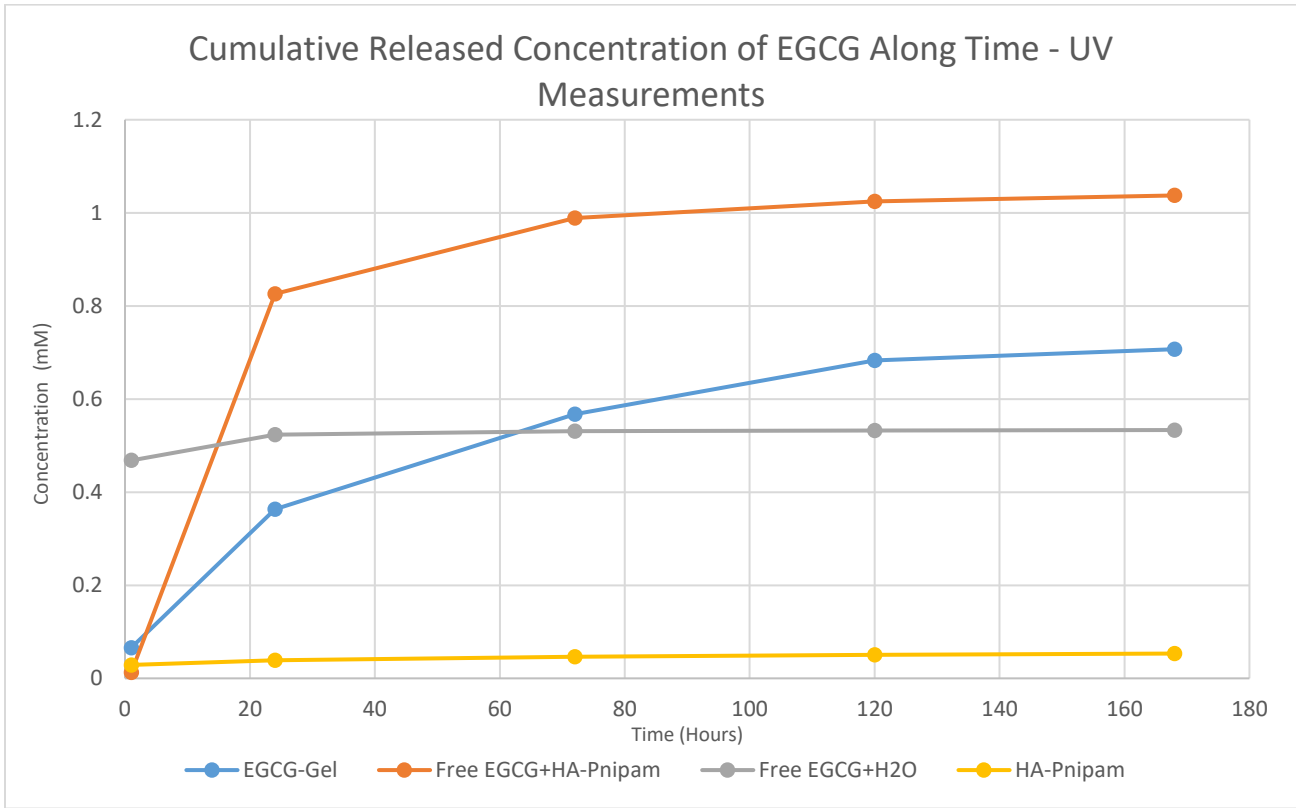


Figure 72. Cumulative Release Rates of EGCG Along Time through UV Measurements (Experiment No.3)

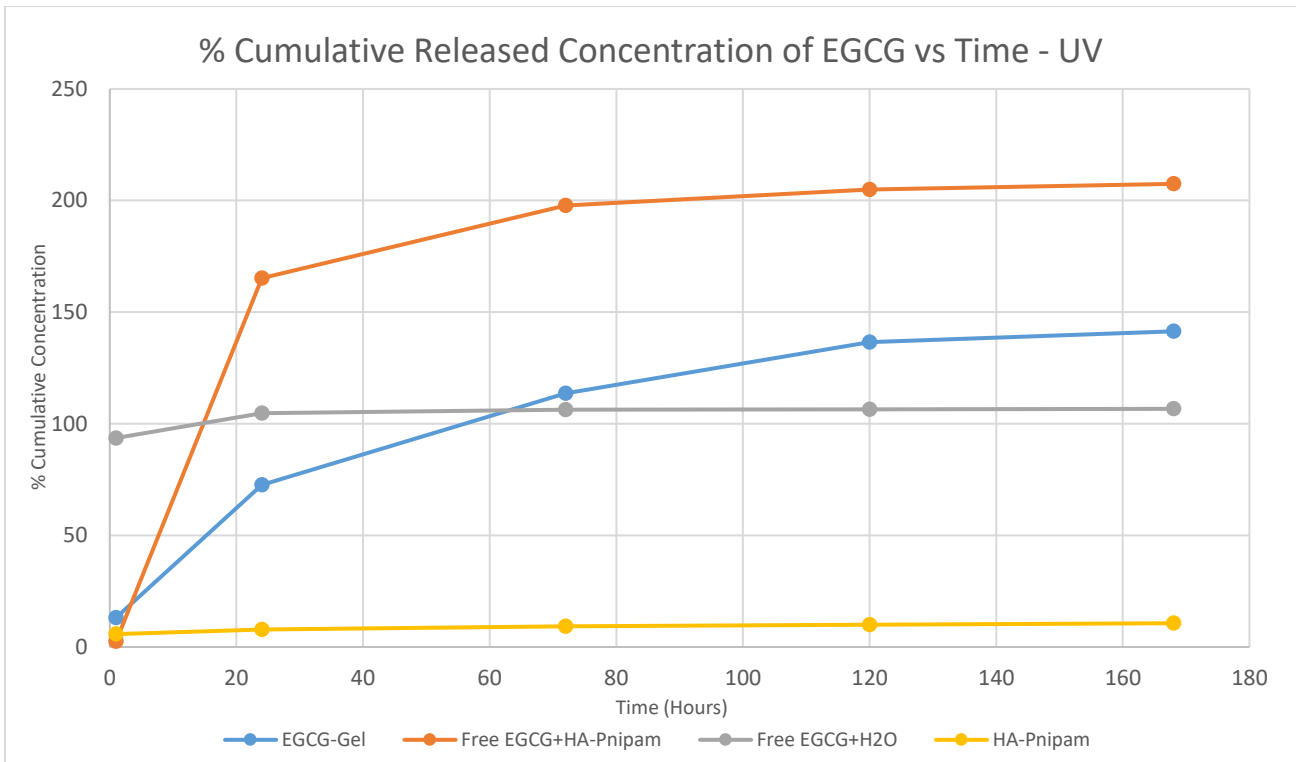


Figure 73. % Cumulative Release Rates of EGCG Along Time through UV Measurements (Experiment No.3)

During the last repetition of the release experiment, there is gel collapsing in both DDS samples, that can probably affect any of the measurements. The maximum release rate of encapsulated EGCG is 0.3mM (figure 71). For this repetition, the maximum release rate of encapsulated EGCG measured with Ferrous Tartrate (0.335mM) coincides with the value derived by UV measurements (0.3mM). Also, there is gel collapsing in both samples of Control2 and the release rates of EGCG reach 0.8Mm, compared with 1.3mM derived by Ferrous Tartrate. The initial released concentration of EGCG Control2 samples is almost 0.47mM, which corresponds to the expected one, according to the dilution law ( $C_1V_1=C_2V_2$ ). Finally, there is also gel collapse in one of Control3 samples.

For cumulative and % cumulative release graphs (Figures 72, 73), encapsulated EGCG and free EGCG mixed with hydrogel seem to be released beyond 100%. A reason for this, is probably gel collapsing of these samples and the wavelength spectrum that gel may absorb in. As in previous experiment, also here, the total of the released and the entrapped into the gels EGCG concentration is not equal to 5mM, according to absorption measurements (Figure 74).

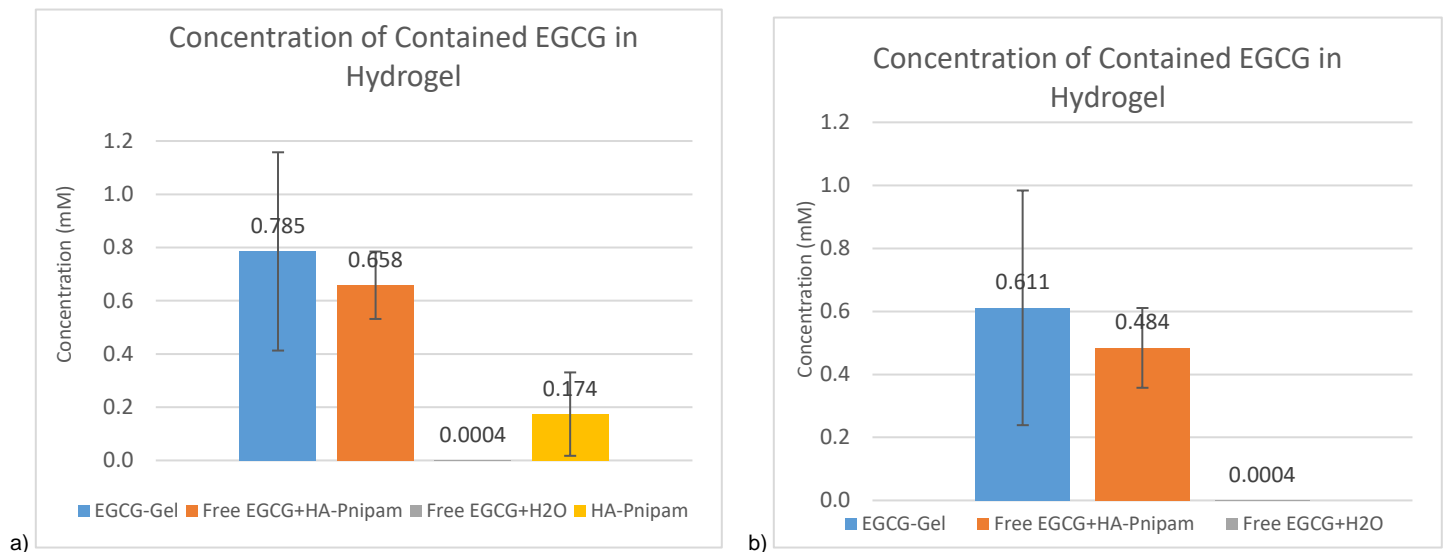


Figure 74. EGCG Concentration Contained in the Remaining Hydrogel (if stated) by the end of the Experiment (Experiment No.1). In graph (b) the absorbance rate of bare HA-pNIPAM has been subtracted in contrast with graph (a) (Experiment No.3). Statistical analysis with Kruskal-Wallis test ( $p=0.1$ ,  $n=12$ )

#### ❖ Overall results

The cumulative release rates (Figure 75) of the individual repetitions described separately above, are represented below. Also, the respective results indicated by absorbance in UV spectrum are represented on the following graphs (Figures 76-78).



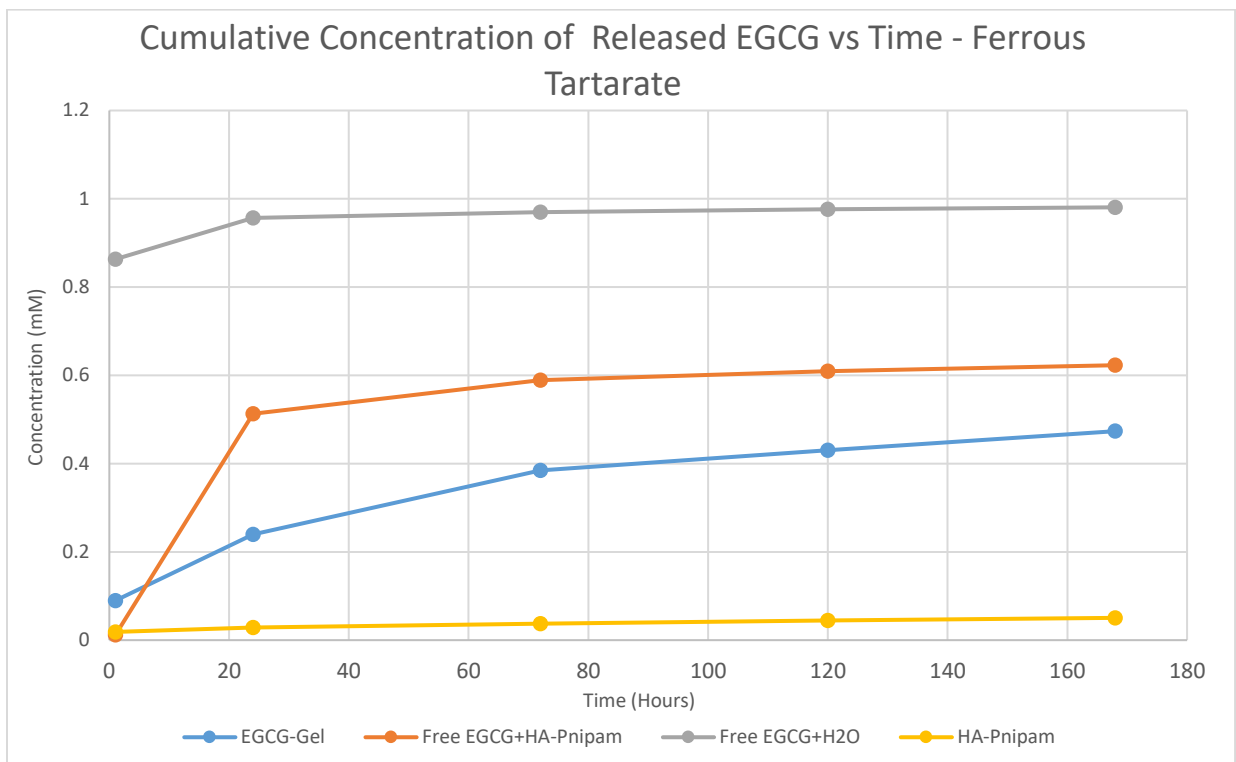


Figure 75. Cumulative Concentration of Released EGCG in the medium of NaCl 0.9%, Along Time. The release rates of the encapsulated EGCG is much lower (0.49mM), than free EGCG in hydrogel (0.64mM) and free EGCG in water (1.05mM). (Overall Results) Statistical analysis with Kruskal-Wallis test ( $p=0.1$ ,  $n=12$ )

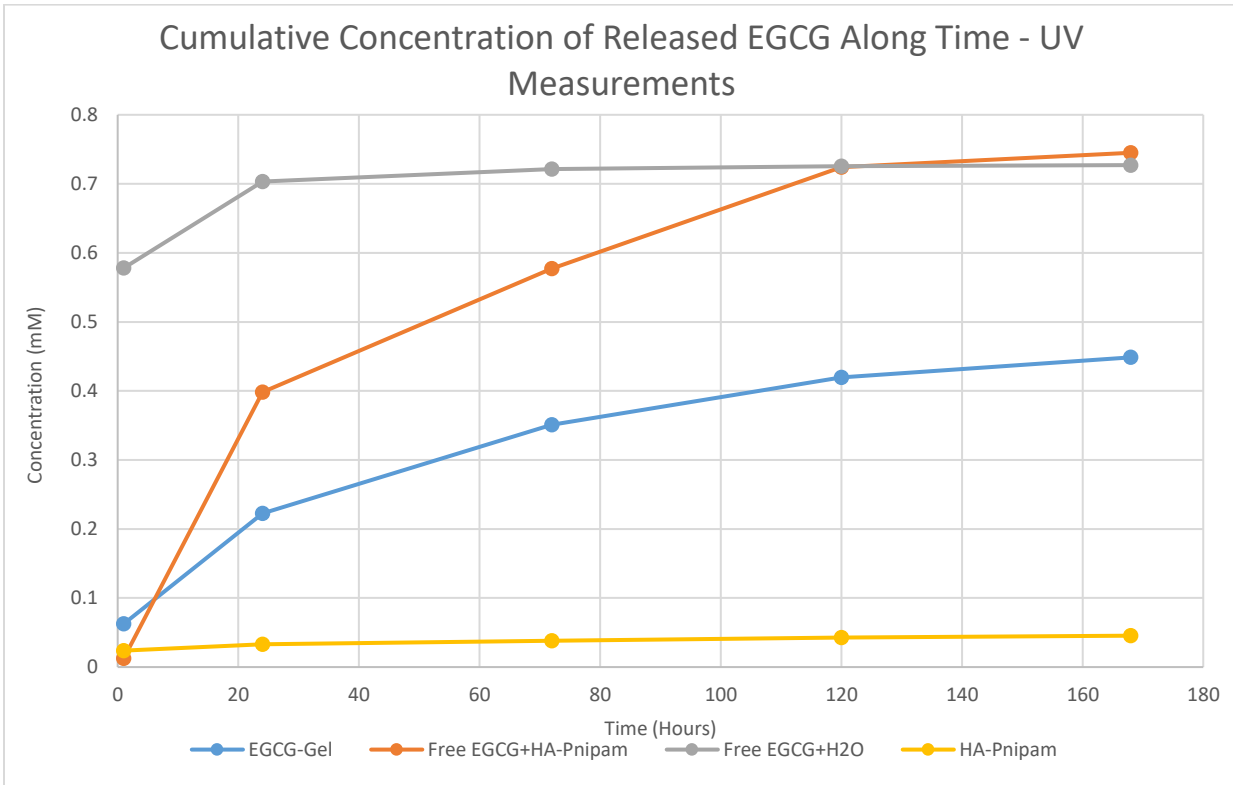


Figure 76. Cumulative Release Rates of EGCG Along Time through UV Measurements (Overall Results) Statistical analysis with Kruskal-Wallis test (p=0.1, n=12)

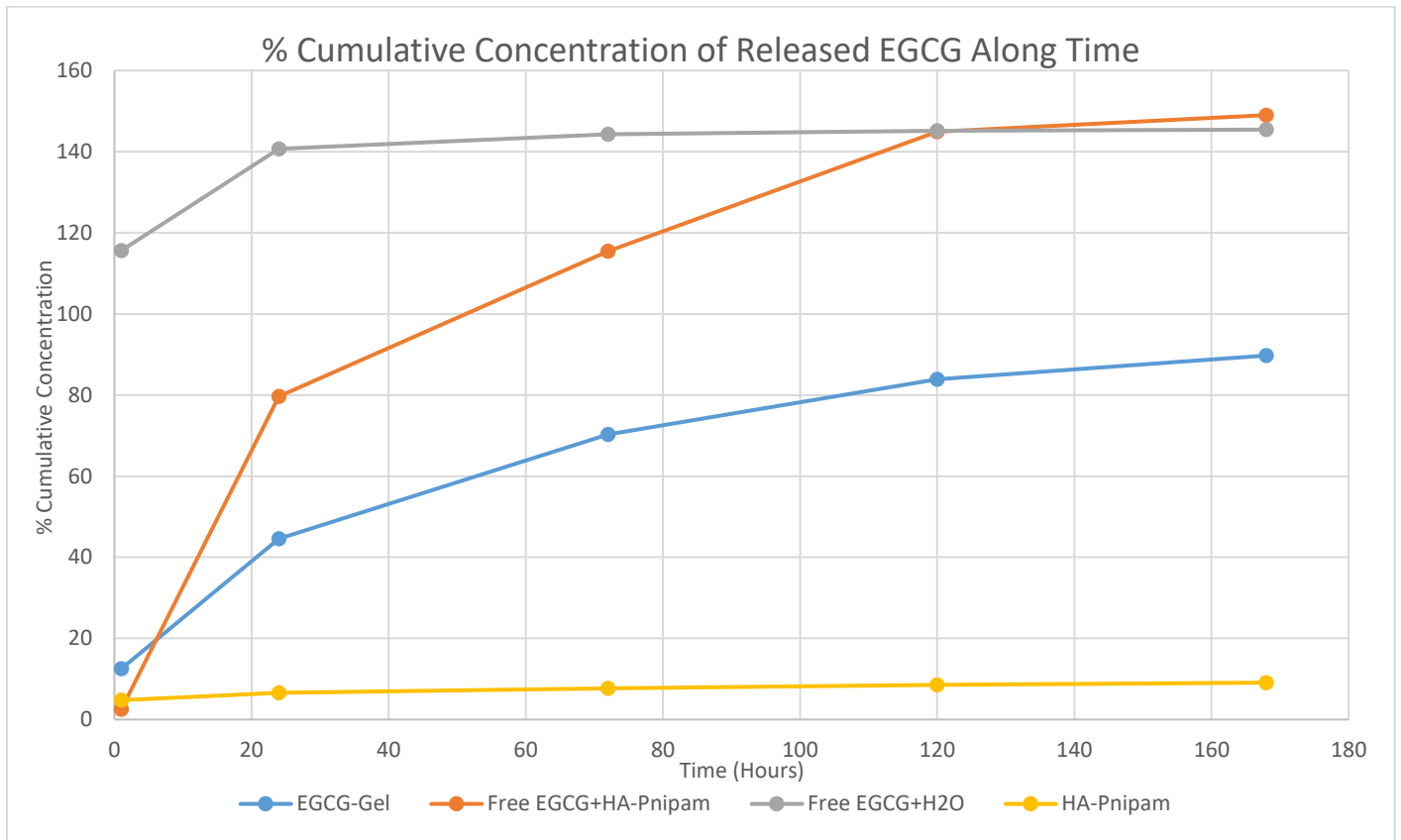


Figure 77. % Cumulative Release Rates of EGCG Along Time through UV Measurements (Overall Results) Statistical analysis with Kruskal-Wallis test ( $p=0.1$ ,  $n=12$ )

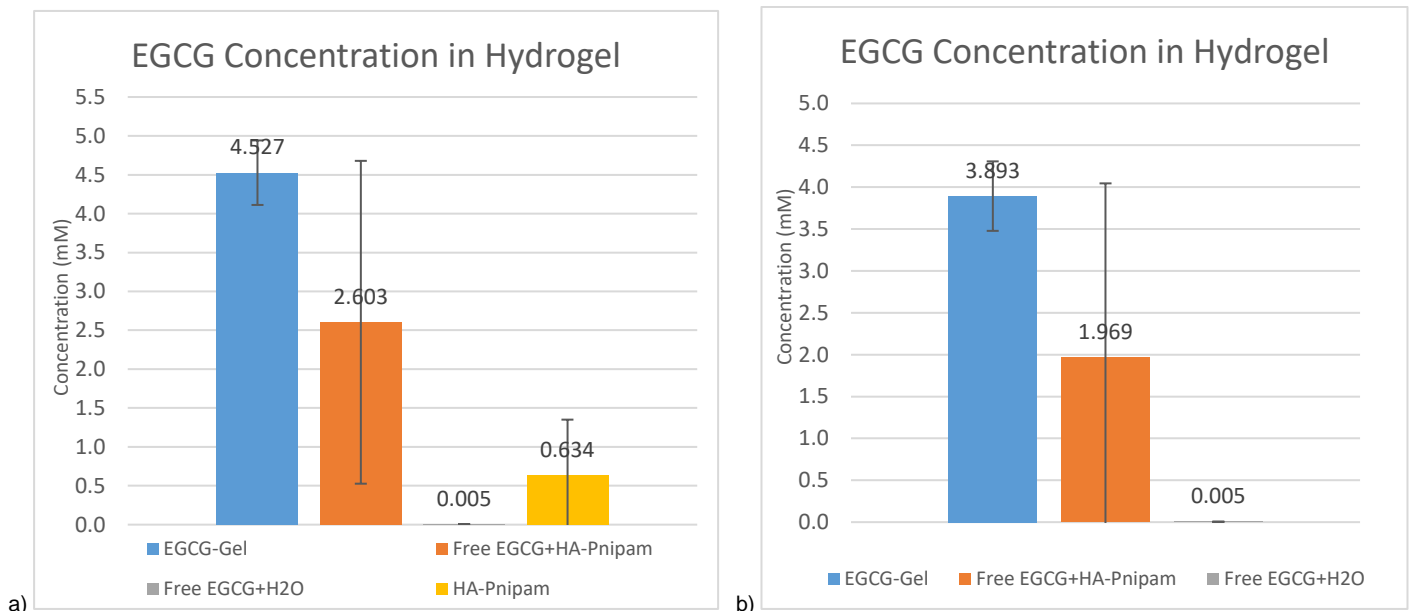


Figure 78. EGCG Concentration Contained in the Remaining Hydrogel (if stated) by the end of the Experiment (Experiment No.1). In graph (b) the absorbance rate of bare HA-pNIPAM has been subtracted in contrast with graph (a) (Overall Results) Statistical analysis with Kruskal-Wallis test ( $p=0.1$ ,  $n=12$ )

## 5. EGCG Activity During Release Experiments (DPPH Assay)

### ❖ Experiment No.1

EGCG activity is calculated in respect to blank DPPH solution in ethanol (negative control). The results represented in % Activity as a function of time (Figure 79), demonstrate that encapsulated EGCG features limited activity (12.3%), in comparison with free EGCG mixed with hydrogel (Control1, 36.9%) and free EGCG in water (Control2, 82.8%), while all of them decrease rapidly by the end of the experiment. However, these activity values are directly related with the respective concentration values of EGCG. Therefore, the graph of normalized activity represents a clearer interpretation of EGCG activity (Figure 80). Indeed, in this graph the profiles of EGCG activity for all different kind of samples (DDS and Controls) appears to be more stable and have different trends than Figure 79. In more details, activity of encapsulated EGCG ranges between 0.23-2.43 units, while activity of free EGCG in hydrogel and free EGCG in water controls range between 2.33-2.44 and 1.33-2.66, respectively.

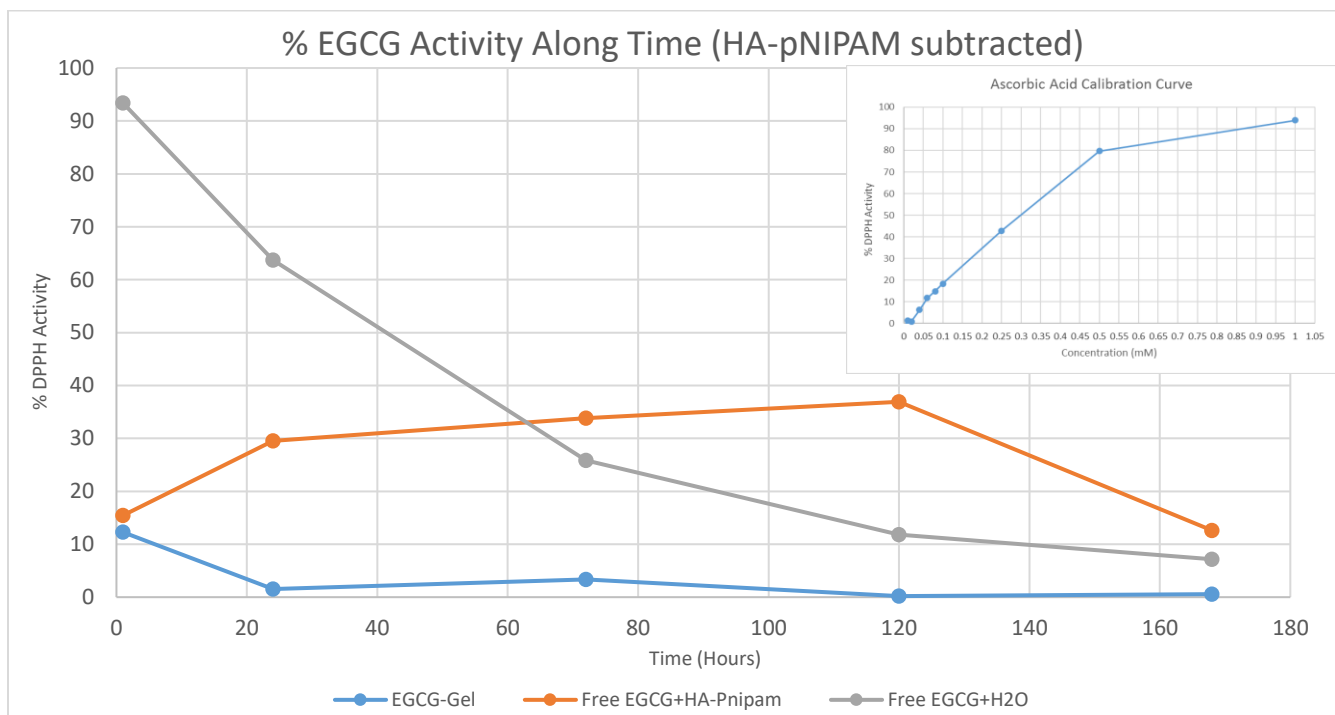


Figure 79. % Activity of Released EGCG as a Function of Time. The respective values of HA-pNIPAM control have been subtracted, to have the original activity of EGCG for Each sample. The calibration curve of L-Ascorbic Acid (Positive Control) has been added as legend on the graph (Experiment No.1).

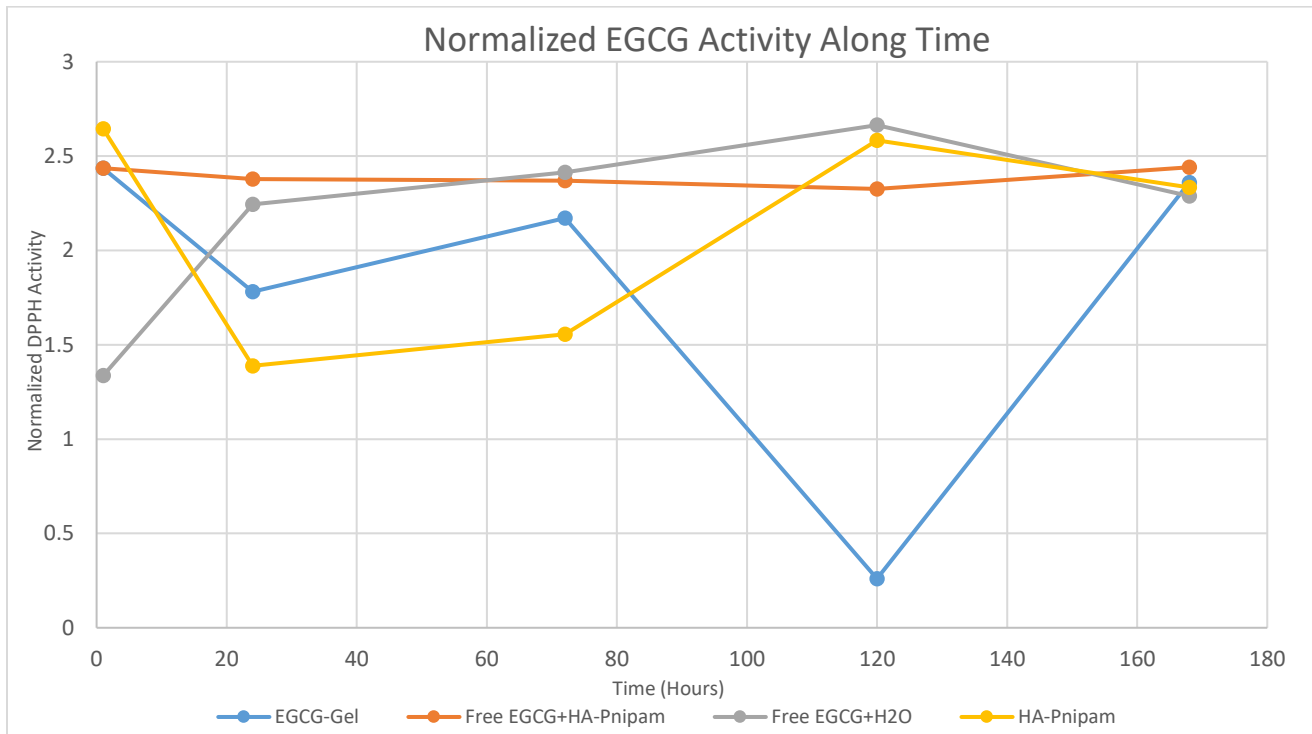


Figure 80. % Activity of Released EGCG as a Function of Time. The normalization has been obtained in respect of concentration. By this, the activity profiles of each sample have a different shape (Experiment No.1).

#### ❖ Experiment No.2

As in previous repetition, activity results are represented in % Activity along time graph (Figure 81). According to this, EGCG-Gelatin microparticles display activity equal to 13% (in experiment No.1 it was 12.3%), in comparison with Control2, which indicated activity equal to 21.7% (in experiment No.1 it was 36.9%), and Control3, which indicated activity equal to 90.2% (in experiment No.1 it was 82.8%). Obviously, activity values of experiment No.1 and 2 range close to each other.

The graph of normalized activity represents a clearer interpretation of EGCG activity (Figure 82). According to this graph, the profile of EGCG activity for each different sample appears to be more stable. Encapsulated and free EGCG mixed with hydrogel represent the same trend as in Figure 81. In more details, activity of encapsulated EGCG ranges between 0.76-0.89 units, while activity of Control1 and Control2 range between 0.7-0.97 and 1.37-0.58, respectively.

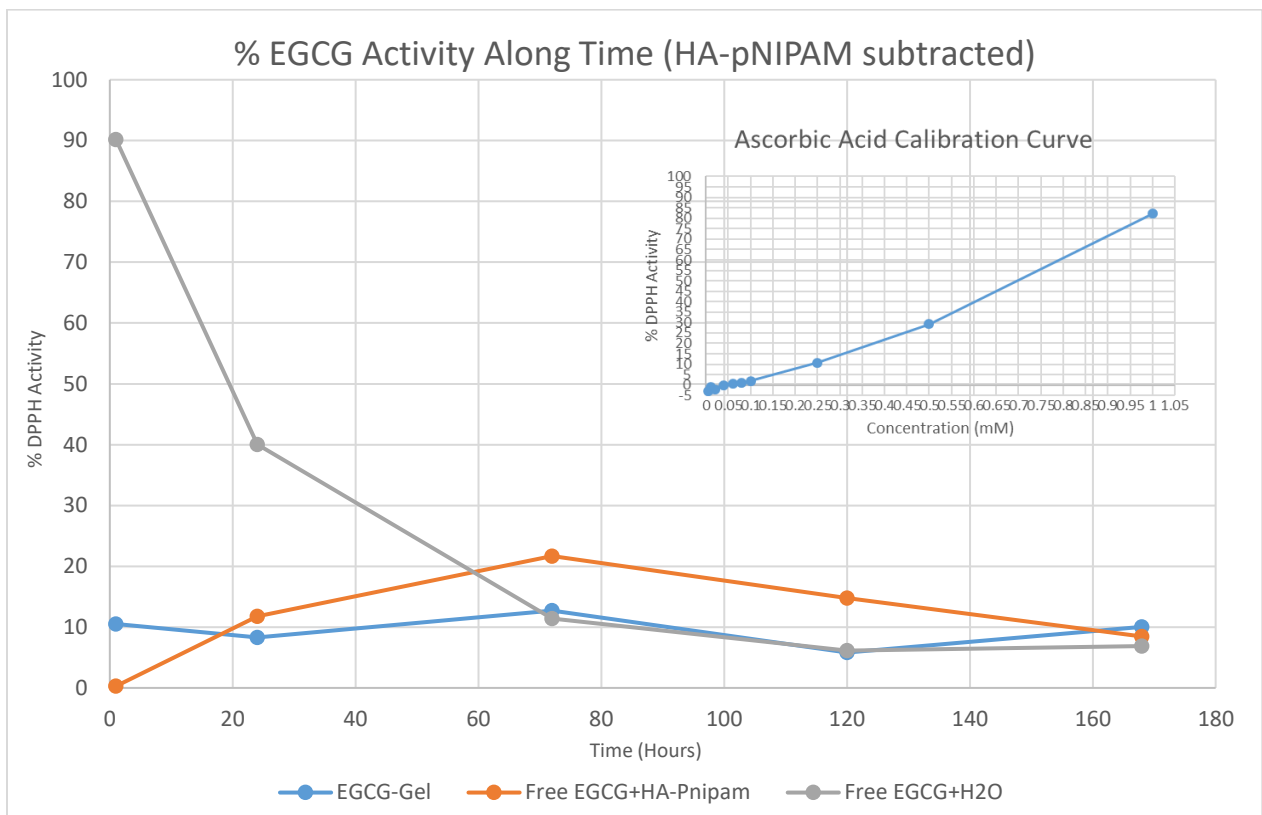


Figure 81. % Activity of Released EGCG as a Function of Time. The respective values of HA-pNIPAM control have been subtracted, in order to have the original activity of EGCG for Each sample. The calibration curve of L-Ascorbic Acid (Positive Control) has been added as legend on the graph (Experiment No.2).

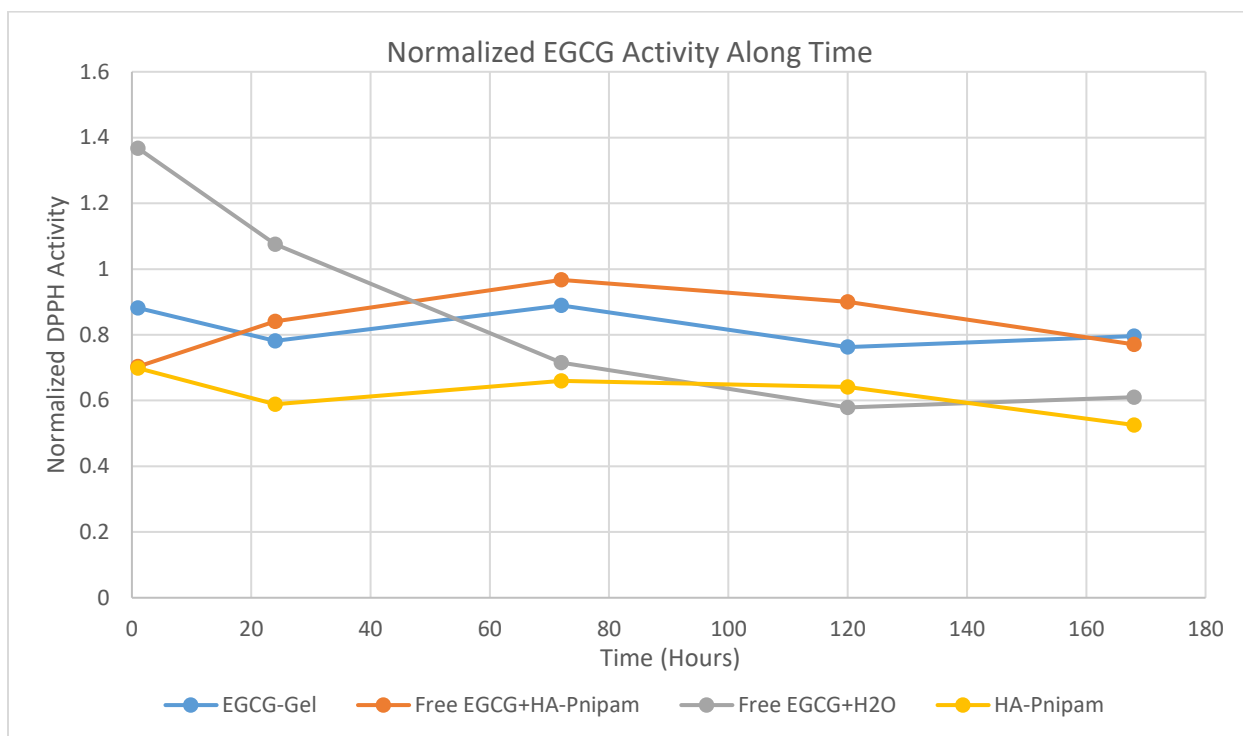


Figure 82. % Activity of Released EGCG as a Function of Time. The normalization has been obtained in respect of concentration. By this, the activity profiles of each sample have a different shape (Experiment No.2).

❖ Experiment No.3

In the last repetition of release and activity experiments, EGCG of the designed DDS display activity equal to 20.86% (13% and 12.3% in previous), in comparison with Control1, which indicated activity equal to 51.27% (21.7% and 36.9% in previous), and Control2, which indicated activity equal to 90.59% (90.2% and 82.8% in previous). In this case, the activity rates are a bit higher for encapsulated EGCG and Control1 (Figure 83), than in the first two repetitions. Contrariwise, Control2 indicated rates almost equal for all the three repetitions.

The graph of normalized activity represents a clearer interpretation of EGCG activity (Figure 84). According to this graph, the profile of EGCG activity for each different sample appears to decrease gradually between the first and the fifth day. In more details, the activity of encapsulated EGCG ranges between 1.53-2.48 units, while activity of Control1 and Control2 range between 0.63-2.46 and 0-2.35, respectively.

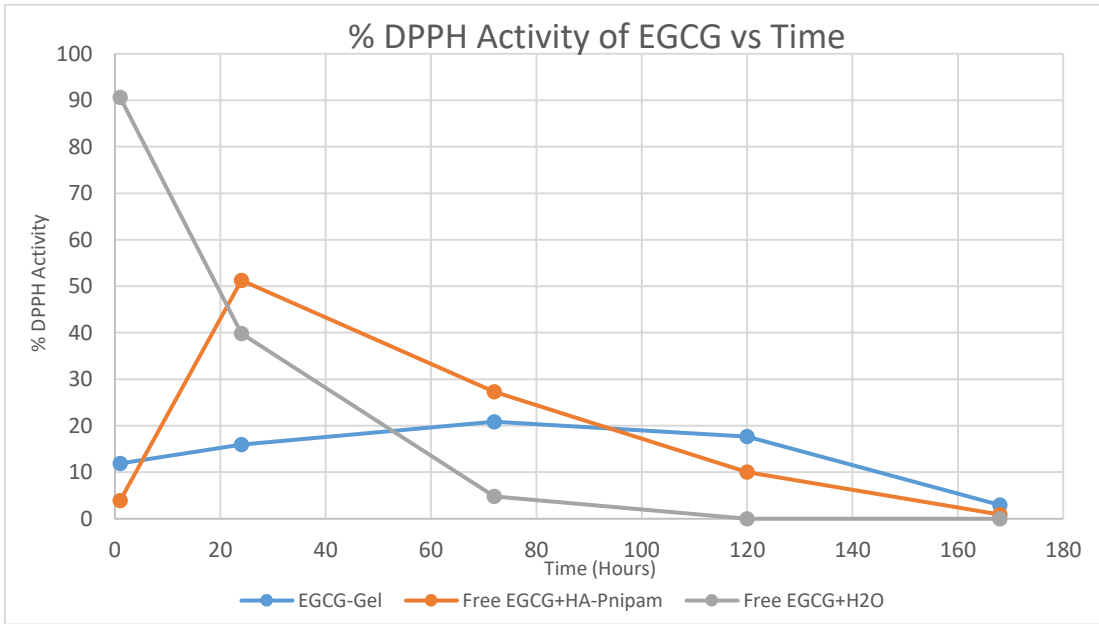


Figure 83. % Activity of Released EGCG as a Function of Time. The respective values of HA-pNIPAM control have been subtracted, in order to have the original activity of EGCG for Each sample. (Experiment No.3)

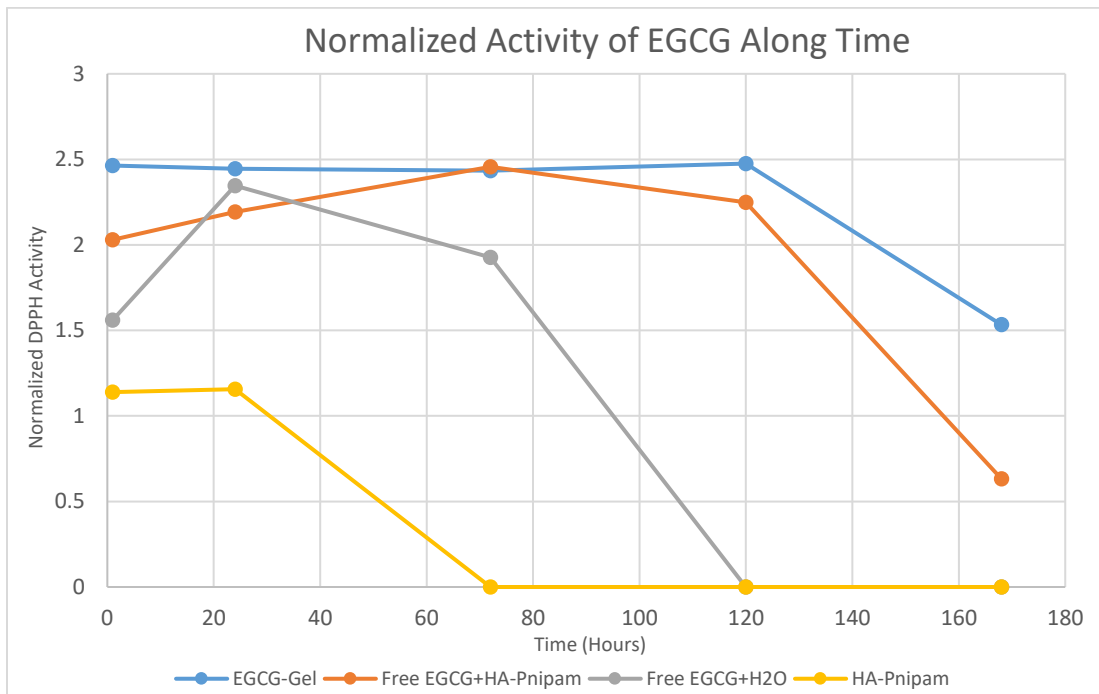


Figure 84. % Activity of Released EGCG as a Function of Time. The normalization has been obtained in respect of concentration. By this, the activity profiles of each sample have a different shape (Experiment No.3).



## 6. Protocols

### Electrospraying of Gelatin Microparticles

#### 1. 4 (or 6) %w/v Gelatin Solution

- ❖ Materials
  - Acetic acid 20% in water (solvent)
  - Gelatin Type A (G1890 - Sigma)
- ❖ Prepare 50mL of 4% gelatin solution by dissolving 2gr of gelatin powder in 50mL of 20% Acetic Acid.
- ❖ Stir at 40 °C for 4-6 hours (until gelatin is totally dissolved)
- ❖ Cool down to room temperature overnight, before spraying
- ❖ The solution might be sealed with parafilm, to avoid any evaporation

#### 2. Gelatin – GA Solution

- ❖ Prepare 5mL of 5% w/v solution of GA (G6257, 25% in H<sub>2</sub>O) in PBS
- ❖ Prepare any of the following solutions

	4% gelatin (mL)	5% GA (µL)
1	5	5
2	<b>5</b>	<b>15</b>
3	5	25
4	5	35

- ❖ Vortex immediately after (or simultaneously) adding GA in the gelatin solution
- ❖ Leave the mixture for 30-60min before spraying

#### 3. 5mM EGCG – Gelatin/15GA Solution

- ❖ Add in solution of 4% Gelatin / 15GA (described above), proper amount (weight on scale) of EGCG powder, in order to have a concentration of 5mM
- ❖ Mix (vortex) properly, so EGCG is totally dissolved in the solution
- ❖ Work in dark (EGCG is sensitive and degradable)
- ❖ Use the solution for electrospraying (20kV, 2µL/min, 24 °C, 40%hum.)
- ❖ After electrospraying, keep the remaining EGCG solution in the freezer (or fridge)

# Release (Ferrous Tartrate, UV) and Activity (DPPH) Assays

## Release Test

- Materials
  1. Normal 96-well plates and ones for UV
  2. 0.9% NaCl (9 grams NaCl per 1 l of water) [release medium]
  3. EGCG dyeing solution [1 g ferrous sulfate (F8633, Sigma) + 5 g potassium sodium tartrate tetrahydrate (S2377, Sigma) in 1000 mL of distilled water] mixed with 0.067 M potassium phosphate buffer (pH 7.5) as 1:4 (Ferrous Tartarate)
- Method:
  1. Mix EGCG particles (powder – 41mg) with (10 or 15%) HA-pNIPAM (powder) in water, in order to get 1mL of 5 mM EGCG-gel mix., in 15 ml tubes
  2. Place in the fridge overnight (4 °C)
  3. Place at 37 °C and let it gelate for 10 mins (eppendorf)
  4. Add 10 mL of pre-warmed release media (use 5 mL pipet and pipet tips)
  5. Media will be collected and replaced with fresh release media at different time points for some days.
    - a. Collect and replace the whole media (10 mL)
    - b. Collect and replace 1 ml of release media (time: 1h, 24h, day 3,5,7)  
(different experiment)
  6. Freeze (in the freezer -20°C) the collected samples of the release media immediately
  7. The tubes will be kept for the total duration of the experiment in the eppendorf (37°C)
  8. use as control:
    - a. free EGCG in p-NIPAM
    - b. free EGCG without p-NIPAM frozen at the beginning of the experiment)
    - c. free EGCG without p-NIPAM (as stability control (2) (frozen at the end of the experiment – day 7)
- ❖ Use 100 uL of the release medium collected by the 15mL tubes and calculate absorbance in UV-VIS (274 nm)
- ❖ Use another 100 uL of the collected release media with ferrous tartarate solution for analysis [colorimetric spectroscopy (540 nm)]

## DPPH Assay:

- Materials
  1. (DPPH) radical scavenging assay ((250 µM in ethanol; D9132, Sigma) (wrapped in aluminum foil)
  2. 100 uL of the collected release media described above
- Method:
  1. 100 µl of EGCG solution (collected release medium) will be incubated with 500 µl of DPPH for 1 hour at room temperature

2. Calculate the absorbance at 517 nm (normal plate)
  3. L-Ascorbic acid (A4403, Sigma) and ethanol (O2860, Sigma) in equal amounts will be used as positive and negative controls
- ❖ prepare EGCG calibration curve for each release media both methods (UV-VIS and ferrous tartarate), for EGCG 5 mM – 5  $\mu$ m (\*For each plate prepare new standard curve)
- \* work in duplicates